School of Civil and Mechanical Engineering
Department of Civil Engineering

Experimental Study on Unsaturated Direct Shear and California Bearing Ratio Tests with Suction Monitoring on Sand-Kaolin Clay Mixtures

Yusep Muslih Purwana

This thesis is presented for the Degree of
Doctor of Philosophy
of
Curtin University

June 2013

DECLARATION

To the best of my knowledge and belief this thesis contains no material previously published by any other person except where due acknowledgement has been made.

This thesis contains no material which has been accepted for award of any other degree or diploma in any university.

Signature:

Yusep Muslih Purwana

Date:

ABSTRACT

The laboratory study on unsaturated soil may comprise the study of devices or apparatus used and the study of the behaviour of soil itself. In both, suction is the main issue of the study's concern. One of the common devices for unsaturated soil strength-testing is a suction-controlled direct shear box. With this device, suction is generated by controlling water pressure and air pressure during the test. A relatively rare method in unsaturated soil testing is suction-monitored direct shear. In this test, soil suction is not controlled; rather it is directly monitored by attaching the tensiometer to the top cap of the shear box.

For flexible pavement design, a very common laboratory test is the California Bearing Ratio (CBR). The CBR has been used as a semi-empirical approach for predicting the bearing capacity of sub-grade soil since the 1920's. The effect of water content on the CBR is commonly investigated in this type of study. Even though suction is one of the key parameters affecting unsaturated soil behaviour, the effect of soil suction on the CBR is not usually taken into account. This may be due to the difficulty in measuring soil suction while the performing the CBR test.

The main objective of this study is to review the behaviour and capability of a suction-monitored direct shear device and to introduce a modified CBR test device in which suction is taken into consideration during the test. A series of laboratory tests was carried out consisting of a saturated direct shear test, an unsaturated direct shear test, and a suction-monitored CBR test on both soaked and unsoaked CBR using the artificial soil of sand and sand-kaolin clay mixtures. During the tests, suction was generated naturally by controlling the specimen in different water content values. For this, the soil water characteristic curve (SWCC) was a very useful tool for predicting the desired specimen water content and/or matric suction.

Suction-monitored direct shear and CBR devices were successfully used for the specimens where matric suction was less than 80 kPa. The tensiometer performed effectively during the test. The results indicated that the presence of kaolin clay in the mixture, to some extent, led to the increase in unsaturated shear strength and the CBR. In general, matric suction versus unsaturated shear strength and matric suction versus CBR curves exhibited bi-linear curves with the inflection points occurring around the air entry value (AEV).

The correlation between CBR and unsaturated shear strength was developed by plotting the failure envelopes resulting from unsaturated direct shear and unsaturated CBR tests. The range of R-square was between 0.87 and 0.99. The high R-square value of the equations indicated that the correlations were reasonable. This correlation may be applicable only for these particular specimens in the range of suction between 0 and 80 kPa.

Keywords: *sand-kaolin clay mixture, suction-monitored CBR, suction-monitored direct shear, tensiometer, unsaturated soil*

ACKNOWLEDGEMENTS

I would like to express special thanks to my supervisor Prof. Hamid Nikraz, for giving me the opportunity to conduct research in a challenging area; unsaturated soil. He has given me a lot of advice and encouragement and the spirit to learn and study this particular area of geomechanics. I am grateful for his kindness and willingness to help with and solve many of the problems encountered during the study.

Thank you to Dr. Peerapong Jitsangiam, Dr. Apiniti Jotisankasa from Kasetsart University, Dr. Komsun Siripun and Mr. Mark Whittaker and all technical staff at the Geomechanics Laboratory for their assistance in the experimental work.

I acknowledge and strongly appreciate the support and funding from the Indonesian National Education Department through the Dikti Scholarship Project.

Last but not least, my special thanks are due to all my housemates; Mr. Isnandar Slamet, Mr. Bowo Ekocahyono, Mr. Edy Saputra, Mr. Sony Gunawan and Mr. Suratman. They are all PhD candidates at the time of writing this acknowledgement.

LIST OF PUBLICATIONS

During the study, the following publications have been resulted:

Purwana, Y.M., Jitsangiam, P., Nikraz, H., and Josinakasa A. (2011). "*Experimental Studies on Suction-Monitored Direct Shear Apparatus on Perth Poorly Graded Sand*". Proceedings, International Conference on Advances in Geotechnical Engineering, Perth, Westren Australia, November 7-9, pp. 273-278.

Purwana, Y.M., Nikraz, H., Jitsangiam, P. (2012). "*Experimental Study of Suction-Monitored CBR test on Sand-Kaolin Clay Mixture*". Proceedings, 2nd International Conference on Geotechnique, Construction Materials and Environment, Kuala Lumpur, Malaysia, November 14-16, pp. 85-90

Purwana, Y.M., Nikraz, H. (2012). "*Review and Reintroduction to Suction-Monitored Direct Shear Test for Unsaturated Soil*", Proceedings, 16th Annual Scientific Meeting, Indonesian Society for Geotechnical Engineering (ISGE), Jakarta, December 4-5, pp. 161-166.

Purwana, Y.M., Nikraz, H., Jitsangiam, P. (2012). "*Experimental Study of Suction-Monitored CBR test on Sand-Kaolin Clay Mixture*", Int. J. of Geomate Vol. 3 No. 2. Japan, pp. 419-422 (accepted paper)

Purwana, Y.M., Chegenizadeh, A., Nikraz, H. (year). "*Suction-Monitored Direct Shear Apparatus; A Simple Device for Unsaturated Soil Testing*". Australian Geomechanics Journal (accepted paper)

TABLE OF CONTENTS

LIST OF FIGURES

LIST OF TABLES

LIST OF NOTATIONS

A	=	activity of fine grained material
c'	=	effective cohesion
C_c	=	curvature coefficient of gradation curve
C_u	=	uniformity coefficient of gradation curve
d_f	=	estimated horizontal displacement at failure of direct shear test
d_r	=	displacement rate of direct shear
ϕ'	=	effective internal friction angle
ϕ^b	=	the angle indicating the rate of change in shearing strength due to the contribution of matric suction
G_s	=	specific gravity
γ_w	=	unit weight of water
h_c	=	capillary rise
P	=	partial pressure of pore water vapour
P_0	=	saturation pressure of water vapour over a flat surface of pure water at the same temperature
π	=	osmotic suction
r	=	radius of tube of capillary model
R	=	universal gas constant (8.31432 J $mol^{-1}K^{-1}$)
R_s	=	radius of curvature of capillary rise theory
σ	=	normal stress
σ_n		normal stress at failure plane
t_f	=	total elapsed time to failure of direct shear test
t_{90}	=	time required for the specimen to achieve 90% consolidation
T	=	absolute temperature (273.16 + t^oC)
T_s	=	surface tension of Kelvin's capillary model
τ_f	=	shear strength at failure
τ_u	=	unsaturated shear strength
θ	=	volumetric water content
θ_s	=	saturated water content
Θ	=	normalised volumetric water content
V	=	molecular volume of water
u_a	=	pore air pressure

u_w	=	pore water pressure
ψ	=	total suction
ψ_b	=	air entry value of SWCC
ψ_r	=	residual water content of SWCC
w_f	=	filter paper water content
χ	=	parameter between 0 and 1 as a function of degree of saturation of Bishop's theory of strength

CHAPTER 1
INTRODUCTION

1.1 Backgound

In general, the laboratory study of unsaturated soil may be divided into two groups; (a) the study on the devices or apparatus used for unsaturated soil testing, and (b) the study on the behaviour of the soil itself in unsaturated conditions. In both groups, soil suction is the main issue of the study. For group (a), various devices and test methods have been proposed and developed by researchers (Donald, 1957; Hilf, 1956; Gan et al., 1988; Likos et al., 2010; amongst other) . One of the most common devices for unsaturated soil strength testing is the suction-controlled direct shear apparatus. With this device, suction is generated by controlling water pressure and air pressure during the test. A relatively rare method in unsaturated soil testing is suction-monitored direct shear. In this test, soil suction is not controlled; rather it is directly monitored by attaching a tensiometer to the top cap of a shear box (Jotisankasa and Mairaing, 2010). Compared to the first method, the second one is very rarely reported in the literature.

Another very common laboratory test utilises the California Bearing Ratio (CBR). The CBR has been used since the 1920's as a semi-empirical approach and test for predicting the bearing capacity of the sub-grade layer for flexible pavement design. The effect of water content on the CBR was commonly investigated in the study. Even though suction is one of the key parameters affecting unsaturated soil behaviour, the effect of soil suction on the CBR is commonly not taken into account. This may be due to the difficulty in measuring soil suction while performing the CBR test.

In group (b), researchers have studied the behaviour of soil in unsaturated conditions. Some unsaturated soil property functions such as hydraulic conductivity for steady state seepage, water storage function for transient state seepage, shear strength function for stability analysis and thermal conductivity function for thermal analysis have been proposed (Fredlund and Houston, 2009). In many cases, the behaviour of artificial soil can be controlled and this makes it useful for the purposes of experimental study. Another advantage of using artificial soil is that it allows for reliable test duplication.

1.2 Research objectives

In the study undertaken in this paper, groups (a) and (b) were investigated using suction-monitored direct shear and suction-monitored CBR methods. Artificial materials of sand and sand-kaolin mixture were used to investigate soil behaviour in both saturated and unsaturated conditions.

Based on the background above, the objectives of this study are:

1. To review the behaviour and capability of a suction-monitored direct shear device by performing laboratory tests in saturated and unsaturated conditions.
2. To introduce and develop a CBR test device in which suction is taken into consideration using direct suction measurement. The modification was made by attaching 3 tensiometers on a CBR surcharge weight and mould.
3. To investigate the strength behaviour of sand and sand-kaolin clay mixture in saturated and unsaturated conditions.
4. To develop the correlation of strength obtained from unsaturated direct shear test and unsaturated CBR tests.

1.3 Scope of work

To achieve the research objectives, a series of procedures were performed. The scope of work comprises:

1. Preliminary laboratory tests on specimens from some areas in Perth. It has been conducted by randomly selecting and picking sub-grade soil samples from 4 different locations to find out their index properties.
2. Preliminary laboratory tests on artificial soil made of sand, kaolin clay, and kaolin clay mixtures with differing proportions of 95:5, 90:10, 80:20, and 60:40. For the purposes of this study, artificial soil was used to ensure the repeatability of the test.
3. Reviewing the the properties of of sand, kaolin clay, and sand-kaolin claymixture, with an emphasis on the physical and chemical properties of kaolin clay.
4. Reviewing unsaturated soil theory including soil-water characteristic curve, unsaturated shear strength theory and their test methods.

5. Laboratory compaction tests on sand, kaolin clay and kaolin-clay mixtures to obtain compaction characteristic.
6. Soil-water characteristic curve test using a tensiometer and filter paper method.
7. Experimental laboratory tests using a conventional direct shear device for saturated conditions and a modified direct shear device for unsaturated conditions. The modification was made by attaching a tensiometer on the top cap of the direct shear.
8. Analysing the direct shear results and reviewing these along with the general framework of unsaturated soil theory.
9. Experimental laboratory tests using a modified CBR device for soaked and unsoaked conditions. The test was performed to develop the CBR device with direct suction measurement using tensiometers.
10. Developing the correlation of strength obtained from unsaturated direct shear tests and unsaturated CBR tests.

1.4 Outline of thesis

This thesis is organised into six chapters with the outline of each chapter as follows:

Chapter 1 introduces the background and general idea of this study, the objectives and scope of work.

Chapter 2 presents the literature review of the thesis. This chapter outlines previous studies of laboratory tests on unsaturated soil with particular emphasis on direct shear and CBR. The chapter also presents the theory of shear strength in unsaturated conditions, stress state variables, soil suction, and the methods of suction measurement. The concept of the soil-water characteristic curve (SWCC) and its mathematical models is also described here.

Chapter 3 continues with the literature review. This chapter focuses on the theory and previous studies of sand-kaolin clay mixture. The properties of sand, kaolin clay, and sand-kaolin clay mixture are reviewed in this chapter. The mineralogy of clay, especially of kaolin clay, and its physical properties is also presented.

The experimental program of the study is described in Chapter 4. This chapter outlines specimen selection and preparation, specimen preliminary tests (index property tests and compaction test), suction measurement methods, SWCC test methods, and unsaturated strength tests. Two methods of SWCC tests using a tensiometer and filter paper are described in this chapter. Finally, two methods of unsaturated strength testing; suction-monitored direct shear and suction-monitored CBR tests are elaborated upon.

Chapter 5 presents the result of the laboratory tests described in Chapter 4. It is divided into five subsections; specimen index properties, compaction characteristics, SWCC, unsaturated shear strength, and unsaturated CBR. The analysis and discussion is carried out for each subsection using the framework of the literature review in Chapters 2 and 3.

Finally, Chapter 6 presents the summary of the study along with conclusions and recommendations.

CHAPTER 2
UNSATURATED SOIL AND LABORATORY TESTING

2.1 Introduction

This chapter presents the theory of, and literature review on unsaturated soil issues. It includes a brief history of the emerging concept of unsaturated soil theory, the concept of soil suction, unsaturated stress variables, suction measurement, the soil water characteristic curve (SWCC), and its laboratory test, and unsaturated shear strength theory. Finally, an unsaturated strength test is presented, in which matric suction is taken into consideration.

2.2 The emergence of unsaturated soil theory

According to Fredlund and Rahardjo (1993), the concept of unsaturated soil theory was pioneered in the early 1900's by researchers in soil science in relation to soil-water-plant systems. Information regarding soil's capacity to hold water is vital to the agricultural industry. As most plants are grown in unsaturated soil, researchers focused on this area and developed a theory of soil suction. This included aspects such as the influence of soil type on water storage capacity, water supplies to plantations and the effect of root suction on water content. (Corey et al., 1967; Slavéková, 1967).

In the field of geotechnical engineering, engineers have been considering the role of soil suction on soil behaviour for over fifty years, when problematic issues such as expansive soil first emerged. The term 'unsaturated soil' was initially proposed at the 2nd International Society of Soil Mechanics and Foundation Engineering ISSMFE in 1969. Research interest and appreciation of the issues regarding unsaturated soil increased to the point where this term is now accepted widely. In fact, the phenomenon of unsaturated soil in geotechnical engineering has long been recognised. Terzaghi (1942) studied and wrote on soil moisture and the capillary phenomenon in soil. Unsaturated soil in geotechnical structures was discussed at the 1st International Conference on Soil Mechanics and Foundation Engineering in 1936. This was considered as a forum to attempt to explain shear strength behaviour with respect to matric suction on the stability of earth dams. A series of international

conferences on expansive soil was seen as a significant forum for discussion with regard to establishing a theoretical basis around unsaturated soil mechanics (Fredlund, 1996).

A milestone of unsaturated soil theory in geotechnical engineering was passed when Bishop (1959) proposed the remarkable effective stress parameter and stress state variables for unsaturated soil; net normal stress and negative pore pressure. The work of Donald (1956) contributed to a very significant development in systematic laboratory testing on unsaturated soil strength, as Donald performed shear strength tests using modified direct shear with suction measurement. An extensive study by Fredlund and Morgenstern (1977), Fredlund (1979), Fredlund and Rahardjo (1993) and others also helped establish a theoretical framework for unsaturated soil in the geotechnical engineering area by introducing the concept of independent two stress state variables in unsaturated soil.

2.3 The terminology of unsaturated soil

In terms of the presence of water in soil, the natural soil profile is divided into two categories; saturated and unsaturated soil. The soil layer below the water table can be considered as saturated soil, whereas the soil layer above the water table can be considered as unsaturated soil. The entire zone above the groundwater table is called the vadose zone. Due to gravitational forces, the pore water pressure in a saturated soil layer is positive, whereas in unsaturated layers (the vadose zone), pore water pressure is negative. The soil can be deemed as being in an unsaturated condition when even the smallest bubbles of air are found in the system.

In saturated soil, all soil pores in the soil body are occupied by water. In this condition, the concept of effective stress is applicable. Conversely, in an unsaturated condition some of the soil pores are occupied by water whilst other pores are occupied by air. The presence of air in the soil results in a negative pore water pressure. In this situation, the concept of effective stress in which only one state stress variable is present (σ - u_w) is not applicable. Rather, there are two stress state variables in the soil body; net normal stress (σ - u_a) and matric suction (u_a - u_w). Figure 2.1a shows the illustration of soil pores in a saturated and unsaturated

condition, whereas Figure 2.1b shows the application of state stress variables in both conditions.

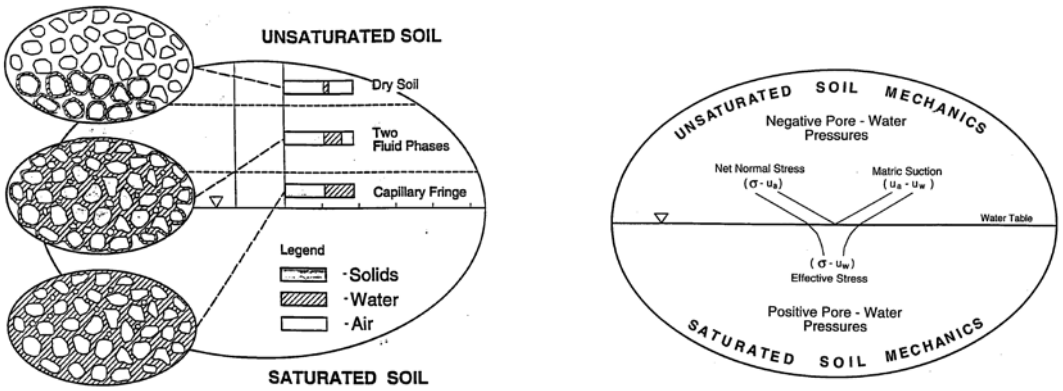

(a) (b)

Figure 2.1 The illustration of saturated and unsaturated layers (Fredlund, 1996)

2.4 Suction in soil body

Soil suction is one of main parameters used in unsaturated soil mechanics. The role of this parameter is vital, as pore water pressure measurement effective stress concept in saturated soil mechanics (Houston et al., 1994a).

Suction can be defined as the unit attraction force of the soil with regard to water. The attraction of water is necessary to transform a soil water molecule from the liquid phase into the vapour phase (Bulut and Wray, 2005). Suction can also be defined as the ability of the soil to absorb additional water (Murray and Sivakumar, 2010). It represents the thermodynamic potential of pore water relative to free water. Unsaturated soil, when in contact with a hypothetical reservoir of free water, has the potential to draw the water through the liquid phase and the gas phase. This potential is commonly referred to as suction, which can also be defined as the free energy state of soil water in terms of the partial pressure vapour of soil pore water in equilibrium (Fredlund and Rahardjo, 1993).

Soil suction consists of two components: matric suction and osmotic suction.

(1) Osmotic suction is a component of free energy derived from the measurement of the partial negative pressure of water vapour and it must be in equilibrium with an identical composition of soil water. This is relative to the partial pressure of water vapour in equilibrium with free pure water (water without dissolved solutes). This suction comes from dissolved solutes or salt concentration differences between one point and another point in the soil mass through chemical interaction between dissolved salt and free water. Osmotic suction only occurs when the soil water is in contact with pure water through a semi-permeable membrane via which only water molecules, not solutes, can pass.

(2) Matric suction is another component of suction. It is free energy derived from the measurement of the partial pressure of water vapour in equilibrium with the soil water, relative to the partial pressure of water vapour in equilibrium with a solution identical in composition to soil water. Matric suction comes from the combined effect of capillary tension and short-range adsorption forces in the soil matrix (Lu and Likos, 2004). Houston (1994) defined matric suction as the affinity of soil has for water in the absence of any salt content gradient in the water.

Thermodynamically, suction above the free surface of pure water can be determined by using Kelvin's equation:

$$\psi = \frac{RT}{V} ln\left(\frac{P}{P_0}\right) \qquad \text{(kPa)} \qquad (2.1)$$

where

R = universal gas constant (8.31432 J $mol^{-1}K^{-1}$)

T = Absolute temperature (273.16 + t^oC)

V = molecular volume of water, volume of 1000 moles of liquid water (0.018 m^3)

P = partial pressure of pore water vapour (kPa)

P_0 = saturation pressure of water vapour over a flat surface of pure water at the same temperature (kPa)

Equation (2.1) is commonly expressed using the relative humidity (*RH*) term as:

$$\psi = \frac{RT}{V} ln(RH) \qquad (2.2)$$

where $RH = P/P_0$

In an unsaturated condition, the interface between pore air and pore water is developed as an elastic membrane (Figure 2.2). This membrane is referred to as a contractile skin which possesses the property of surface tension (T_s). The contractile skin is subjected to pressure from the air (u_a) and pressure from the water (u_w). The difference between pore air and pore water pressure on the contractile skin is referred to as matric suction ($u_a - u_w$). If the radius of curvature (R_1 and R_2) in all directions is the same, the relation between the surface tension and the matric suction can be expressed as:

$$(u_a - u_w) = \frac{2T_s}{R_s} \qquad (2.3)$$

where $(u_a - u_w)$ is matric suction, T_s is surface tension, and R_s is the radius of curvature.

Equation (2.3) is commonly referred to as Kelvin's capillary model equation.

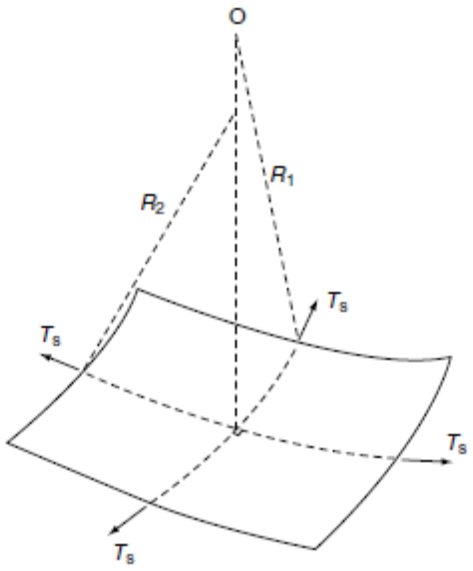

Figure 2.2 Illustration of surface tension on a membrane (Fredlund and Rahardjo, 1993)

The radius of curvature is analogous to the radius of the soil pore. The presence of surface tension in the soil causes capillary action. Water in the soil pores is pulled up by surface tension to a certain level until an equilibrium state with gravitational force is achieved. The height of capillary rise can be expressed as:

$$h_c = \frac{2T_s}{\gamma_w r} \tag{2.4}$$

where γ_w is the unit weight of water and r is the radius of the tube; this radius being analogous to the pore radius of the soil.

Equations (2.3) and (2.4) can be used to prove that there is a strong relation between matric suction, grain size (or pore radius) and capillary rise. Soil with fine particle sizes such as clay or silt would cause higher matric suction and a higher capillary rise compared to soil with coarse particle sizes such as sand or gravel.

It is evident that suction comes from the combination of matric suction and osmotic suction, and this can be expressed as:

$$\Psi = (u_a - u_w) + \pi \tag{2.5}$$

Where ψ is total suction, $(u_a - u_w)$ is matric suction, and π is osmotic suction.

There is a relationship between water content and soil suction. The change of water content in the soil is responsible for the changes in matric and osmotic suction. However, in most geotechnical problems the changes in matric suction are more significant when compared to changes in osmotic suction (Fredlund and Rahardjo, 1993). In the following section, the term 'suction' refers to matric suction, unless otherwise stated.

2.5 Suction as a stress state variable

It is vital to determine stress variables for unsaturated soil as the stress condition of unsaturated soil is quite different to the soil in a saturated condition. Unsaturated soil has 3 phases: solid (soil particle), liquid (pore water) and gas (pore air) whereas saturated soil has only two phase: solid and liquid.

A stress state variable is defined as a limited set of dynamics in the system, such as pressure, temperature and volume. These are sufficient to describe or to specify

completely the state of the system under consideration (Ng and Menzies, 2007). Fredlund and Morgenstern (1977) proposed any two of three possible stress variables as sufficient for unsaturated soil, (σ - u_a), (σ - u_w) and (u_a – u_w). The possible combinations of stress variables are:

1. (σ - u_a) and (u_a – u_w) (2.6 a)
2. (σ - u_w) and (u_a – u_w) (2.6 b)
3. (σ - u_a) and (σ – u_w) (2.6 c)

The study which was carried out found that the independent combination of (σ - u_a) and (u_a – u_w) was the best choice as this combination produced an easier transition to the fully saturated condition and was the most satisfactory from a practical standpoint (Fredlund, 1979; Fredlund and Rahardjo, 1993).

Figure 2.3 illustrates the stresses at a particular point in the soil, where soil particles and pore water are assumed to be incompressible. The stress state variables of unsaturated soil can be written as two independent stress tensors:

$$\begin{bmatrix} (\sigma_x - u_a) & \tau_{yx} & \tau_{zx} \\ \tau_{xy} & (\sigma_y - u_a) & \tau_{zy} \\ \tau_{xz} & \tau_{yz} & (\sigma_z - u_a) \end{bmatrix} \quad (2.7)$$

and

$$\begin{bmatrix} (u_a - u_w) & 0 & 0 \\ 0 & (u_a - u_w) & 0 \\ 0 & 0 & (u_a - u_w) \end{bmatrix} \quad (2.8)$$

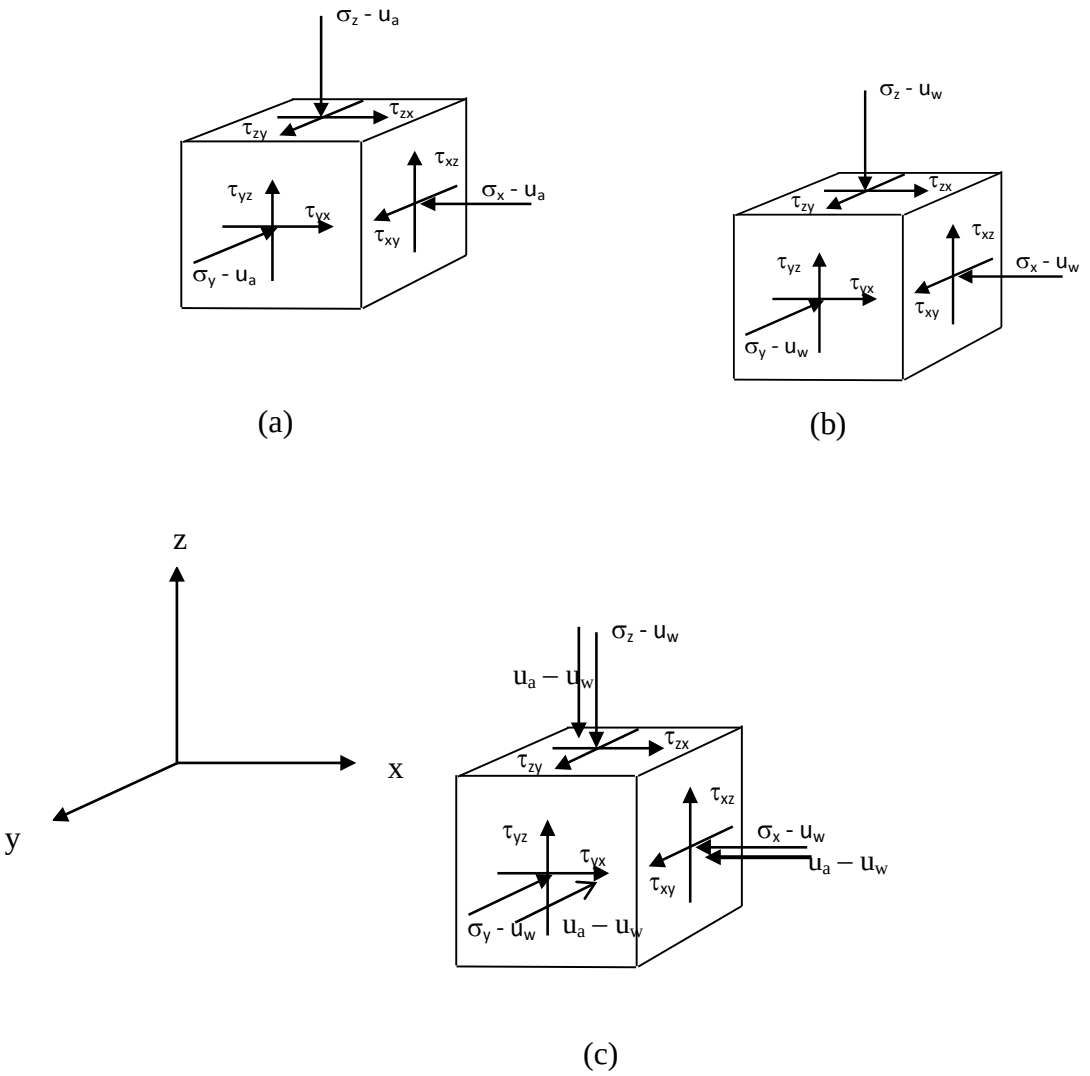

Figure 2.3 The illustration of stress state variables at a particular location: (a) Dry soil (b) Saturated condition and (c) Unsaturated condition (modified from Fredlund (1996))

2.6 Suction measurement

One of the important issues in dealing with unsaturated soil is suction measurement. Suction measurement can essentially be grouped into two categories: direct and indirect. Ridley and Wray (1995) and Murray and Sivakumar (2010) summarised a number of direct and indirect suction measurement methods for both matric and total suction. Based on suction capacity, Rahardjo and Leong (2006) divided suction measurement techniques into three groups: low range (0 - 100 kPa), medium range (100 - 1,000 kPa), and high range (1,000 - 10,000 kPa). As previously described in

section 2.4, in most geotechnical problems matric suction is more responsible for the behaviour of unsaturated soil than total suction, a technique which will not be presented here. Table 2.1 shows the methods of matric suction measurement and their characteristics.

Table 2.1 Methods of matric suction measurement

Method	Range (kPa)	Equilibrium time	Direct/indirect
Filter paper	10 – 30,000	7 -14 days	Indirect
Porous block	30 – 30,000	Weeks	Indirect
Pressure plate	30 – 1,500	Hours to days	Direct
Tensiometer	0 – 100	Minutes	Direct
Suction probe	0 – 1,500	Minutes	Direct

In this study, filter paper and tensiometer were utilised extensively. The filter paper method was employed as it is a relatively simple method, with the ability to measure suction up to a pressure of 30,000 kPa. The tensiometer was used due to its short response time (within minutes). The tensiometer is also a device which can perform direct matric suction. However, each method has its own disadvantage. The use of filter paper is an indirect method with a correspondingly slow time of equilibration (7 – 14 days), whereas the tensiometer has a very low matric suction reading capacity (0 – 100 kPa). For these reasons, the combination of both methods is employed simultaneously.

2.6.1 Filter paper method

The idea of utilising filter paper for measuring soil suction is that in equilibrium in a closed system, the suction value of the soil will be the same as the suction value of the filter paper. Hence, prior to measuring the suction in the soil body, the filter paper is calibrated to establish the relation between its suction and water content.

According to Al-Khafaf and Hanks (1974), the method of measuring soil suction using filter paper was recognised by researchers in the early 1930's. Gardner (1937) was considered to be one of the first researchers who utilised filter paper for measuring matric suction. Schleicher and Schuell filter paper No. 589 was utilised to establish a calibration curve, and sulphuric acid and a centrifuge were used for generating high and low suction respectively. The calibration curve of the filter paper was used as a reference for calculating the suction of the soil.

McQueen and Miller (1968) used a pressure plate and pressure membrane extractor to determine a wider range of calibration curves from saturation to dry air, using Schleicher and Schuell filter paper No. 589. They studied the effect of the placement of filter paper in three different conditions: good contact, uncertain contact, and no contact of the filter with the soil. The effect of temperature in measuring suction was also taken into account. When a filter paper was placed where it had a good contact with the soil, water from the soil was absorbed and taken up by the filter paper with capillary force; this is referred to as matric suction. When a filter paper was placed in a closed container without contact with the soil, water from the soil was absorbed by vapour diffusion, referred to as total suction.

The effect of temperature on the filter paper method has been studied by Al Khafaf and Hanks (1974) using Schleicher and Schuell filter paper No. 589. The results indicated that temperature is not an important factor, as long as a constant temperature is maintained during testing to avoid water loss from condensation as the room temperature changes.

Other investigators have studied the use of filter paper for suction measurement using Whatman filter paper No. 42 with different types of measuring devices (Chandler and Gutierrez, 1986; Fawcett and Collis-George, 1967; Hamblin, 1981). The calibration curves resulting from each study were unique. However, from the results it can be concluded that the filter paper method offers a promising simple technique for suction measurement, and can be reliably used across a wide suction range (10-90,000 kPa).

A comprehensive review of published literature was undertaken by Leong et al., (2002) on the differences in calibration curves using Schleicher and Schuell filter paper No. 589 and Whatman filter paper No. 42. They concluded that the differences between them may have been attributable to calibration procedures, along with the quality of the filter paper, suction source, hysteresis, and equilibration time. Leong et al., (2002) summarised the equations of calibration curves obtained from the literature, as shown in Table 2.2.

According to Leong et al., (2002) and Houston et al. (1994a), the procedure for determining calibration curves for matric suction must be different from the procedure for total suction. Matric suction calibration curves can be obtained using a

pressure plate apparatus (drying procedure), whereas total suction calibration curves are obtained by placing the filter paper using a non-contact method over salt solutions (wetting procedure). It is these different procedures that produce differing total and matric suction calibration curves. Leong et al., (2002) suggested that for pressures up to 1000 kPa, contact filter paper may be reliably used for matric suction measurement, whereas for suction greater than 1000 kPa, the filter paper will only measure total suction, regardless of whether a contact or non-contact procedure is used. Table 2.3 shows the equations for calibration curves suggested by Leong et al. (2002).

Table 2.2 Filter paper calibration curves (Leong et al., 2002)

Whatman filter paper No. 42			Eq.
Reference	Calibration curve equation	Range	
Hamblin (1981)	$log\,\Psi = 8.022 - 3.683\ log\ w_f$		(2.9)
Chandler and Gutierrez (1986)	$log\,\Psi = 4.84 - 0.0622\ log\ w_f$	$w_f < 47$	(2.10)
Chandler et al. (1992)	$log\,\Psi = 6.05 - 2.48\ log\ w_f$	$w_f \geq 47$	(2.11)
Greacen et al. (1987)	$log\,\Psi = 5.327 - 0.0779\ log\ w_f$	$w_f < 45.3$	(2.12)
ASTM (1997)	$log\,\Psi = 2.413 - 0.0135\ log\ w_f$	$w_f \geq 45.3$	(2.13)
Schleicher and Schuell filter paper No. 589			
McQueen and Miller (1968)	$log\,\Psi = 5.238 - 0.0723\ log\ w_f$	$w_f < 54$	(2.14)
	$log\,\Psi = 1.8966 - 0.01025\ log\ w_f$	$w_f \geq 54$	(2.15)
Al-Khafaf and Hanks (1974)	$log\,\Psi = 4.136 - 0.0337\ log\ w_f$	$w_f < 85.3$	(2.16)
	$log\,\Psi = 2.0021 - 0.009\ log\ w_f$	$w_f \geq 85.3$	(2.17)
McKeen (1980)	$log\,\Psi = 4.9 - 0.0624\ log\ w_f$	$w_f < 66$	(2.18)
	$log\,\Psi = 1.25 - 0.0069\ log\ w_f$	$w_f \geq 66$	(2.19)
Greacen et al. (1987)	$log\,\Psi = 5.056 - 0.0688\ log\ w_f$	$w_f < 54$	(2.20)
ASTM (1997)	$log\,\Psi = 1.822 - 0.0102 log\ w_f$	$w_f \geq 54$	(2.21)

Ψ = suction (kPa); wf = filter paper water content (%)

Table 2.3 Calibration curve equations suggested by Leong et al. (2002)

Whatman filter paper No. 42			Eq.
Suction	Calibration curve equation	Range	
Matric	$log\,\Psi = 2.909 - 0.0229\ w_f$	$w_f \geq 47$	(2.22)
	$log\,\Psi = 4.945 - 0.0673\ w_f$	$w_f < 47$	(2.23)
Total	$log\,\Psi = 8.778 - 0.222\ w_f$	$w_f \geq 26$	(2.24)
	$log\,\Psi = 5.31 - 0.0879\ w_f$	$w_f < 26$	(2.25)
Schleicher and Schuell filter paper No. 589			
Matric	$log\,\Psi = 2.659 - 0.018\ w_f$	$w_f \geq 54$	(2.26)
	$log\,\Psi = 5.438 - 0.069\ w_f$	$w_f < 54$	(2.27)
Total	$log\,\Psi = 8.778 - 0.191\ w_f$	$w_f \geq 32$	(2.28)
	$log\,\Psi = 5.26 - 0.0705\ w_f$	$w_f < 32$	(2.29)

Figure 2.4 shows the calibration curve of Whatman filter paper No. 42 according to the Eq. (2.12) and (2.13), and Eq. (2.22)-(2.25).

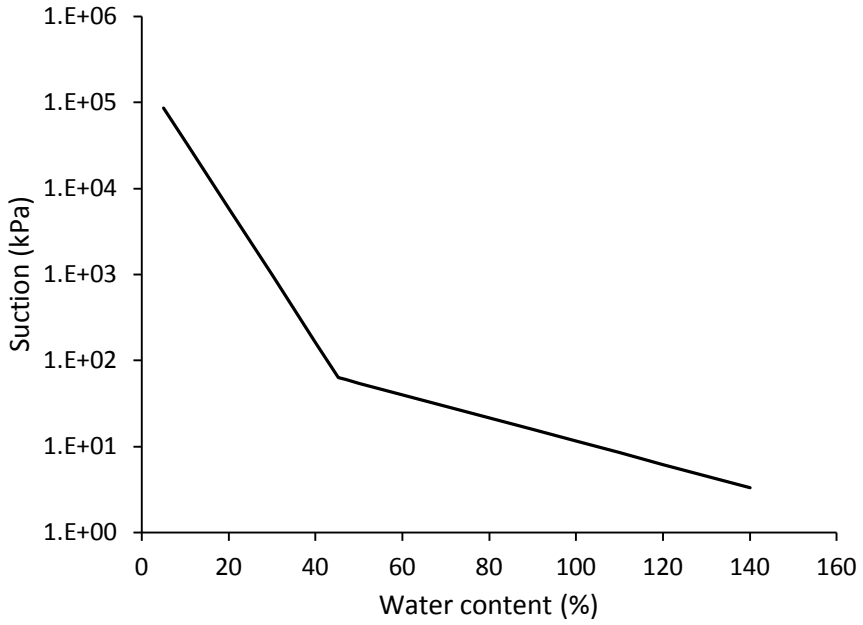

(a)

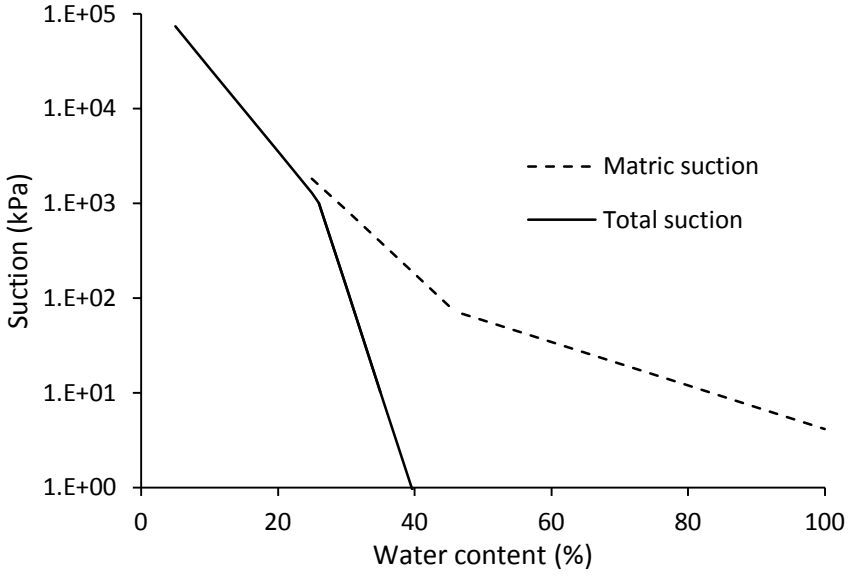

(b)

Figure 2.4 Whatman filter paper No. 42 calibration curves for: (a) Based on Eq. (2.12) and (2.13) from Leong et al. (2002), and (b) Based on Eq. (2.22)-(2.25) from ASTM D 5298-94 and Greacen (1987).

Once the calibration curve has been determined, matric and total suction measurement can be performed using a similar brand and number of filter paper.

The procedure of soil suction measurement has been described by numerous investigators (Al-Khafaf S. and Hanks, 1974; Bulut and Wray, 2005; Fawcett and Collis-George, 1967; Houston et al., 1994b; Murray and Sivakumar, 2010). ASTM D 5298-03 provides the standard test of suction measurement using filter paper, and also provides the calibration curves for Schleicher and Schuell filter paper No. 589 and Whatman filter paper No.42. Figure 2.5 illustrates the setup of matric and total suction measurements using the filter paper method.

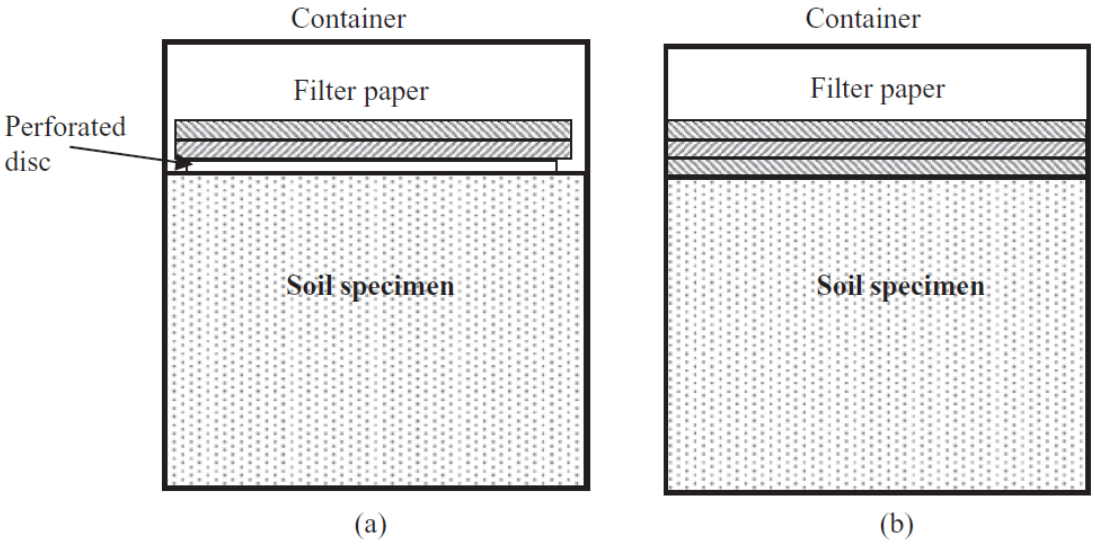

Figure 2.5: Illustration of the filter paper method: (a) Total suction measurement, (b) matric suction measurement (Murray and Sivakumar, 2010)

2.6.2 Tensiometer

The tensiometer is one of the devices used for direct measurement of matric suction. It consists of a high air entry disk (HAED), water reservoir, and sensor transducer. The HAED is made from ceramic material with uniform size pores and it acts as a membrane between the water in the reservoir and the air in the soil. In saturated conditions, the HAED has the ability to allow the passage of water and at the same time it can prevent air passing through due to the presence of the contractile skin developing on the surface of the ceramic disk. Once the HAED surface contacts with soil, the water pressure in the reservoir is developed. This pressure is then sent

through a sensor transducer for digital readout as a voltage. Calibration is required to correlate pressure and voltage, in which a single value of pressure corresponds to a single value of voltage. Calibration is essentially performed using a controlled vacuum pump and a multimeter. With these devices, a suction-voltage curve can be established. Once the curve is created, the voltage from the multimeter can be converted into a pressure unit. Figure 2.6 (a) and (b) show photographs of the miniature tensiometers and (c) shows the schematic diagram of the IC tensiometer.

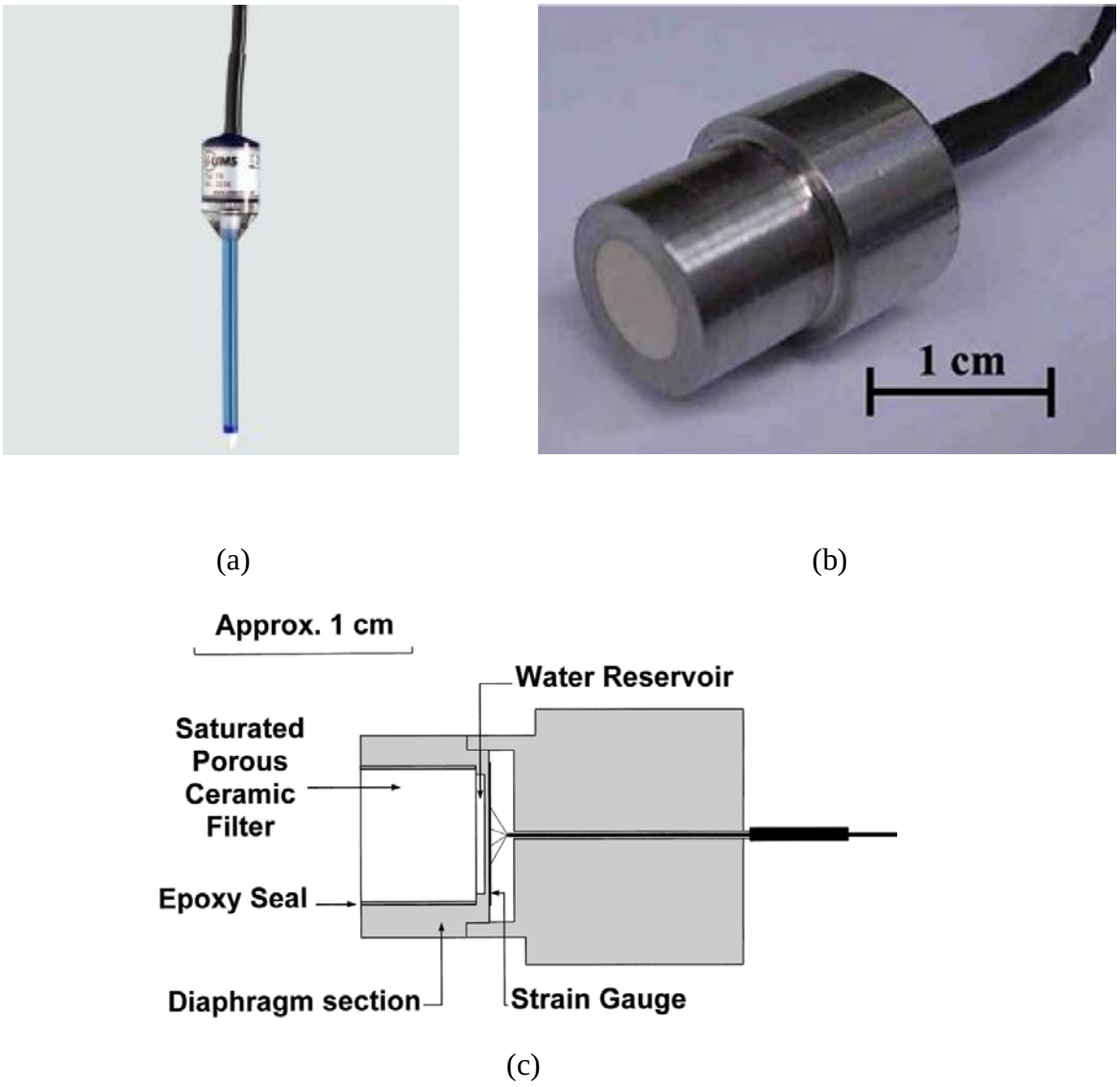

Figure 2.6 The miniature tensiometers, (a) Photograph of Tensior 5 made by Eijkelkamp (www.eijkelkamp.com), (b) Imperial College (IC) tensiometer (Ridley and Burland, 1993), and (c) Schematic diagram of IC miniature tensiometer (Ridley and Burland, 1999)

During the test, air must not be present in the tensiometer. The presence of even a few air bubbles in the tensiometer will affect the performance by increasing the response time. Saturation is required for evacuating the air from different parts of the device using a vacuum pump. The tensiometer was submerged in pure water-filled desiccators for vacuuming at 90 kPa, as described by Jotisankasa (2010). During the process, air bubbles were produced from the water but eventually disappeared when saturation was complete.

Prior to installation, the performance of the tensiometer required checking, using a material that could easily be absorbed by water. Tissue paper was placed onto the surface of the HAED. When the response time was rapid, it was deemed that no air bubbles were present in the tensiometer and performance was effective. Otherwise saturation process has to be repeated until no air bubbles in the tensiometer.

2.7 Soil water characteristic curve

2.7.1 Nature of the soil water characteristic curve

The behaviour of unsaturated soil is strongly affected by matric suction, and matric suction is strongly affected by water content. As a consequence, matric suction and water content are vital parameters, and these are commonly represented by a curve expressing the relationship between matric suction and water content. In geomechanics, the curve is commonly referred to as a soil water characteristic curve (SWCC). Suction is plotted in logarithmic scale and water content is plotted in arithmetic scale. The terms used to describe water content can be expressed as degree of saturation S, gravimetric water content w, or volumetric water content θ which is defined as $\theta = S.e/(1+e)$. The SWCC quantifies the capacity of the soil to hold water with a particular degree of suction, and the slope of the SWCC describes the rate of water loss corresponding to suction (Agus et al., 2001). A typical SWCC and the terms related to the curve are shown in Figure 2.7.

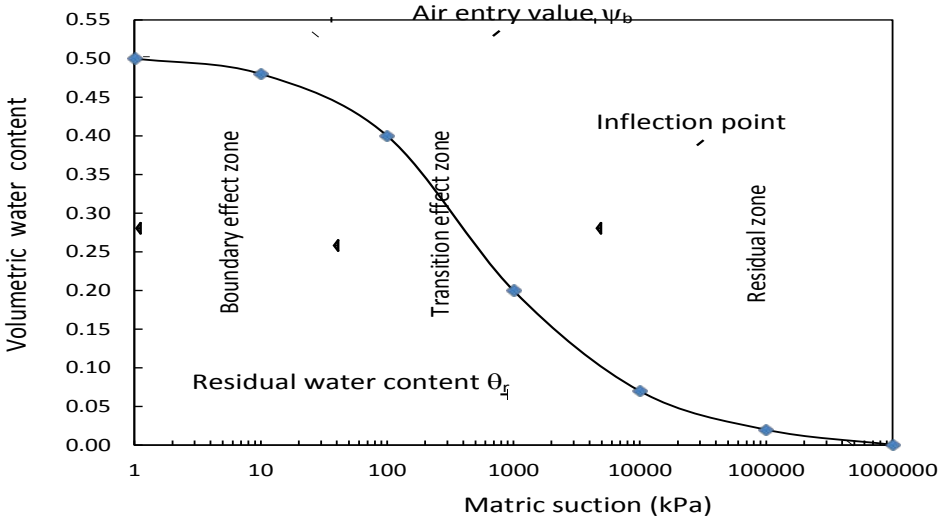

Figure 2.7 Typical soil water characteristic curve, modified after Vanapalli (1999)

There are numerous descriptions relating to the SWCC. Vanapalli et al. (1999) and Siller et al. (2001) elaborated upon the mechanism of the SWCC with regard to a soil sample when it was desaturated from its fully saturated condition. The SWCC consists of 3 zones: the boundary effect zone, the transition zone, and the residual zone. With the boundary effect zone (saturated condition) there is no inter-granular surface tension due to all soil pores being occupied by water. When negative pressure or suction is applied, the water in the soil pores is expelled from the largest pores first and the water space becomes occupied by air. The suction required for removing water from the largest pores is known as bubbling pressure $(u_a - u_b)_b$ or air entry value ψ_b, and the area between zero suction and the air entry value is called the boundary effect zone. Beyond the air entry value, the increase of suction causes a rapid rate of water content loss until the residual water content, θ_r is reached. Suction corresponding to residual water content is referred to as residual suction ψ_b, at which the desaturation ends, and the water begins to be held in the soil by adsorption forces. The area between the air entry value and the suction in which the residual condition is reached is called the transition zone. In the residual zone, the curve exhibits an asymptotic line at a low degree of saturation. Water still exists but considerable suction is needed to expel even a small amount of water from the pores.

There is no a single or unique SWCC for a particular soil (Fredlund, 2000). Many variables can affect the shape of the SWCC such as soil type (Marinho, 2005; Miller et al., 2002; Tinjum et al., 1997), grain size distribution (Fredlund et al., 1997; Fredlund et al., 2002) and initial water content (Miller et al., 2002; Vanapalli et al., 1999). The shape of the SWCC is also affected by stress history and how the treatment is applied to the soil. The SWCC of natural soil exhibits a different shape of SWCC compared to remoulded soil, even that with the same density and water content (Ng and Pang, 2000). Extensive studies indicate a hysteresis phenomenon in the SWCC, where the curve resulting from drying differs to the results obtained from wetting (Poulovassilis A., 1962; Yang et al., 2004). The effect of temperature on suction has also been reported by Chahal (1965) and Wikinson and Klute (1962).

2.7.2 Mathematical models of SWCC

Obtaining SWCC's is a time-consuming, costly and complex procedure involving the sampling and preparation of laboratory specimens along with the installation, maintenance and monitoring of instruments (Lu and Likos, 2004; Agus, et al., 2010). Laboratory test data is sometimes insufficient to capture the variability of soil properties. To overcome this difficulty, some studies have been conducted to establish mathematical expressions for the SWCC, in order for the relationship between the SWCC and other soil parameters to be more easily understood.

Based on the nature of the SWCC, many mathematical expressions have been proposed to model the SWCC. Most of the models used saturated water content, high air entry suction and residual suction as the base parameters. SWCC modelling was first pioneered by such investigators in soil science as Gardner (1958), Brooks and Corey (1964), Farel and Larson (1972), van Genuchten (1980), William (1983), McKee and Bumb (1984). The models of Brooke and Corey (1964), van Genuchten (1980), and Fredlund and Xing (1997) are the most commonly used models in geotechnical applications (Lu and Likos, 2004) and these models are briefly explained in the following section.

Leong and Rahardjo (1997) in their review, deduced that all the relevant equations can be derived from the following generic form:

$$a_1\Theta^{b_1} + a_2 \exp(a_3\Theta^{b_1}) = a_4\psi^{b_2} + a_5 \exp\left(a_6\psi^{b_2}\right) + a_7 \qquad (2.30)$$

Where a_1, a_2, a_3, a_4, a_5, a_6, a_7, b_1, b_2 are constants, and Θ is normalized volumetric water content, i.e. $\Theta = (\theta - \theta_r)/(\theta_s - \theta_r)$.

It can be observed that the natural shape of the SWCC is commonly sigmoidal. However, not all SWCC models present in this condition. The curve resulting from the model can be sigmoidal or non-sigmoidal. The models proposed by van Genuchten (1980), McKee and Bumb (1987), and Fredlund and Xing (1994) produce a sigmoidal curve whereas the models proposed by Brooks and Corey (1964), Farel and Larson (1972), William et al. (1983) produce a non-sigmoidal curve.

Brooke and Corey (1964) proposed the equation for the SWCC as:

$$\theta = \theta_s \qquad for\ \psi \leq \psi_b$$
$$\theta = \theta_r + (\theta_s - \theta_r)\left(\frac{\psi_b}{\psi}\right)^{\lambda} \qquad for\ \psi > \psi_b \qquad (2.31)$$

where ψ_b is the air entry value, θ_r is the residual volumetric water content, θ_s is the saturated volumetric water content, and λ is the constant. It can be observed that equation (2.31) is obtained from equation (2.30) by making $a_2 = a_5 = a_7 = 0$, $b_1 = 1$, and $b_2 = \lambda$, and the curve resulting from this equation is non-sigmoidal.

Van Genuchten (1980) proposed the equation of the SWCC to be:

$$\theta = \frac{\theta_s}{\left[1+\left(\frac{\psi}{a}\right)^{n}\right]^{m}} \qquad (2.32)$$

where a, m, n are constants. It can be observed that this equation is obtained by making $a_2 = a_5 = 0$, $a_1 = a_7$, $a_4/a_1 = \alpha^n$, $b_1 = m$, $b_2 = n$ of equation (2.30) and it produces a sigmoidal curve. This model has been used for predicting the hydraulic conductivity of sandstone, silt loam and loam and clay, and it produces very reliable results.

Fredlund and Xing (1994) proposed a model based on an empirical approach and the assumption that soil consists of a set of randomly distributed interconnected pores. The model applies an entire range of soil suction from 0 to 1.000.000 kPa.

$$\theta = C(\psi)\frac{\theta_s}{\left\{ln\left[e+\left(\frac{\psi}{a}\right)^n\right]\right\}^m} \quad (2.33)$$

where a, m, n are constants that can be determined using a non-linear regression procedure. With the constant 'a', suction is greater than the air entry value corresponding to the inflection point on the curve. The constant n is the soil parameter relating to the slope of the SWCC at the inflection point. Constant m is the parameter relating to the results around the residual water content, and e is a 'natural' number, 2.71828...

C(ψ) is the correctional factor defined as:

$$C(\psi) = \left[1 - \frac{ln\left(1+\frac{\psi}{\psi_r}\right)}{ln\left(1+\frac{1{,}000{,}000}{\psi_r}\right)}\right] \quad (2.34)$$

The equation (2.34) is obtained from equation (2.33) by making $a_1 = a_5 = 0$, $a_3 = 1$, $a_7/a_1 = e$, $a_4/a_2 = (1/a)^{b2}$, $b_1 = m$, $b_2 = n$. This equation is recommended for use as it is deemed 'best fit' amongst the choice of equations.

2.7.3 Laboratory tests of SWCC

Various kinds of methods and devices can be used for obtaining the SWCC including a pressure plate, filter paper and tensiometer. Determining the most suitable device and method depends on the range of suction, material, purpose and the availability of devices. The pressure plate test is one of the most popular methods for SWCC testing with a range of suction from 0 to 1,500 kPa. For coarse-grained material such as sand with a lower matric suction (0 – 100 kPa), the tensiometer may be suitable, whereas for fine-grained soil with relatively higher suction, the filter paper method may be used.

The procedure of SWCC testing using a pressure plate is outlined in much of the literature (Agus et al., 2001; Anand J. Puppala et al., 2006; Khanzode et al., 2002; Leong and Rahardjo, 1996; Miller et al., 2002; Tinjum et al., 1997). Essentially, the test is performed by placing the saturated specimen onto the high air entry disk of a pressure plate. The desired pressure is then applied to the specimen, expelling some of the pore water through the burette. Once equilibrium is reached, the specimen is removed from the pressure plate and the weight of the sample is recorded. The

specimen is placed back onto the pressure plate and a higher pressure is applied. This procedure is repeated until the desired level of final suction is reached.

Two procedures of SWCC testing, using a tensiometer, can be employed; discrete drying and continuous drying (Lourenço et al., 2011). In the first procedure, matric suction is obtained by touching the surface of the high air entry in the tensiometer to the surface of the specimen. The weight of the specimen corresponding to the matric suction is then recorded. The specimen is then kept in contact with the free air for evaporation over a certain period of time. The specimen is then covered with a plastic sheet for suction equilibration within the specimen. The tensiometer is then placed onto the surface of the specimen for matric suction measurement. The procedure is then repeated for selected matric suctions. The continuous drying procedure is basically similar to the discrete method. However, the recording of the matric suction and the weight of the specimens is carried out continuously without covering with the plastic sheet.

Filter paper can also be used for the SWCC test. The filter paper is sandwiched between two specimens and left for 7-14 days for equilibration in a closed container. After equilibration, the water content of both filter paper and specimen is measured. Matric suction is calculated indirectly by using a provided calibration curve. The specimen is then kept in contact with the free air for evaporation for a certain period of time, and the procedure is repeated for selected matric suctions.

2.8 Unsaturated shear strength

Terzaghi (1943), proposed an effective stress theory for analysing the stress and strength of the soil. The theory was developed from the Mohr-Coulomb failure criterion with the assumption that the soil is in a saturated condition, where all the voids in the soil are occupied by water. The soil shear strength in saturated condition can be written as:

$$\tau_f = c' + (\sigma_n - u_w)tan\phi' \tag{2.35}$$

where τ_f is shear strength, c' is effective cohesion, σ_n is normal stress at failure plane, u_w is pore-water pressure, and ϕ' is effective angle of internal friction. The

term $(\sigma_n - u_w)$ is known as effective normal stress, and is sometimes denoted as $\sigma_n^{'}$. The theory became very popular and widely accepted in the soil mechanics area.

When soil is in an unsaturated condition, some or all of the soil voids are occupied by air. As a consequence the concept of effective stress is no longer applicable. A study was conducted to find soil strength in an unsaturated condition. Donald (1957) is considered to be the first investigator who conducted a laboratory study dealing with the effects of matric suction on unsaturated soil shear strength (Vanapalli and Lacasse, 2010). He performed a series of shear strength tests on unsaturated sand using a modified direct shear apparatus for controlling the matric suction during the test. Even though the shear strength behaviour of unsaturated soil was understood, no new mathematical expression to relate matric suction and shear strength had been reported until Bishop (1959) proposed the equation of unsaturated soil strength. He introduced a parameter, χ into Terzaghi's effective shear strength equation:

$$\tau_f = c' + [(\sigma_n - u_a) + \chi(u_a - u_w)]tan\phi' \quad (2.36)$$

where τ_f is shear strength, σ_n is normal stress, u_a is pore air pressure, $(u_a - u_w)$ is matric suction, and χ is a parameter between 0 and 1 as a function of degree of saturation (0 for dry soil, and 1 for fully saturated soil). It can be observed that equation (2.35) from Terzaghi is a particular case of equation (2.36) when pore air pressure is zero and χ is 1.

Fredlund et.al (1978) proposed another unsaturated soil strength test using two independent state stress variables $(\sigma_n - u_a)$and $(u_a - u_w)$. The equation can be written as:

$$\tau_f = [c' + (\sigma_n - u_a)tan\phi'] + \left[(u_a - u_w)tan\phi^b\right] \quad (2.37)$$

where $(\sigma_n - u_a)$ is net normal stress, ϕ^b is the angle indicating the rate of change in shearing strength due to the contribution of matric suction. The equation (2.37) can be represented in a three dimensional graphical expression as a planar surface of the failure envelope, showing that both ϕ' and ϕ^b are constant. In other words, the increase in strength as a contribution of net normal stress is characterised by ϕ', and the increase in shear strength as a contribution of matric suction is characterised by ϕ^b. The failure envelope is an idealisation as an extension form from the two-

dimensional Mohr-Coulomb failure criterion with matric suction as the third axis (Figure 2.8).

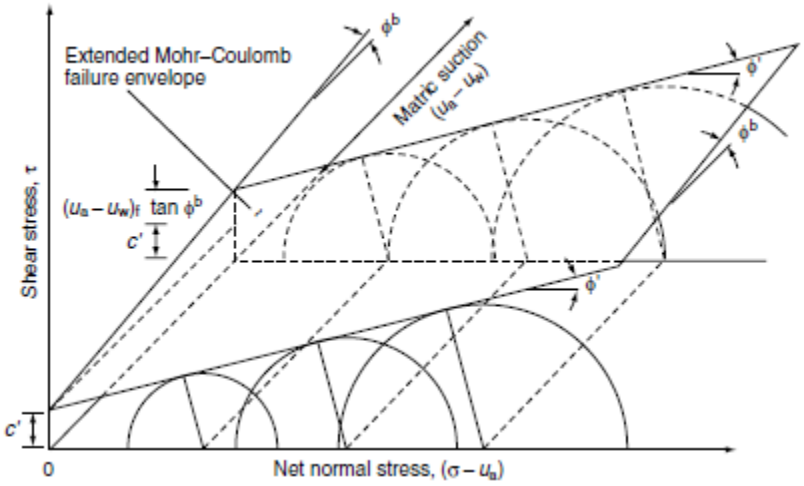

Figure 2.8 The idealisation of failure surface from extended Mohr-Coulomb failure criterion (Fredlund and Rahardjo, 1993)

The effect of matric suction on shear strength can be presented by a failure envelope curve in a two-dimensional diagram. The curve is divided into two regimes; linear and non-linear as shown in Figure 2.9 and as suggested by Vanapalli and Lacasse (2010). At low matric suction (zero suction until air entry suction), the soil remains saturated and the parameter of ϕ^b is a linear function of matric suction. The effect of pore-water pressure and total normal stress are characterised by the effective internal friction angle, ϕ'. Beyond the air entry suction, the parameter ϕ^b is changing non-linearly as matric suction is increasing. In other words, the value of ϕ^b varies from very close to ϕ' in the saturated condition, to less than ϕ', zero and even negative for very high matric suction depending on the type of soil. In particular, with soil at a very low matric suction, the value of ϕ^b can be higher than ϕ'. The study carried out by Likos at al. (2010) on sand using controlled direct shear apparatus at matric suction and stress less than 10 kPa indicates that $\phi^b > \phi'$. He described that this phenomenon may come from the effects of dilation on strength development.

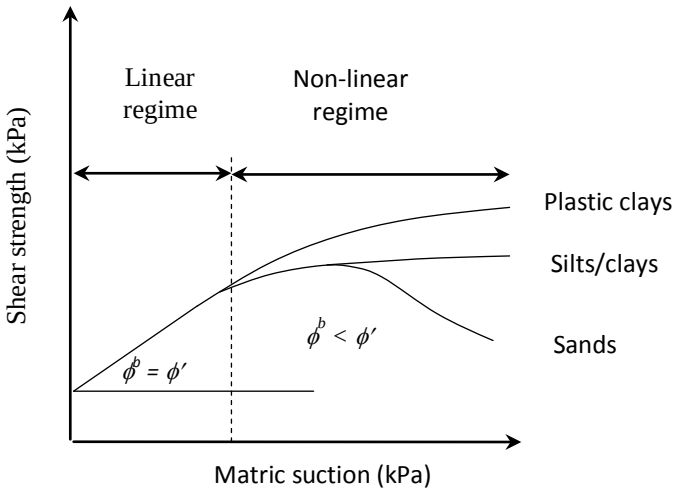

Figure 2.9 Non-linearity of shear strength versus matric suction (modified from Vanapalli and Lacasse (2010))

2.9 Laboratory strength tests of unsaturated soil

One of the mechanical properties of unsaturated soil is strength. The strength parameter can be obtained from shear strength tests such as the triaxial test, direct shear and unconfined compression tests. For sub-grade material, a very common strength parameter is the California Bearing Ratio (CBR). In this section, shear strength and CBR tests with matric suction measurements are presented.

2.9.1 Direct shear test with suction measurement

There are two types of unsaturated direct shear tests; suction-controlled and suction-monitored types. The first type is carried out by applying the desired matric suction during the test, generally using the axis translation technique. Matric suction is developed by directly controlling pore air and pore water pressure. This type of test was pioneered by Donald (1956), and the suction-controlled type is the most common unsaturated direct shear test. The second type is the suction-monitored direct shear test. In this test, the matric suction is not controlled. Rather it is monitored by using tensiometer(s) attached to the shear box (for example,Tarantino and Tombolato, 2005; Jotisankasa and Mairaing, 2010). Figures 2.10 and 2.11 show a schematic diagram of suction-controlled and suction-monitored direct shear tests respectively. Even though the capacity of a tensiometer is very low (< 90 kPa),

suction-controlled direct shear is suitable for material with a low air entry value such as sand. The literature on the suction-monitored direct shear test is still very limited and requires further study.

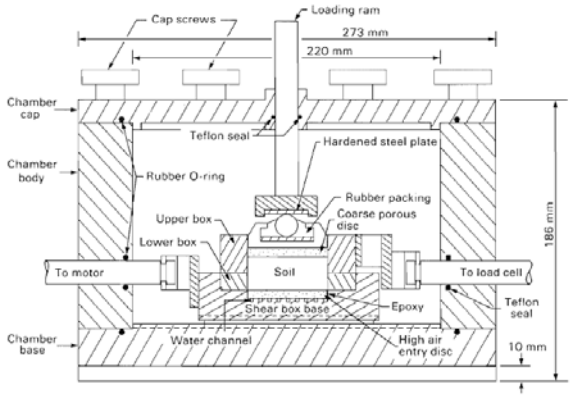

Figure 2.10 Schematic diagram of suction-controlled direct shear test (Gan J.K.M. et al., 1988)

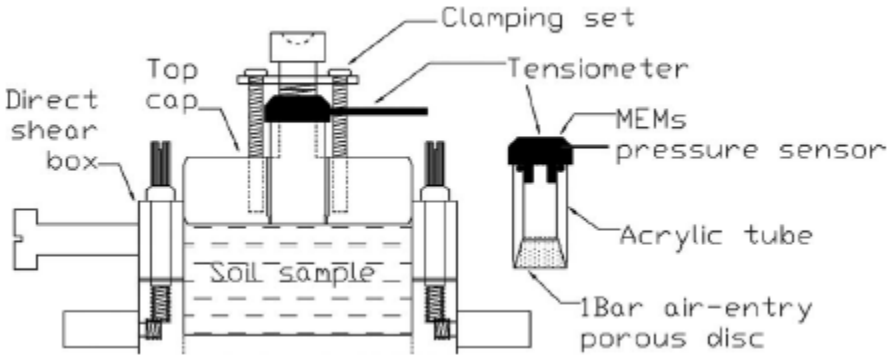

Figure 2.11 Schematic diagram of suction-monitored direct shear test developed by Jotisankasa and Mairaing (2010)

2.9.2 CBR test with suction measurement

The CBR has been widely used since the 1920's as a semi-empirical approach for predicting the bearing capacity of sub-grade for flexible pavement design. This method is relatively simple and low cost. The test is performed by penetrating a plunger with a constant penetration rate of 1.27 in/min into the compacted specimen on a rigid mould as described in ASTM D 1883-07. Essentially there are two types of CBR test associated with the treatment of the sample: soaked and unsoaked. The

unsoaked CBR test is performed to simulate natural conditions, whereas the soaked test is performed to replicate unfavourable and undesirable conditions in the field such as a high water table.

A remarkable study on CBR, using a relatively wide variation of soils from heavy clay to sandy gravel was conducted by Davis (1946). He presented the relationship of CBR to water content and dry density in a semi-logarithmic diagram, showing that the log value of the CBR was affected by water content, dry density and the structure of soil particles. As the water content increased, the CBR value went down linearly for plastic soil, whereas for non-plastic soils the relationship was non-linear. The non-plastic soil exhibited an increase in CBR with initial water content, and the CBR decreased as the water content increased. This non-linearity was believed to be the effect of compaction on the structure of the soil. The measurement of matric suction was not performed during his test.

Black (1962) may be the first investigator who utilised matric suction of a particular soil to estimate the CBR value. Firstly, he used the soil plasticity of cohesive soil and its moisture content to predict soil suction and the true angle of friction. The bearing capacity was then calculated using the predicted suction and the true angle of friction. Finally, the CBR was estimated using the calculated bearing capacity. It can be observed that the use of soil suction-with water content appeared impractical and that the true angle of friction-plasticity index curves appeared complex. The measurement of matric suction during the test was also not performed.

The use of the bearing capacity test to predict the CBR was also studied by Paraire (1987). The matric suction obtained in unsaturated conditions during the test was generated using a suction plate apparatus, while the water content was also measured. The bearing capacity test was conducted using a small cone with an angle of 30^{o} and a diameter of 2.03 cm to penetrate the surface of specimens of silt and quartz sand with similar dimensions to the CBR mould. The CBR was then indirectly predicted using the wide range of data on suction-bearing capacity. In this test, the sample was simply placed on the suction plate without using the CBR mould in order not to simulate the actual CBR laboratory test.

The non-linearity of the CBR with respect to matric suction was also the result obtained from the study carried out by Sivakumar and Tan (2002). They investigated

the effects of compacted water content on the CBR of tills, while the matric suction was taken into consideration using a pressure plate. The effect of matric suction was presented indirectly by the water content of the specimen. The result indicated that water content has a significant effect on the CBR. The rate increase in the CBR on the wet side of optimum water content was lower than that on the dry side.

Ampadu (2007) carried out a study on CBR affected by the matric suction of a decomposed granite specimen. Matric suction was obtained indirectly from the SWCC using the filter paper method. In this study, he focused on the effect of the drying and wetting of remoulded specimens on the CBR. The results indicated that as the water content decreased from OMC, the CBR tended to increase rapidly. Beyond the OMC, the CBR would then drop as the water content increased due to the soaking of the specimens.

The aforementioned studies indicate that the effect of matric suction on the specimen during the test was determined indirectly. More investigations regarding the effect of matric suction on CBR are still required. The study using the CBR test with direct suction measurement might prove to be a promising method in the future.

2.10 Summary

1. Soil suction consists of two components; matric and osmotic suction. In most geotechnical problems, the effect of matric suction on soil behaviour is more significant than the effect of osmotic suction.
2. For unsaturated geotechnical analyses, two stress state variables are used; namely net normal stress $(\sigma - u_a)$ and matric suction $(u_a - u_w)$.
3. Soil suction measurement can be grouped into direct and indirect methods. The determination of the most suitable method depends on the range of suction, material, purpose and the availability of devices.
4. The soil-water characteristic curve (SWCC) is essential in unsaturated soil analysis. For this purpose, some mathematical models of SWCC have been proposed.
5. Two types of unsaturated direct shear test are used in practice; suction-controlled and suction-monitored direct shear. The latter type is still very rare in literature and requires further study.

6. Most of the previous studies on the CBR used the indirect suction measurement. Further studies on CBR with direct suction measurement are required.

CHAPTER 3
SAND-KAOLIN CLAY MIXTURE

3.1 Introduction

It is well recognised that the physical and engineering properties of soil are closely related to its particle size distribution. The latest studies indicate that the properties of soil are not solely affected by grain size, but also by the presence of clay minerals and their atomic structure. Some clay minerals exhibit low water absorption/adsorption and low shrinkage/swelling capacity, whilst other clay minerals may possess properties in the reverse. The knowledge of clay minerals is fundamental to an understanding of the properties of soil.

In this section, a brief review of the properties of sand and clay minerals will be presented. It includes the physical/chemical and engineering properties of those materials. An additional review with a particular focus on clay mineralogy will also be presented. The literature concerning clay minerals in this section is mostly obtained from Grim (1962 a), Murray (1991), and a comprehensive study from Grim (1962 b) concerning clay mineralogy. At the end of this chapter, previous and more recent studies on sand-clay mixtures and their properties will be presented.

3.2 The properties of sand

Sand is formed from the mechanical weathering of rock-forming minerals such as quartz, feldspar, mica, calcite, dolomite. The influence of molecular attractions and electrical charges of sand is very small so that particles can easily occupy soil voids (Soos and Bohac, 2002). The most important physical characteristic of sand is particle size distribution. According to ASTM D 422 (2007), sand is categorised as coarse material with a grain size of between 0.075 mm and 4.75 mm (particles through passing a # 4 sieve and retained in a # 200 sieve). Furthermore, sand can be divided into three groups: coarse, medium and fine sand. Coarse sand has a particle size of between 2 mm and 4.75 mm (passing through a # 4 sieve and retained in a # 10 sieve). Medium sand has a particle size of between 0.425 mm and 2 mm (passing through a # 10 sieve and retained in a # 40 sieve). Fine sand has a particle size of

between 0.075 mm and 0.425 mm (passing through a # 40 sieve and retained in a # 200 sieve).

In terms of strength and compressibilty, sand has relatively beneficial engineering properties compared to clay. It has high internal friction, low compressibility, non-plasticity, low swell-shrinkage potential, and in general, the behaviour of sand is rarely affected by water content. A small amount of cohesion may be generated through the capillary tension among the particles, due to the presence of water. The increase in moisture content, to some extent, can cause this increase in cohesion. With the increment of moisture, cohesion also increases significantly. However, when the moisture content reaches a certain value, cohesion will decrease and even disappear when a saturated condition is reached (Wu and Sun, 2008).

The engineering properties of sand are mainly influenced by particle size, gradation and particle shape. Other influencing factors are density, particle arrangement and isotrophy (Mitchell and Soga, 2005). Poorly graded sand tends to have a narrower range of density compared to well-graded sand. Particle size distribution can also affect the properties of sand. The increase in the range of particle size (increase in the coefficient of uniformity, *Cu*) causes a decrease in void ratio. For example, the presence of smaller particles such as silt may affect the properties of sand. Silt particles occupy the voids between larger sand particles, causing a decrease in void ratio. However, an excessive quantity of silt would cause an increase in void ratio. In this situation, the sand particles float inside the silt matrix.

The shape of the particles also strongly influence the engineering properties of sand. The shape can be angular, sub angular, rounded or semi-rounded. The compaction result of sand containing angular particles tends to be less dense when compared to sand with rounded particles. For ideal uniform-size spherical particles, Mitchell and Soga (2005) proposed five different possible packing arrangements. The packing can be (a) simple cubic, (b) cubic tetrahedral, (c) tetragonal sphenoidal, (d) pyramidal, and (e) tetrahedral, as illustrated in Figure 3.1. Simple cubic packing has the loosest stability and highest void ratio of 0.91, whereas tetrahedral packing has the densest arrangement and the lowest void ratio of 0.34.

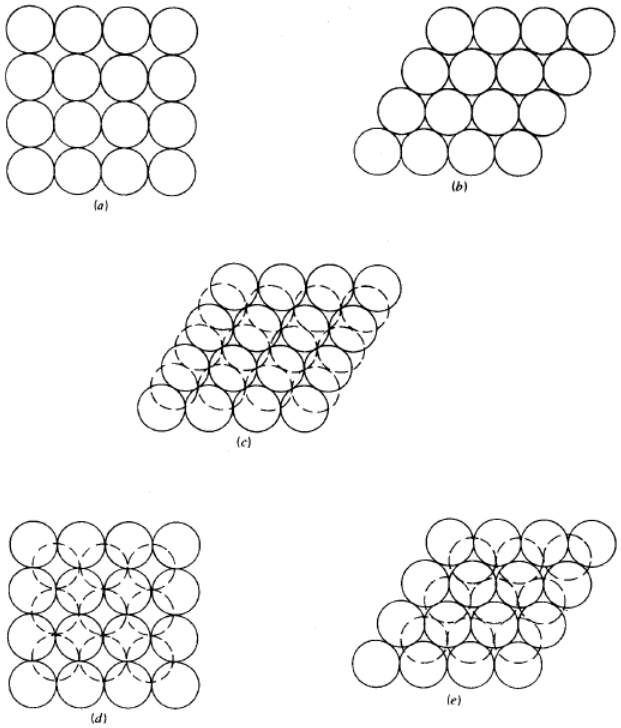

Figure 3.1 Different packing arrangement for ideal uniform size spherical particles (Mitchell and Soga, 2005)

In reality, the structure of granular soil is not composed of single size particles, rather it may contain different sizes of particles, different particle groups, and different couplings of particle groups. Some structures can be seen visually by the naked eye (macrostructure) and some other structures can only be seen using a microscope (microstructure). They may form single grains (loose or dense) or honeycombed structures (Holtz and Kovacs, 1981). Figure 3.2 shows the illustration of loose single grain structures (a), dense single grains (b), and honeycombed structures (c). The dense single grain can result from a static or vibrating compaction of a loose single grain. The honeycombed structure can support the static load, but due to a very high ratio, it is very sensitive to collapse when a vibrating load is applied. This engineering properties of the honeycombed structure are also vulnerable to change with the presence of water.

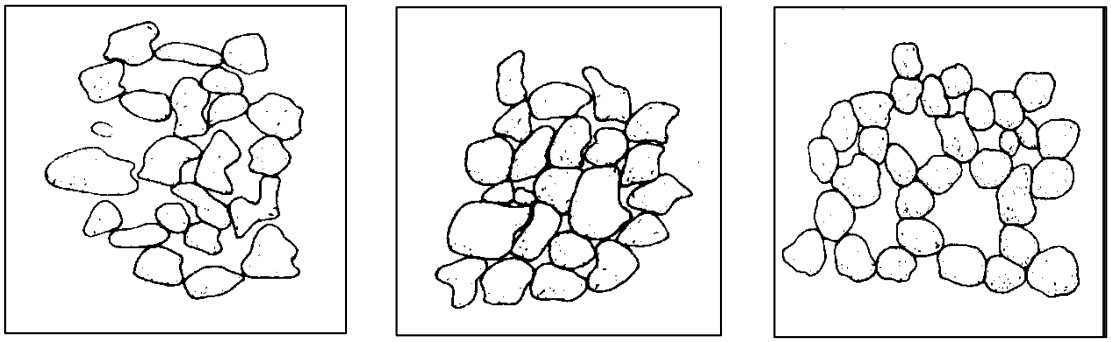

(a) (b) (c)

Figure 3.2 The structure of granular soil of (a) loose single grain, (b) dense single grain, and (c) honeycomb (Holtz and Kovacs, 1981)

3.3 The properties of kaolin clay

Kaolin clay is a versatile material that has a wide range of uses. Murray (1991) summarised kaolin clay's uses in various industries such as in: ceramic raw material, cement, fibreglass, paint extender, paper filling/coating, filler in rubber, filler in plastic, as a catalyst, in foundries, desiccants, pencil leads, adhesive, tanning leather, pharmaceuticals, enamels, pastes and glues, insecticides, medicine, sizing, textiles, food additives, bleaching, fertilizer, plaster, filter aids, cosmetics, crayons, detergent, roofing granules, linoleum, polishing and compounds. In geotechnical engineering, kaolin clay has been used for slope stabilisation and erosion protection (Jotisankasa et al., 2012) and as a barrier for waste disposal facility.

The extensive use of kaolin clay is due to its unique properties. The properties of clay-size material are not only dependent on its particle size, but also on its mineralogy. The presence of clay-size minerals in the soil can markedly affect the engineering properties of that soil. In the following section, a brief review on the mineralogy of clay (with the emphasis on kaolin clay) will be presented.

3.3.1 Particle size and shape

According to ASTM D 422 (2007), clay is defined as a material with a particle size of less than 0.005 mm. Australian Standard AS 1726 (1993) and British Standard BS 1377 specify that the size of a clay particle must be less than 0.002 mm. The shape of a clay particle is not equidimensional like gravel or sand, rather it is formed as a

needle-like, plate-like or flake-type crystal. The range of particle sizes of clay is very wide. Kaolin clay forms a platy crystal with the length of particle being 0.2 μm to 2 μm with a thickness of 0.05 μm to 0.2 μm. The needle-like structure of attapulgite has 2 μm length with a thickness of 0.1 μm. The platy crystal form of montmorillonite has 0.1 μm to 1 μm length with the thickness of 0.01 μm. Figure 3.3 shows an illustration of the particle size of kaolin, attapulgite and montmorillonite. Amongst other clay minerals, kaolin is a mineral with the largest particle size.

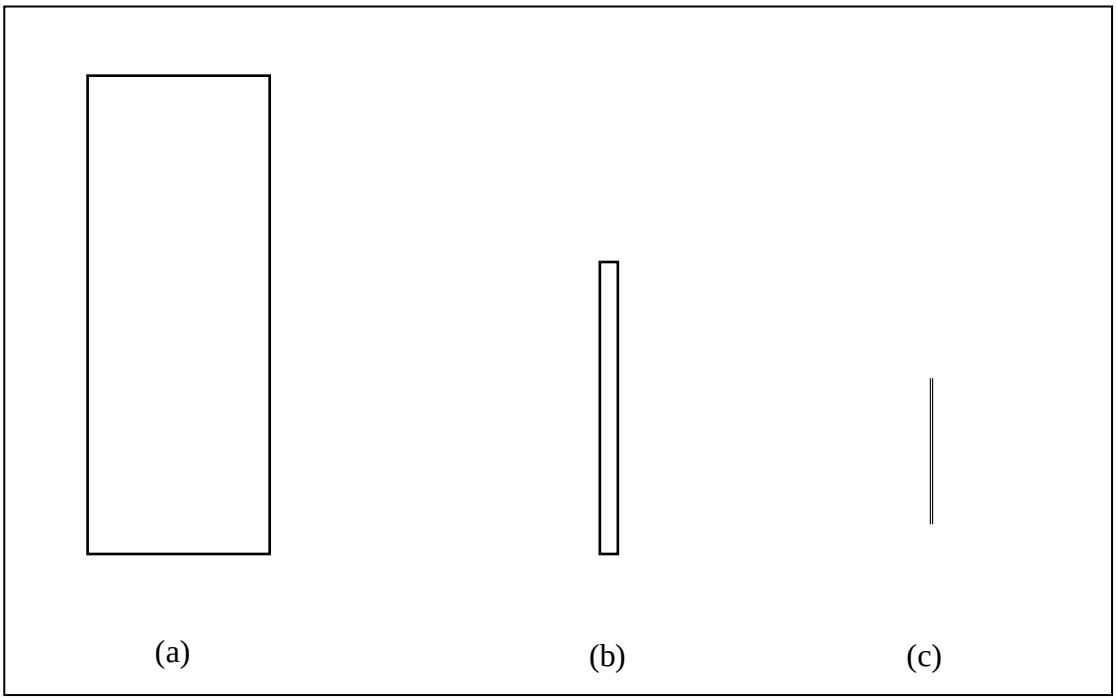

Figure 3.3 Illustration of particle size of (a) kaolin, (b) attapulgite and (c) montmorillonite

3.3.2 Mineralogy of clay

In general, clay minerals are formed in nature by a physical and mechanical alteration or a weathering process of primary minerals (Mackenzie and Mitchell, 1966). Clay minerals are tetrahedral and may comprise alumina, silica and water and sometimes iron or magnesium or both. They also may contain non-clay mineral particles such as quartz and calcite. The flakes may consist of many crystal sheets, staked together with different types of bonding. Silica tetrahedral molecules consist of a single atom of silicon, surrounded by four oxygens at the corner. This combination of silica tetrahedral forms tetrahedral sheets. An octahedral unit consists of an atom of aluminium, magnesium, iron or other atom, surrounded by six oxygens

or hydroxyls. This combination of octahedral units forms octahedral sheets. There are at least three physical properties attributed to clay minerals; atomic structure, cation exchange capacity, and specific surface.

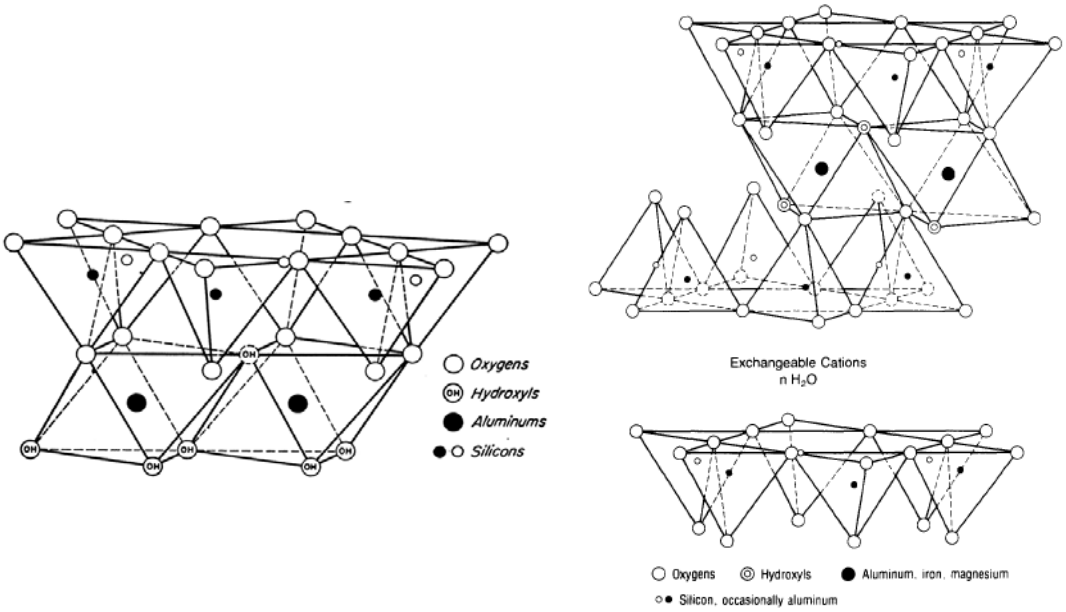

(a) (b)

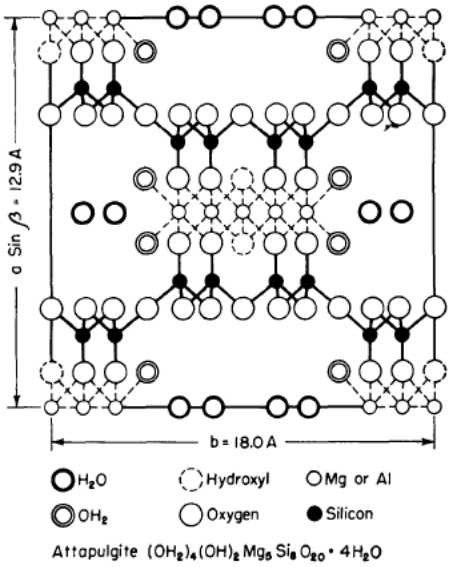

(c)

Figure 3.4 Atomic structure of clay mineral (Grim (1962 a) and Murray (1991): (a) Two layered structure of kaolinite, (b) three layered structure of smectite, and (c) fibrous structure of attapulgite

There are three general structures of clay mineral; two-layered, three-layered and fibrous. The clay mineral with a two-layered structure consists of a sheet of silica tetrahedral and a sheet of alumina octahedral. Both sheets are tied together in a common sheet with shared oxygens and hydroxyls. Kaolinite, halloysite, dickite and nacrite are examples of two-layered structures of clay mineral. The three-layered clay mineral has two silica tetrahedral sheets and a sheet of central octahedral. Smectite, montmorillonite, and vermiculite are examples of three-layered structures of clay mineral. Smectites are very thin flakes with a very small particle size, which gives a high surface area, and consequently, a high degree of absorbency. Smectite minerals are dominant in bentonite. The third structure of clay mineral is fibrous. It consists of ribbon-like sheets of silica tetrahedral units tied together by a central octahedral unit through common oxygens. Attapulgite is an example of fibrous material. Figure 3.4 shows a typical atomic structure of a clay mineral.

Another fundamental characteristic of clay is cation exchange capacity. This is defined as the ability of clay to absorb certain cations around the outside of the silica-alumina structural unit. The different engineering properties among soils are due to this physical property, and generally capacity increases as particle size decreases. Cation exchange capacity is measured in milliequivalents per 100 grams. Common exchangeable cations are calcium, magnesium, hydrogen, potassium, ammonium, and sodium. Table 3.1 shows a list of cation exchange capacity of clay minerals.

Another property of clay minerals is specific surface area; that is surface area per unit of mass or volume. The adsorption of molecules, swelling potential, water retention capacity, and cation exchange capacity are related to a specific surface area. The specific surface area is inversely proportional to grain size; the smaller the particle size, the higher the specific surface area.

Table 3.1 shows the physical properties of some clay minerals.

Kaolin clay is categorised as a silicate mineral. Kaolinite clay is one of the minerals in the kaolin group including haloysite, dickite, and nacrite. Theoretically, the main components of kaolinite are alumina (Al_2O_3), 39.8%, silica (SiO_2), 46.3% and water, 13.9%. Kaolinite clay consists of alternating layers of one silica tetrahedral sheet and one alumina octahedral (or gibbsite) sheet tied with oxygens and hydroxyls. The common molecule formula for kaolinite is $Al_2Si_2O_5(OH_4)$. Table 3.2 shows the

typical results from chemical analyses of different sources of kaolinite clay from Georgia, England, along with from Unimin Pty Ltd, Australia.

Table 3.1 Physical properties and characteristics of certain clay minerals (modified from Grim (1962 b) and Das (2008)

Mineral	Atomic Structure	Cation exchange capacity (meq/100 g)	Specific surface (m^2/g)
Kaolinite	two-layer	3 -15	10 - 20
Halloysite	two-layer	5 - 40	12 - 40
Montmorillonite	three layer	80 – 150	800
Illite	three-layer	10 - 40	80 - 100
Vermiculite	three-layer	100 - 150	5 - 400
Chlorite	three layer	10 - 40	5 - 50
Sepiolite-Attapulgite	Fibrous	20 -30	

Relative to other minerals, kaolinite particles have a small surface area and a very low cation exchange capacity, and as a consequence, kaolin clay is classified as inactive clay (< 0.5). Results from studies carried out on various sources of clay minerals indicate that kaolinite clay, relatively, has the lowest plasticity index, the lowest adsorption capacity, and the lowest swelling potential.

Table 3.2 Typical chemical analysis of kaolin clay

Component (%)	Georgia [1)]	England [1)]	Unimin Australia batch 1 [2)]	Unimin Australia batch 2 [2)]
SiO_2	45.3	46.77	49.2	49.1
Al_2O_3	38.38	37.79	39.4	39.2
Fe_2O_3	0.3	0.56	1.01	1.01
TiO_2	1.44	0.02	0.935	0.932
MgO	0.25	0.24	0.358	0.366
CaO	0.05	0.13	0.51	0.506
Na_2O	0.27	0.05	< DL	< DL
K_2O	0.04	1.49	0.18	0.178

1) After Murray (1991)
2) After Shankar et al. (2010)

3.3.3 Physical and engineering properties

According to Grim (1962 b), kaolin clay is formed mainly by decomposition from the chemical weathering of feldspars, granite, and aluminium silicates.

There are some physical and engineering properties attributable to kaolin clay and clay-size minerals in general; particle size, plasticity, activity, strength, permeability, water absorption and swelling/shrinkage potential.

Plasticity may be defined as the ability of a material to be deformed under stress without cracking, and the shape remains unchanged when the stress is removed. The plasticity of clay minerals is developed when a certain amount of water is added to them. In geotechnical engineering, plasticity is commonly referred to as the liquid limit (LL), plastic limit (PL), and plasticity index (PI). The plasticity index of the soil is strongly related to the specific surface area of particles. The smaller the particle size, the higher the specific surface area, the higher the plasticity index. The wide range of plasticity of kaolin clay is due to the different chemical components of kaolin clay.

Fine grained material may contain only plastic material such as clay, or non-plastic material such as silt or clay and silt mixture. Accordingly, fine grained material can be plastic or non-plastic. The plasticity of fine grained material is strongly affected by the quantity of clay or silt. Skempton (1953) proposed an important parameter, namely Activity (A) for the identification of fine grained material. According to Skempton (1953), Activity (A) is defined as the ratio of plasticity index (PI) to the amount by weight of clay friction finer than 2μ , and can be written as:

$$A = \frac{PI}{clay\ friction < 2\ \mu} \tag{3.1}$$

Skempton (1953) suggested 5 classes of activity of the soil as shown in Table 3.3.

Table 3.3 Soil activity group (Skempton, 1953)

Group	Value	Activity
1	< 0.5	Inactive
2	0.5 – 0.75	Inactive
3	0.75 – 1.25	Normal
4	1.25 - 2	Active
5	> 2	Active

Table 3.4 shows the liquid limit, plastic limit, plasticity index and activity of kaolin clay and two other clay minerals of montmorillonite and Attapulgite. It can be seen

from the table that compared to other clay minerals, kaolin clay has the lowest plasticity and activity.

Table 3.4 Plasticity and activity of kaolinite clay, montmorillonite and attapulgite (Grim, 1962 b)

Engineering properties	Clay mineral		
	Kaolinite	Montmorillonite	Attapulgite
Liquid limit	29 - 113	123 - 700	158 - 232
Plastic limit	26 - 38	51 - 97	97 - 124
PI	1 - 41	34 - 603	57 - 123
Activity	0.01 -0.41	0.32 – 7.09	0.57 – 1.23

Active clay has a high water holding capacity, high compaction under load, high cation exchange capacity, low permeability, and low shear resistance. Therefore, very active soils can be problematic for engineers (1962 b). The presence of certain types of clay mineral in the soil affect its engineering properties. Soil with a high activity has high swelling when wetted and high shrinkage when dried. Activity can also be used for predicting the amount of clay fraction in the soil and is a very useful indicator for predicting the swelling/shrinkage potential of soil. Conversely, inactive soils may not cause problems for engineers, as it has little cohesion. The strength of inactive soil is mainly caused by internal friction.

The activity of kaolin clay is relatively low and the lowest compared to other clay minerals (see Table 3.1). According to a soil activity group defined by Skempton (1953), kaolin clay is categorised as inactive clay.

Another engineering property of clay materials is strength; the ability of materials to withstand external shearing forces. Common laboratory tests for such properties are the unconfined compression strength test, direct shear, or triaxial test. The composition of minerals, particle size distribution and water content (amongst other factors) are controlling factors in shear strength. Different clay minerals have different strengths.

Permeability is affected by mineral composition, particle size distribution, texture, void ratio, exchangeable cation composition, characteristics of fluid, and the degree of saturation (Grim, 1962 b). In general, permeability decreases when particle size

decreases. It would be expected that the permeability of a flake shaped mineral is less than that of granular shaped material.

An additional engineering property of clay materials is water adsorption ability. Studies indicate that some clay minerals have a very high water adsorption capacity such as Na montmorillonite (> 800% within 1000 minutes), attapulgite (± 200 %), Ca montmorillonite (± 240 %), poorly ordered illite (160 %), kaolinite (80 -140 %). Water adsorption ability also leads to swelling. The higher the water adsorption capacity, the higher the swelling potential.

3.4 The mixture of sand-kaolin clay

3.4.1 The properties of sand-kaolin clay mixture

In general, the engineering properties of sand are relatively sound. In terms of strength, it has a relatively high internal friction, and accordingly has a relatively high shear strength and high bearing capacity. In term of compressibility, sand has very low swell/shrinkage potential and is categorised as a non-plastic material. Another property of sand is that it has high permeability. The most important property of sand is that its behaviour is relatively unaffected by water content. One disadvantage of sand is that it has relatively low cohesion.

In contrast to sand, kaolin clay is a fine-grained material. The engineering properties of this clay are strongly affected by water content. In terms of strength, clay has very high shear strength when it contains very little water, but very weak shear strength when water content is high. The lower the water content, the higher the strength. In terms of compressibility, clay has high compressibility, high plasticity and high swell/shrinkage potential. In general, problems in geotechnical engineering are due to the presence of clay in the soil.

The shortcomings of sand or clay can be overcome by mixing both materials in certain porportions. The inclusion of kaolin clay in sand and vice versa can produce a new material with new properties. The cohesionless properties of sand can be improved to some extent by the addition of kaolin clay. The presence of kaolin clay amongst sand particles will produce a new material with improved properties. In the

same way, the lack of internal friction in kaolin clay can be improved to some extent by the addition of sand.

3.4.2 Recent studies on sand-kaolin clay mixture

Mullin and Panayiotopolous (1984a) studied the effects of kaolin clay content in a sand-kaolin clay mixture on the void ratio. They used two sets of narrowly-graded fine sand and coarsed-fine sand mixed with the different proportions of kaolin clay. Water was added to the mixture to create a saturated condition. The mixtures were compacted using a static load of 1.5 MPa. The results indicated that for narrowly graded fine sand, an increase in kaolin clay content led to a decreased void ratio. However, for coarsed-fine sand, the increase in kaolin clay to some extent led to a decrease in void ratio. After reaching a certain kaolin clay content, the increase in kaolin clay caused an increase in void ratio (Figure 3.5).

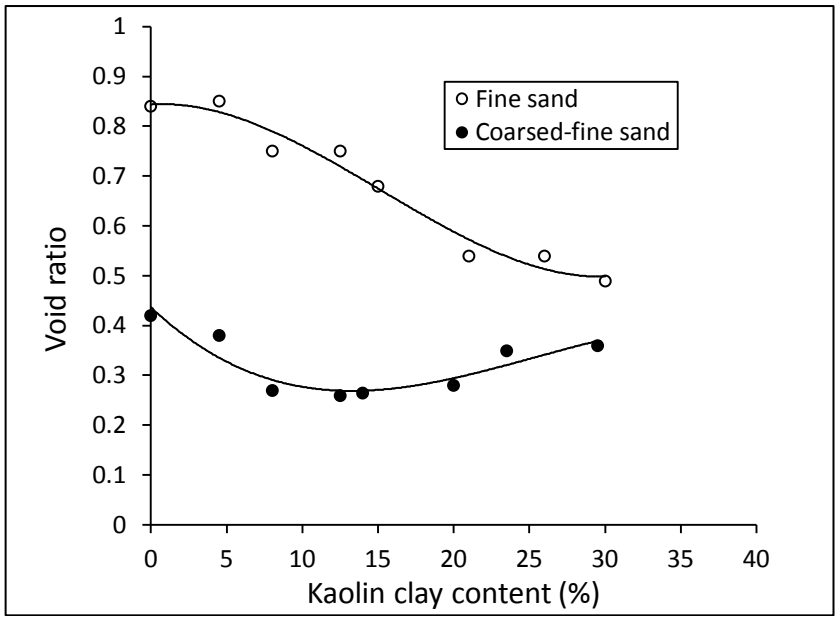

Figure 3.5 The influence of kaolin clay content on void ratio of sand-kaolin clay mixture. (Modified from Mullin and Panayiotopolous (1984a))

In addition to the study, Mullin and Panayiotopolous (1984b) also investigated the effect of kaolin clay content on the unconfined compression strength of different sand-kaolin clay mixtures of 0.5%, 2%, and 8% water content. The results indicated that with a certain water content, the increase in kaolin clay content led to an increase in strength. The results also showed that an increase in water content in the mixture caused a decrease in strength.

Sand-kaolin clay mixtures have also been studied by Chiu and Shackelford (1998). They used three different compacted sand-kaolin clay mixtures of 0%, 5%, 10% and 30% to investigate the effects of kaolin clay content on the hydraulic conductivity of the mixtures. Figures 3.6 and 3.7 show the effect of kaolin clay content on compaction characteristic and hydraulic conductivity of sand-kaolin clay mixtures respectively. It can be observed that the increase in kaolin clay content causes the increase in maximum dry density, decrease in optimum water content, and the increase in hydraulic conductivity.

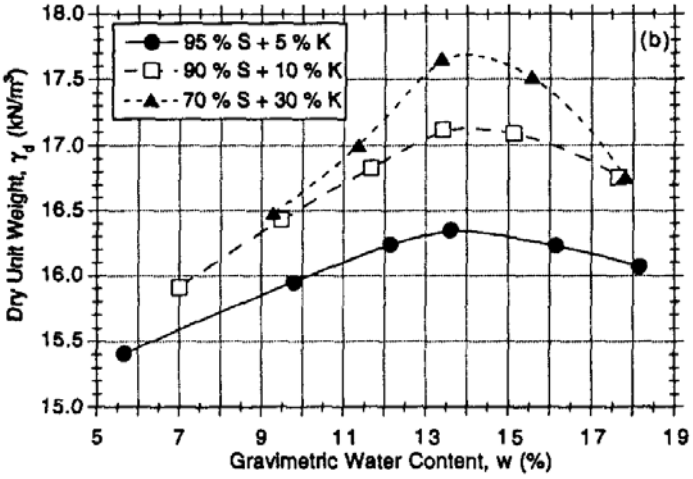

Figure 3.6 The effect of kaolin clay content on compaction characteristics of sand-kaolin clay mixtures (Chiu and Shackelford (1998))

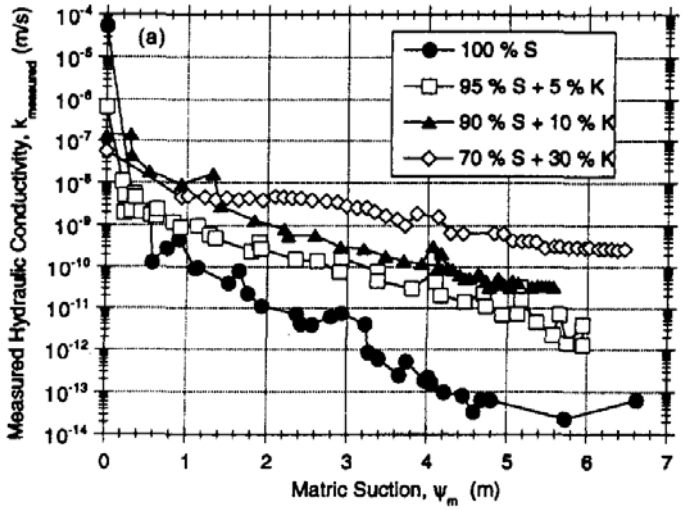

Figure 3.7 The effect of kaolin clay content on hydraulic conductivity of sand-kaolin clay mixtures (Chiu and Shackelford (1998))

There are some other studies concerning the engineering properties of sand-kaolin clay mixture, for example Frenkel and Levy (1992), Boutin (2011), Jigheh and Zare (2012). However, the information about this mixture is still very rare and more studies are required.

3.5 Summary

1. In term of strength and compressibilty, sand has relatively sound engineering properties; high internal friction, non-plasticity, low compressibility and low swell/shrinkage potantial. In general the behaviour of sand is minimally affected by water content. However, the cohesion qualities of sand are relatively low.
2. The properties of kaolin clay are strongly affected by water content. It has a very high shear strength at low water content but is very weak with a high water content.
3. The compressibility, plasticity and swell/shrinkage potential of kaolin clay is very high. In general, the the presence of clay in the soil causes problems in geotechnical engineering.
4. The inclusion of kaolin clay into sand and vice-versa can produce a new material with more sound engineering properties.

CHAPTER 4
EXPERIMENTAL PROGRAM

4.1 Introduction

This chapter describes the experimental program of the study. The background of material selection, specimen preparation, index properties, unsaturated shear strength tests along with matric suction measurements during the test, and testing standards/procedures are presented. The main laboratory work in the experimental program consisted of direct shear and CBR tests for obtaining the strength behaviour of sub-grade material in unsaturated conditions. The chapter then describes the SWCC test procedures using the filter paper method and tensiometer. The description of the use of tensiometer is highlighted in this chapter as it was the main apparatus used for matric suction measurement. In general, the experimental program consisted of a preliminary test, compaction, soil water characteristic curve (SWCC) test, and shear strength test using direct shear and CBR methods with suction measurement.

4.2 Materials selection

The original intention of this study was to investigate the engineering behaviour of unsaturated sub-grade material found in Western Australia, particularly in Perth. However the choice of materials shifted following preliminary studies, as described below.

A preliminary study was performed by taking random sub-grade material samples from four locations in Perth. The samples were identified as specimens A, B, C and D. An index properties test on the specimens indicated that according to ASTM D-2487, three specimens were classified as poorly graded sand (SP), and the fourth classified as poorly graded sand with clay (SP-SC). The quantity of sand particles of the specimens was around 95 % for the SP-SC and 99.7 % for the SP samples. The gradation curves and Atterberg limits of the specimens are shown in Figure 4.1 and Table 4.1.

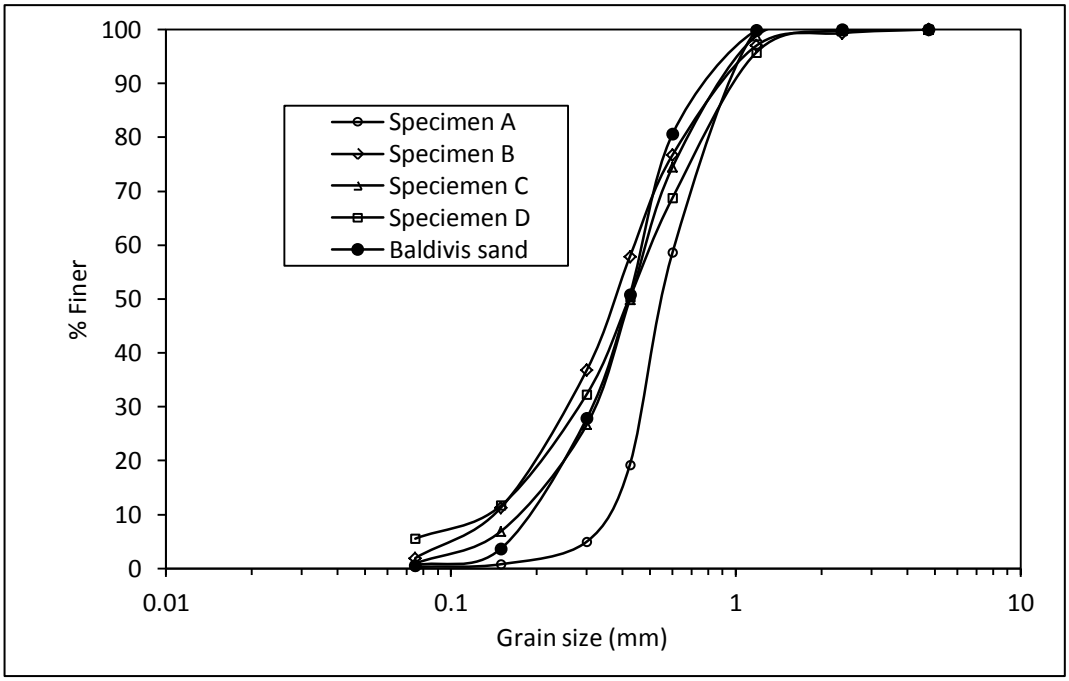

Figure 4.1 Gradation curves of different sub-grade soil of Perth

Table 4.1 Fraction, Atterberg limits, and classification of some sub-grade soils of Perth

Soil	Fraction				Atterberg limits			USCS Symbol
	Sand			Silt and clay	LL	PL	PI	
	Fine	Medium	Coarse					
Specimen A	18.93	80.76	0.00	0.32	NA	NA	NP	SP
Specimen B	55.92	41.48	0.68	1.93	NA	NA	NP	SP
Specimen C	48.99	49.87	0.22	0.93	NA	NA	NP	SP
Specimen D	44.83	49.50	0.15	5.53	19.1	13.8	5.3	SP-SC
Baldivis	50.24	49.17	0	0.26	NA	NA	NP	SP

It can be observed from the figures in the diagrams that the gradation curves of specimens A, B, and C are relatively similar but not identical. It was predicted that the engineering properties of those specimens would be completely identical, and therefore the laboratory tests on whole specimens with identical index properties were less useful. The curve of specimen A and D is slightly different from the others due to the large portion of medium size of sand and the presence of $\pm$ 5 % of fine grained material respectively. Based on the aforementioned reason, the scenario of the study then shifted toward artificially altered material. Attempts to find the appropriate material finally resulted in the choice of Baldivis sand and kaolin clay.

The Baldivis sand was obtained from the CEMEX Baldivis sand pit, Western Australia and the kaolin clay was an industrial product obtained from Unimin Australia Pty. The decision was made to use three different proportions of Baldivis sand and Unimin kaolin clay mixture. In this study, the sand-kaolin clay mixtures of 100:0, 95:5, and 90:10 were used.

4.3 Index properties of artificial specimens

The first step in classifying the artificial specimens was to order them according to the standards. For this purpose, index property tests were performed. These consisted of specific gravity and grain size analysis, along with an Atterberg limits tests. The tests were performed not only on Baldivis sand and kaolin clay, but also on sand-kaolin mixtures. For simplicity of handling and calculation, the sand and kaolin clay were oven dried for 24 hours at a temperature of 105^{o} C to obtain free-water specimens. The sand-kaolin mixture was then prepared according to the desired proportions, as described in section 4.2. These mixtures were then put in sealed plastic bags and placed in an air-tight plastic container.

The specific gravity test was performed on sand and kaolin clay separately according to method B (procedure for oven-dried specimens) of ASTM D 854-06. The specific gravity of different proportions of sand-kaolin clay mixtures were determined using the following equation:

$$Gs_b = \frac{P_1+P_2+\cdots.+P_n}{\frac{P_1}{Gs_1}+\frac{P_2}{Gs_2}+\cdots+\frac{P_n}{Gs_n}} \qquad (4.1)$$

where Gs_b is the bulk specific gravity of the new mixture. P_1, P_2, P_n are the percentages of material 1, 2, and n. Gs_1, Gs_2, and Gs_n are the specific gravity measures of materials 1, 2, and n.

Grain size analysis was conducted on the Baldivis sand using a series of standard sieves according to ASTM 422-63, with the grain size curve of kaolin clay being obtained from the vendor. The gradation curve of the sand-kaolin mixtures were simply obtained by combining the data of the grain size of the sand and the kaolin clay.

The degree of consistency or firmness was also included in the specimen identification and classification process. The consistency of specimens is commonly determined by Atterberg limits: liquid limit, plastic limit and plasticity index. Atterberg limits are the boundaries of water content at which the plasticity of specimen can be quantified. Atterberg limits have been used extensively as key parameters for the preliminary assessment of a soil. Liquid limit tests can be performed using the Casagrande method (ASTM D 4318) or fall cone method (British standard, BS – 1377). In this study, the fall cone test was used as it was considered to be relatively simple in practice compared to the Casagrande method. The plastic limit test was performed according to ASTM D 4318.

Another property of the specimens is activity (A). The activity is calculated using Equation (3.2), found in Chapter 3.

4.4 Soil compaction

Standard Proctor compaction tests were performed on the sand and the sand-kaolin mixtures to obtain their compaction characteristics (maximum dry density-MDD, optimum water content-OWC, and void ratio-e). Five to six bags of specimens weighing 2500g each were prepared. Different quantities of water were poured onto each specimen to obtain a water content interval of $\pm$ 3 % between each specimen. The mixed sand-kaolin clay-water was then stirred thoroughly and immediately placed in sealed plastic bags for curing. According to ASTM D 698, some of the soil required curing for a period of time to allow the water to permeate the entire specimen. SP, SW, GW, and GP soils did not require curing, whereas the GM and SM required 8 hours curing. With these exceptions the soil in general required curing for 16 hours before compaction. In this study, prior to compaction, a curing period of 72 hours was applied to all proportions of the sand-kaolin clay-water mixtures to ensure water equilibration of the mixtures.

After equilibration, the specimens were then compacted in a standard mould (4.0 in) according to ASTM D 698-07. The compaction was performed layer by layer for a total of three layers, at which 25 blows per layer were applied using a 5.5 lb. (2.5 kg) hammer falling from a height of 12 in (30.5 cm). After compaction, representative parts of the specimen were taken from the mould for the water content test.

4.5 Suction measurement

Suction measurement is one of the most important factors in unsaturated soil testing. There are two different methods of suction measurement: direct and indirect. In this study, the direct method using a tensiometer was employed for the SWCC and unsaturated strength tests, whereas the indirect method using filter paper was employed only for the SWCC test. The overview of both methods is described in the following section.

4.5.1 Tensiometer method

4.5.1.1 General

In this study, two different sizes of tensiometer were used, namely tensiometers KU-T1 and KU-T2. These tensiometers were developed by the GERD Centre, Department of Civil Engineering Kasetsart University (Jotisankasa, 2010). The tensiometers were able to measure pore water pressure from - 80 to 700 kPa. The dimension of tensiometer KU-T1 was $\pm$ 7 mm in diameter and $\pm$ 36.5 mm in length, whereas tensiometer KU-T2 was slightly larger with a $\pm$ 16 mm and $\pm$ 38 mm diameter and length respectively. The tensiometer consisted of a 1-bar air entry ceramic disk, a transparent acrylic water reservoir, and a pressure sensor. Due to their small size, tensiometers KU-T1 and KU-T2 are more like a miniature tensiometer. They are suitable for laboratory use, especially for low matric suction measurement. Figure 4.2 shows tensiometers KU-T1 (a) and KU-T2 (b).

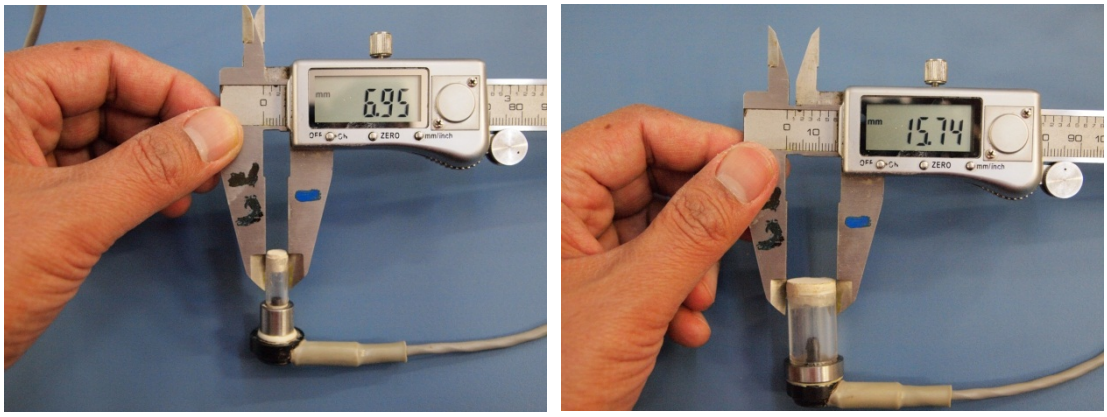

(a) (b)

Figure 4.2 (a) Tensiometer KU-T1 and (b) Tensiometer KU-T2

A tensiometer uses de-aired water as a medium for transferring the pore water pressure in the soil to the pressure sensor. The use of a transparent water reservoir makes visual checking simpler, whether air bubble emerges in the water or not. However, the presence of air bubbles in the water did affect the performance of the tensiometer; the pore pressure of the soil was not able to transfer properly to the sensor, the response time was slow, and as a consequence the results were not reliable. Saturation was therefore required to expel air from the system.

4.5.1.2 Saturation

Saturation is a process of evacuating air bubbles in any part of the tensiometer system (water, reservoir, and sensor). The process is performed by submerging the tensiometer in a pure water-filled desiccator and applying a negative pressure of 90 kPa using a vacuum pump, as described by Jotisankasa (2010). During saturation, air bubbles are developed from the water and eventually disappear when saturation is complete. Two to three hours of vacuuming is usually appropriate for saturation. Figure 4.3 shows the saturation setup.

Figure 4.3 Saturation of tensiometer

After saturation, the performance of the tensiometer was checked using a material that could easily absorb water such as a tissue paper, by touching the surface of the ceramic disk. When the response time was fast, it was considered that the

tensiometer performed well. Otherwise, the saturation process had to be continued until a fast response time was achieved.

4.5.1.3 Calibration

Once good contact between the soil specimen and ceramic disk was achieved, interaction between the pore water in the soil and water in the tensiometer reservoir commenced. Tensile stress developed from the pressure difference between the soil in an unsaturated condition and the tensiometer in a saturated condition. Water in the tensiometer was attracted by the soil through the membrane (ceramic disk) until the pressure in the soil was equal to the pressure of the water in the tensiometer. The tensile stress of water was then read by the assembled sensor transducer, and transferred to the digital readout as voltage. Calibration was required to obtain the relationship between the pressure in the tensiometer and the voltage on the digital readout. The calibration was performed by imposing different values of negative pressure on the tensiometer. The negative pressure was generated by a vacuum pump, while the corresponding voltage was recorded digitally using a multimeter. Figure 4.4 shows the typical calibration curves of tensiometers KU-T1 (a) and KU-T2 (b).

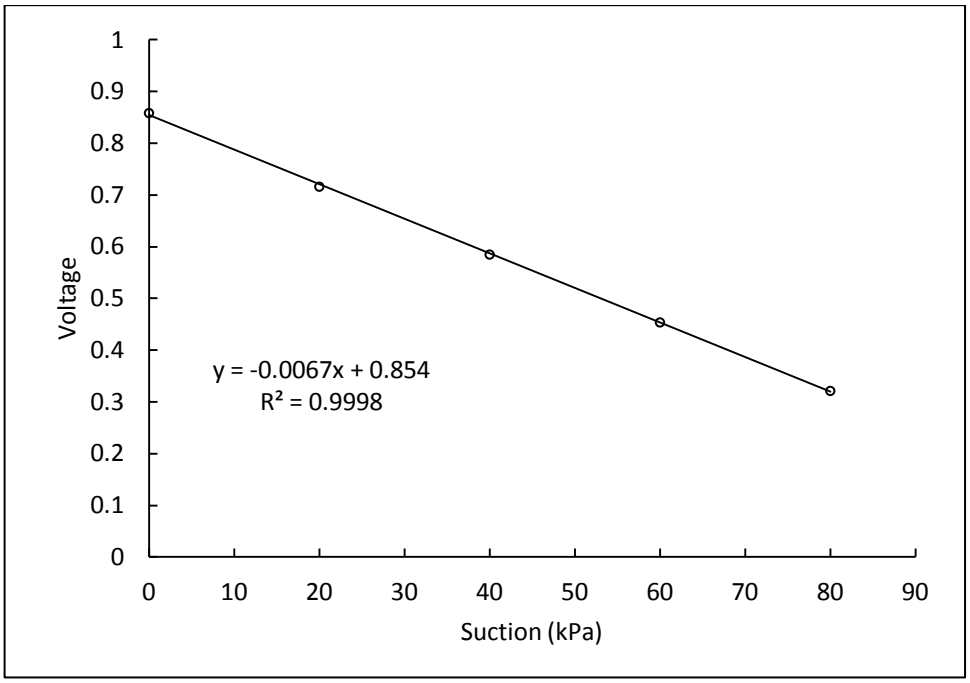

(a)

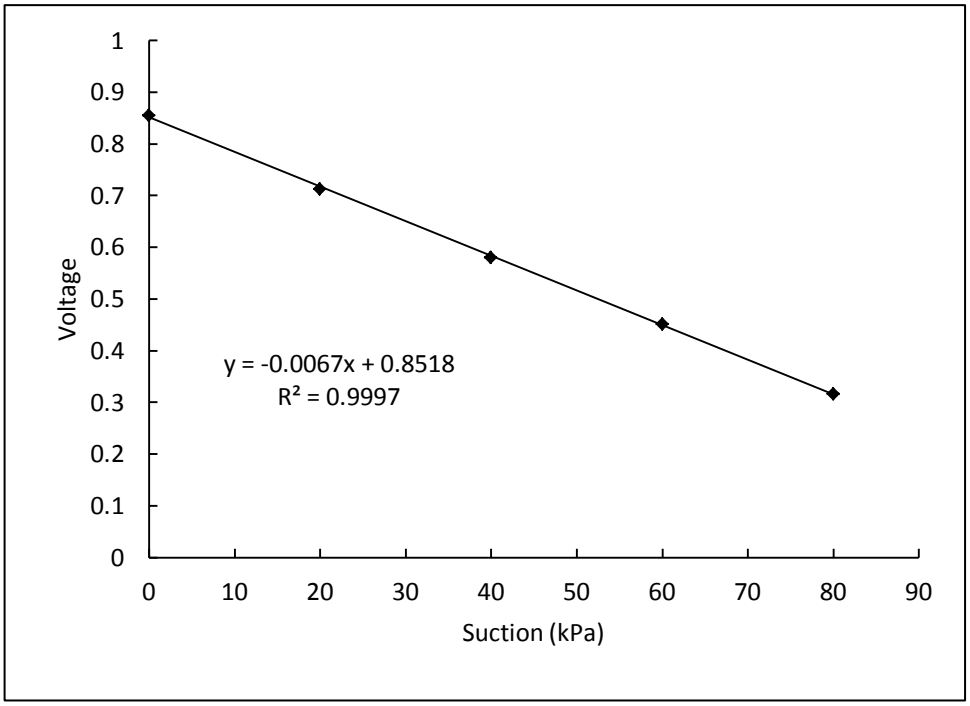

(b)

Figure 4.4 Typical results of calibration curve for tensiometers (a) KU-T1 and (b) KU-T2

4.5.2 Filter paper method

4.5.2.1 General

Matric suction measurement using filter paper has been recognised as one of the simplest methods for use. It is accurate and costs relatively little. The method is based on the assumption that the water potential of the moist soil and the filter paper in contact with the soil will be the same at equilibrium. Once the dry filter paper is placed in the soil, the water travels from the soil to the filter paper and increases its water content. The water will continue to infiltrating the paper until matric suction equilibrium is reached; that is, the condition in which matric suction in the soil is equal to the matric suction in the filter paper. The first step in obtaining matric suction using this method is to construct a calibration curve; that is, a curve corresponding between the filter paper's water content and matric suction. From this, the matric suction of the soil can be determined by the water content of the filter paper.

4.5.2.2 Calibration curve

The filter paper used was made from high technology processes, which ensures quality and homogeneity for the majority of the time. The calibration curves of the filter paper from the different batches of the same brand were identical. Leong and Rahardjo (2002) observed that the calibration curves made by Hamblin (1981), Chandler and Gutierrez (1986), and Swarbrick (1995) were in alignment with those of Fawcett and Collis-George (1967). In general, any differences in calibration curves from one batch to another is insignificant and of little practical importance since these correspond to small absolute potential differences. No. 42 Whatman and S & S 589 filter papers are two very common filter papers in current use. However, according to Leong et al., (2002) Whatman paper No. 42 proves more consistent in quality compared to others. In this study, Whatman filter paper No. 42 was utilised and its calibration curve referred to ASTM D 5298-10.

4.6 Soil water characteristic curve (SWCC) test

4.6.1 Filter paper method

4.6.1.1 Apparatus preparation

The main apparatus for matric suction measurement using the filter paper method were Whatman filter paper No. 42, a rigid PVC mould, two digital scales with respective accuracies of 0.01 g and 0.0001 g, rubber gloves, and tweezers.

The filter paper was obtained from Crown Scientific, Australia. According to the manufacturer, it is categorised as a quantitative ashless filter paper, and has the material properties of: ash 0.007 (%), thickness 200 µm, and weight 100 g/m^2 (www.whatman.com). Two different sizes of filter paper were used, being 55 mm and 70 mm in diameter. The first (55 mm) was used for the actual matric suction measurement, whereas the second was used for protection. Before and during the test, the filter paper was handled carefully (storing, placing, and removing) using rubber gloves and tweezers. Before usage, the filter paper was oven dried at 105^o for 24 hours and stored in the desiccator to maintain dryness.

The second apparatus was a rigid mould. It was made from a thick PVC tube with an internal diameter of 63.2 mm. The bottom part of the tube was attached to an

aluminium cylinder base, and the upper part was kept open. An additional aluminium cylinder with similar dimensions served as a lid. The base and lid were positioned in such a way that the inner height of the mould was 30 mm. To avoid leakage, a thin layer of silicone sealant was injected around the inner part between the tube and the aluminium base. A high quality sealant (branded Blu-Tack) and electric tape were then stuck on the outer part of the PVC tube and base.

Two digital scales were employed for the test; the first one had an accuracy of 0.0001 g, and was prepared for weighing the filter paper, whilst the other one with an accuracy of 0.01 g, was prepared for weighing moulds and specimens.

As matric suction is affected by temperature, the test was performed at a constant room temperature of 20^{o} C. Matric suction tends to decrease as temperature increases (Chahal, 1965; Wilkinson and Klute, 1962).

4.6.1.2 Procedure

Specimens were prepared in three different sand-kaolin clay mixtures; 100:0, 95:5, and 90:10. Each of them was sprayed with pure water to obtain a specified water content, mixed thoroughly, put in a sealed plastic bag and stored in a container for at least three days for water content equilibration. The specimen was then poured into the mould and was compacted layer by layer to achieve a desired void ratio. The quantity of specimens was determined from calculations using the data of the volume of the mould and the specified void ratio. The compacted specimen was then submerged in water for saturation for around 24 hours. Before and after saturation, the weight and height of the specimens were recorded. At this stage, specimens were considered to be in a saturated condition, at which their matric suction was zero.

The second step was to reduce the water content of the specimen by means of air drying. The surface of the specimen was left open for contact with the open air for 12-24 hours for air drying. The desired water content could then be predicted by recording the weight of a specimen before and after air drying. After air drying, a filter paper was sandwiched between two larger sized filter papers and placed on the top of the specimen. The purpose of using larger filter papers was to protect the sandwiched paper so that particles from the specimen would not cling to the sandwiched filter paper. An aluminium lid was then put onto the mould in such a way that the filter papers had a good contact with the specimen. The mould was then

sealed with electric tape, and placed in a room for at least 7 days at a constant temperature for equilibration, as suggested by Fawcett and Collins-George (1967) and ASTM D 5298-10. A cross-section and photograph of the test are shown in Figure 4.5 (a) and (b).

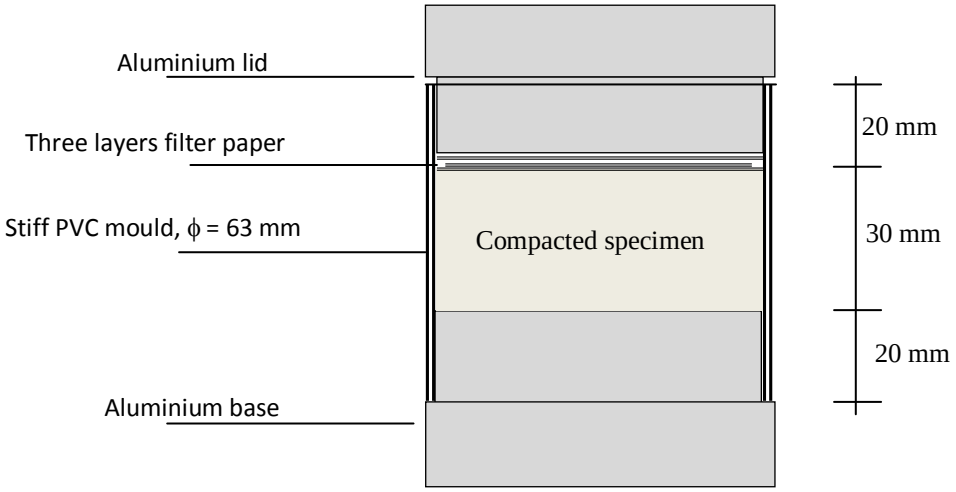

(a)

(b)

Figure 4.5 (a) Cross-section of SWCC test using filter paper, (b) Photograph of PVC mould

After equilibration, the weight of the filter paper and specimen were recorded separately to obtain matric suction and specimen water content respectively. The specimen was then air dried for 12-24 hours to reduce its water content for the second stage. The process was then repeated several times until the difference in specimen weight between the two stages was relatively small. A data series of matric suction and corresponding water content was then plotted to obtain a soil water characteristic curve (SWCC). The procedure for filter paper and specimen water content measurements are follows:

a) The procedure of filter paper water content measurement

The sandwiched filter paper was taken carefully out of the mould and put into a clean dry aluminium cup. The cup lid was then closed immediately after placement of the filter paper, and using 0.0001 g scale, the weight of the cup and the wet filter paper were recorded. The time period between removing the filter paper from the mould and placing it into the cup was crucial, as small amounts of water evaporate very quickly and this affects the result. Therefore a time period of less than a few seconds was preferred. The cup with the wet filter paper inside was then brought to the oven with the lid half open for drying for a minimum of two hours. The hot cup with the dry filter paper inside was then taken out of the oven and put onto a massive aluminium plate for cooling, after which the weight was recorded. During the placement and removal of filter paper, tweezers and gloves were used to avoid direct hand contact with the filter paper. It was vital to the filter paper water content calculation that the weight of the empty cup before and after oven drying was taken into account. Once the filter paper water content was obtained, the specimen's matric suction was then determined by using the calibration curve in accordance with ASTM D 5298-10.

b) Procedure for specimen water content measurement

Water content calculation of the specimen was carried out indirectly by recording the weight of the specimen at every stage using a 0.01 g scale. After completing the final stage, the water content test was performed. The water content obtained from the final stage was then used to calculate the water content at all stages.

4.6.2. Tensiometer method

4.6.2.1 Apparatus

The main apparatus items used in the test were: tensiometer KU-T1, a digital scale of 0.01 g, and a set of data loggers connected to a computer. Three small holes were created at the side of the tube near the base, middle and top of the PVC mould for attaching to the tensiometer.

4.6.2.2 Procedure

The specimens were prepared in the same way as the filter paper method. They were then compacted in a rigid PVC mould 6.32 cm in diameter to achieve the desired void ratio. The tensiometers were then attached through the holes in the mould. The top part of the mould remained open for the pore water to evaporate easily. During the test, the weight and matric suction of the specimens were recorded continuously using a digital scale and a data logger. Figure 4.6 shows the set-up of the SWCC test using the tensiometer.

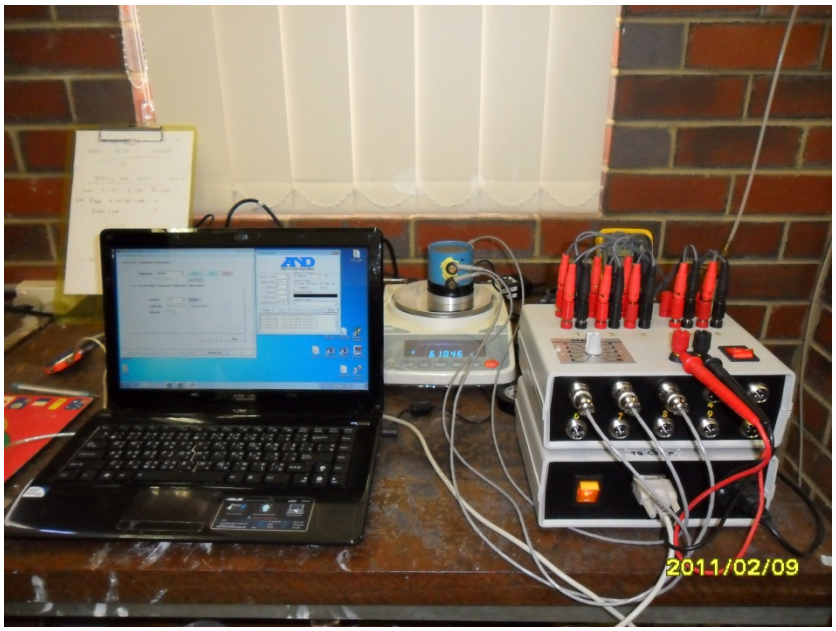

Figure 4.6 Set-up of SWCC test using tensiometer

4.7 Direct shear test

The unsaturated shear strength test using direct shear consisted of testing both saturated and unsaturated specimens. The procedure of the direct shear test under saturated conditions is briefly presented, followed by a detailed account of the test

under unsaturated conditions. It includes the apparatus, specimen preparation, compaction method, equilibration and matric suction monitoring, and procedure up to the point of the loading arrangement. ++

4.7.1 Direct shear test on saturated specimen

A series of direct shear tests on saturated specimens was carried out following the ASTM D 3080-04, the standard of conventional direct shear in which the effective stress concept is applied. The objective of this test was to obtain the effective stress parameters c' and ϕ'. The specimen was compacted directly in the shear box at the optimum water content. The test was performed dynamically layer by layer to achieve its maximum dry density. Prior to the shearing test, the compacted specimen together with the shear box was submerged in distilled water for saturation. The specimen was then consolidated by applying a specified normal force. Three consecutive normal forces of 4, 14 and 24 kg were applied in this study, giving the initial normal stress results of 11.2, 39.2, and 67.1 kPa respectively. The displacement rate d_r was determined using the equation:

$$d_r = \frac{d_f}{t_f} \tag{4-2}$$

where d_f is the estimated horizontal displacement at failure (mm), and t_f is the total estimated elapsed time to failure (min). According to this standard, t_f can be estimated by using a consolidation graph produced from the consolidation test, and can be written as:

$$t_f = 50 \times \frac{t_{90}}{4.28} \tag{4-3}$$

where t_{90} is the time required for the specimen to achieve 90% consolidation under specified normal stress.

4.7.2 Direct shear test on unsaturated specimens

A series of shear tests on unsaturated specimens was carried out using a similar direct shear machine to that for the saturated test. However, in this test the shear box was slightly modified to allow for the monitoring of matric suction during the test. The main difference between the saturated and unsaturated tests was in the treatment of the sample in relation to the water. In the saturated test, the specimen was

thoroughly soaked in water to create fully saturated conditions for the specimen. In the unsaturated test, the water container of the shear box was not filled with water, in order for the specimens' water content to remain unchanged before and after the test.

4.7.2.1 Apparatus

The matric suction-monitored direct shear test was conducted as a modification on the conventional direct shear. Essentially this device was modified in two ways. The first modification was created by attaching a tensiometer to the device. A tensiometer may be placed on the top cap, shear box body, or any part of the shear box. However, the simplest way in this instance was to place the tensiometer(s) on the top cap, as performed by Tarantino and Tombolato (2005) and Jotisankasa and Mairaing (2010). In this study, the modification was carried out by making a small orifice in the top cap for placement of the KU-T2 tensiometer. Its position was strengthened by using a clamping set in such a way that the ceramic disk of the tensiometer had a good contact with the specimen. Figure 4.7 shows the photograph of the installation of the tensiometer to the top cap.

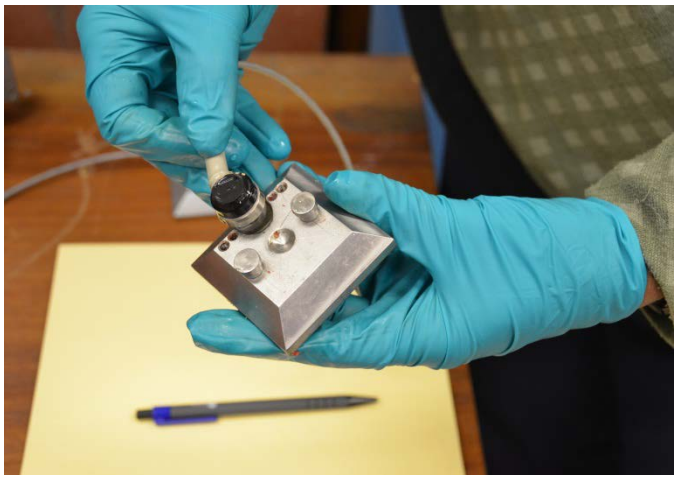

Figure 4.7 The installation of KU-T2 tensiometer on top cap of shear box

The second modification was carried out on the body of shear box. In the unsaturated test, direct contact of the specimen with the open air was avoided in order to keep the water content constant. Water content may be lost through gaps in a shear box so in

this instance the gap between the base plate and the lower half of the shear box was sealed with a thin layer of silicone sealant. This material proved to be both strong and durable enough for the purpose. The gap between the upper half and the top cap was sealed using Blu-Tack, together with petroleum jelly. These materials were extremely easy to use and were reusable for several tests. Another gap found between the lower and upper halves of the shear box was smeared with a thin layer of petroleum jelly around the outside section. Note that porous stones were not required in the unsaturated direct shear test. Figure 4.8 shows the cross-section of the modified direct shear device (Purwana et al., 2011).

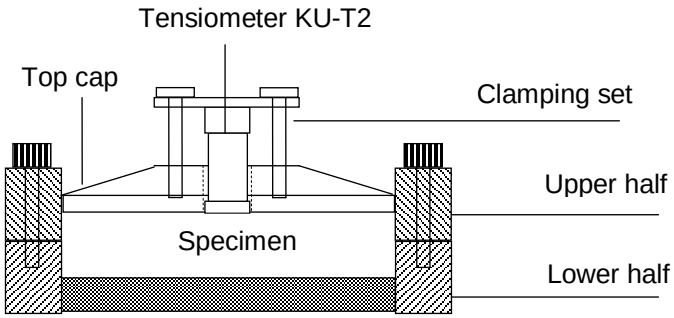

Figure 4.8 The schematic cross-section of modified direct shear (Purwana et al., 2011)

4.7.2.2 Specimen preparation

Specimen preparation (sand-kaolin-water mixing, curing, water equilibration and storing) was basically similar to the preparation for the compaction test in section 4.4. The specimen was poured into the shear box and compacted layer by layer to achieve the desired maximum dry density in accordance with the compaction test. Immediately after compaction, the top cap was placed in such a way that its base was in complete contact with the specimen. The tensiometer was then attached to the top cap and the clamping set was tightened. Care was taken to ensure that the ceramic disk of the tensiometer had a good contact with the specimen. Blu-Tack, and a thin layer of petroleum jelly were then used to block all the vulnerable parts of the shear box to avoid any possible leakage during the testing as described previously. The shear box was then placed into the direct shear machine for the shearing test. Prior to shearing, the tensiometer was connected to the digital readout unit. The specimen

was then left overnight for matric suction equilibration. A number of tests had been previously performed on all mixtures and the result indicated that a time period of 12 hours was sufficient for matric suction equilibration.

The unsaturated direct shear test was also performed on the specimen with the water content being less than the OWC. The specimen was prepared using the air drying method. After compaction to the point of OWC, the specimen was left to air dry with the surface kept in contact with the air. Water loss during air drying was recorded to predict the desired water content. The actual water content was obtained by performing the water content test using the oven drying method after completing the shearing test.

4.7.2.3 Shearing test

In this study, three different normal loads of 4, 14 and 24 kg were applied. A number of preliminary tests had been performed on all mixtures and the result indicated that the displacement rate of 0.122 mm/min was sufficient for the shearing test. During the test, vertical and horizontal stress, vertical displacement, horizontal displacement and the corresponding matric suction were recorded. After completing the shearing test, the entire specimen was removed from the shear box for the water content test. Even though the specimen was placed in a closed system, a small amount of water could have escaped from the specimen. For this reason, the weight of the specimen was recorded before and after the shearing test.

4.8 Suction-monitored CBR test

The procedure for California Bearing Ratio (CBR) test was conducted in reference to the ASTM D 1883-07. According to this standard, the CBR test can be performed on the specimen either in soaked or unsoaked conditions. However, suction is not taken into account at any stage of the condition of the specimen. In this study, a slight modification was carried out so that the matric suction of the specimen could be recorded during the test. This suction-monitored CBR test was performed by attaching tensiometers through the orifices made in the mould and to the attached surcharge weight. A series of tests were performed on the sand-kaolin mixture with the same proportions as the specimens in the direct shear test. The tests were carried

out on soaked and unsoaked specimens, and also on the specimen with different degree of air drying.

4.8.1 Apparatus

The main apparatus types used in this test were a set of conventional CBR devices (compaction set, mould, a surcharge weight, and loading machine unit) and a set of matric suction equipment. Two small orifices of 8 mm in diameter were made in the 6 in. (152 mm) mould, and an orifice of 17 mm in diameter was made in the surcharge weight. The apparatus for matric suction measurement consisted of tensiometers KU-T1 and KU-T2, along with a digital readout unit. The cross-sectional setup of the CBR with matric suction monitoring is shown in Figure 4.9. The location of the upper KU-T1 was 30 mm from the surface, whereas KU-T2 was located 30 mm from the base. The placement of tensiometer KU-T1 was designed in such a way that the matric suction at the lower and upper halves of the specimen in the CBR mould could be monitored. Tensiometer KU-T2 was placed very close to the CBR piston so that the matric suction in the vicinity of the failure area could be monitored. The fixity of those tensiometers was strengthened by a clamping set and Blu-Tack.

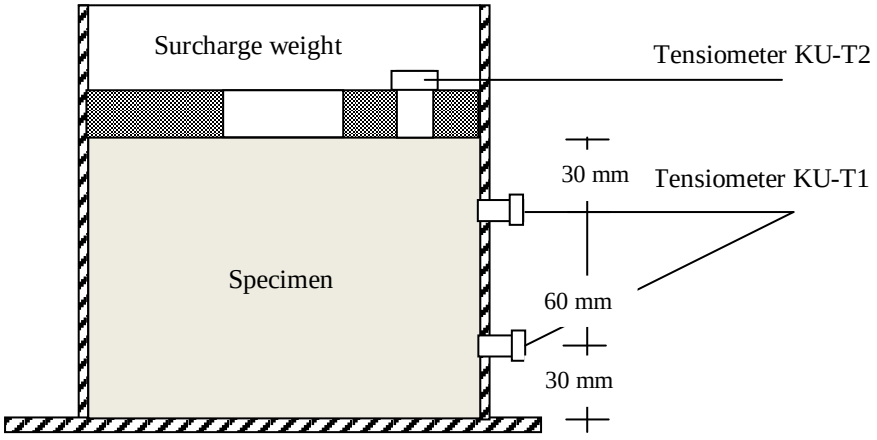

Figure 4.9 Cross-sectional setup of the CBR test (not to scale)

4.8.2 Specimen preparation

The procedure for sand-kaolin-water mixing, curing, water equilibration and storing of the specimen for the CBR test was similar to the specimen preparation for the Proctor compaction and direct shear tests. Prior to compaction, the orifices of the mould were blocked using electrical tape so that no part of specimen could extrude during compaction. The specimen was compacted according to method C of ASTM D 698. Compaction was performed layer by layer @ 56 blows/layer in a 6 in. (152 mm) mould and a by applying a 5.5 lb. (2.5 kg) standard hammer falling at a height of 304.8 mm to achieve 100% maximum dry density.

Three types of specimen were prepared; soaked, unsoaked and "after drying" specimens. The soaked specimen was prepared to simulate the most adverse conditions in the field. For this, the compacted specimen together with the mould was submerged in water for four days, and was loaded with a surcharge weight. The weight and height of the specimen before and after soaking was recorded to calculate the amount of absorbed water and swelling from soaking. The unsoaked specimen was prepared to simulate natural field conditions. There was no "special" treatment given to this type of specimen. The "after drying" specimen was obtained to simulate the condition of the sample when it underwent water content reduction due to air drying after compaction. For this, the surface of the compacted specimen was left to have a contact with the free air so that some of the pore water evaporated. During this period, the weight of the specimen was recorded to predict its water content. When the desired water content was achieved, air drying was discontinued. Prior to CBR penetration, the specimen was covered with a plastic sheet to avoid further evaporation.

4.8.3 Installation of tensiometer

After the specimen preparation was complete, the tensiometers were attached to the mould. The electric tape was removed from the orifice and the tensiometer KU-T1 was installed. A small groove behind the orifice was made so that the tip of tensiometer KU-T1 was slightly embedded into the specimen. Blu-Tack was then stuck around the tensiometer to strengthen the fixity of tensiometer. The tensiometer KU-T2 was also installed through an orifice in the surcharge weight. Care was taken to ensure that the HAED surface had a good contact with the specimen. A clamping

set and Blu-Tack were then assembled to adjust and maintain the fixity of tensiometer. The tensiometers were then connected to a digital readout unit for continuous recording of matric suction measurement.

4.8.4 CBR penetration

The CBR test was performed by penetrating a 49.6 mm in diameter of piston into the specimen. A loading machine with a penetration rate of 1.27 mm/s was set for a penetration period of 15 minutes. During penetration, matric suction was recorded by using the tensiometers as previously described. After completing the penetration, the tensiometers were removed. The water content test was then performed on 1/3 of the upper and 2/3 of the lower part of the specimen.

4.9 Summary

1. The main laboratory work of this study was an unsaturated strength test on different proportions of the sand-kaolin clay mixtures using modified direct shear and CBR. Modification was made by attaching tensiometer(s) onto a conventional direct shear and CBR apparatus so that matric suction could be recorded during the test.
2. Matric suction measurement was performed either directly using a tensiometer or indirectly using the filter paper method.
3. The soil-water characteristic curve (SWCC), was obtained using the filter paper method along with the continuous use of the tensiometer.

CHAPTER 5
RESULT AND ANALYSIS

5.1 Introduction

In this chapter, the results of the laboratory tests, analysis and discussion are presented. Some of the material properties data referred to in the laboratory test were provided by the vendor and as such further laboratory tests were not required. The result of preliminary tests (index properties and compaction test) and a brief analysis are firstly presented, followed by the SWCC, direct shear and CBR test. Due to a large number of laboratory tests, only the summaries of each test are presented. The detail of the data is recorded in the Appendices.

5.2 Specimen index properties

5.2.1 Index properties of sand and kaolin clay

The index properties test consisted of grain size analysis, liquid limit, plastic limit, and specific gravity tests. The tests were performed on Baldivis sand and kaolin clay for determining the classification of the specimen. The result of the sieve analysis on Baldivis sand (in this study, denoted as sand) indicated that the specimen consisted of 50.2 % fine sand, 49.2 % medium, 0 % coarse, and 0.6 % of fines (silt and clay). Based on ASTM D 654, a specific gravity test was conducted, indicating that the specimen had the specific gravity of 2.63. According to ASTM D 2487, this material was classified as poorly-graded sand (SP).

Kaolin clay was obtained from UNIMIN PTY LTD Australia, available commercially as Prestige TM kaolin forming clay. The grain size test on kaolin clay was not performed here as the data was provided by the vendor. The specific gravity of this clay (ASTM D 654) was 2.58. The consistency test indicated that the liquid limit (LL) and plastic limit (PL) of this kaolin clay was 58 and 31 respectively, resulting in a plasticity index (PI) of 27. The values of LL, PL and PI of this kaolin clay were still in the range of that from the data from Grim (1962 b), as presented in Table 5.1. According to ASTM D 2487, the kaolin clay used in this study was classified as high plasticity clay (CH).

Table 5.1 Atterberg limits range of kaolinite clay, montmorillonite and attapulgite (modified from Grim (1962 b)

Atterberg limits	Clay mineral		
	Kaolinite	Montmorillonite	Attapulgite
Liquid limit	29 - 113	123 - 700	158 - 232
Plastic limit	26 - 38	51 - 97	97 - 124
PI	1 - 41	34 - 603	57 - 123

The chemical data obtained from the Prestige TM indicated that this kaolin clay has a mean value (by weight in %) of minerals as follows: 46.41of SiO_2, 36.5 of Al_2O_3, 0.9 of FeO_3, 0.8 of TiO_2, 0.9 of CaO, 0.5 MgO, 0.2 of K_2O, and 0.1 of Na_2O.

5.2.2 Index properties of sand-kaolin clay mixture

The mixture of two or more materials with different index properties may produce a material with new properties. The index property analysis on the new material was required to determine its properties. In this study, new sand-kaolin clay mixtures with different proportions were studied. The gradation curves of sand-kaolin clay mixture were determined simply from the combination of the gradation data of sand and kaolin clay. Figure 5.1 shows the gradation curve of sand, kaolin clay, and sand-kaolin cay mixtures.

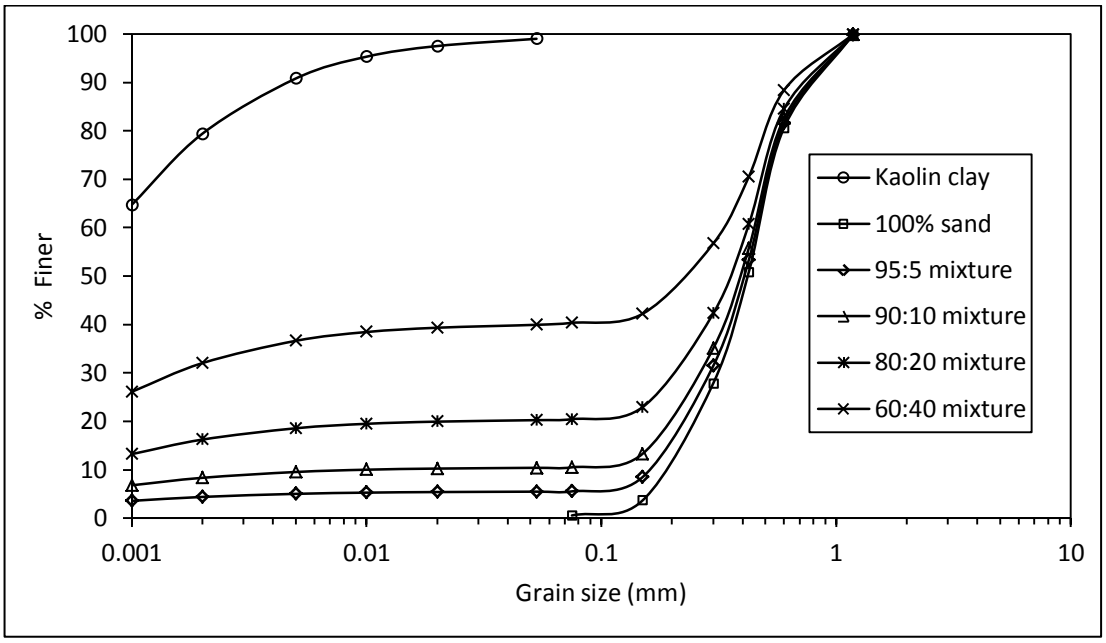

Figure 5.1 Sand-kaolin clay mixture gradation curves

Similarly, a mixture of material with different specific gravities may produce a new material with a new specific gravity. By using Equation (4-1), the bulk specific gravity of a new material of 95:5 and 90:10 mixtures is 2.630 and 2.628 respectively. For simplicity, the specific gravity of 2.63 was applied to all mixtures.

Liquid limit and plastic limit tests on the new mixtures were also performed. The results indicated that the increase in kaolin content caused a decrease in the liquid limit and plasticity index respectively. The classification system was the performed on the new materials according to ASTM D 2487. Due to the addition of a proportion of kaolin clay to the sand, the group of specimens altered from poorly-graded sand (SP) for sand and 95:5, poorly graded sand with clay (SC-SM) for 90:10, to clayey sand (SC) for 80:20 mixtures. Based on plasticity, the sand and 95:5 mixtures were categorised as non-plastic specimens, whereas the rest were low-plastic specimens.

According to Skempton (1953), the correlation between plasticity and the amount of clay mineral particles ($< 2\,\mu$) can be predicted using Activity (A), the activity concept being applicable to fine grained material. In this study, kaolin clay is the only fine grained material, whereas the rest are coarse grained materials. By using Equation (3.1), the activity of kaolin clay is 0.3, and according to Skempton (1953), this specimen was classified as inactive soil.

The summary of the index properties of sand, kaolin clay, and sand-kaolin clay mixtures are presented in Table 5.2.

Table 5.2 Summary of index properties of specimens

Specimen	Gs	LL	PL	PI	Cu	Cc	Class.	Activity
Kaolin clay	2.58	58	31	27	N.A	N.A	CH	0.3
Sand	2.63	N.A	N.A	N.P	2.53	0.99	SP	N.A
95:5 mixture	2.63	N.A	N.A	N.P	3.43	1.3	SP	N.A
90:10 mixture	2.63	21.3	15.4	5.9	22.55	5.88	SC-SM	N.A
80:20 mixture	2.62	26.6	16.7	11.3	667	167	SC	N.A

N.A = not applicable

5.3 Compaction characteristics

The standard compaction test was performed on sand, 95:5 and 90:10 mixtures to obtain their compaction characteristics. Additional compaction tests were also performed on 80:20, 60:40, and 100:0 (kaolin clay) mixtures to attain a broader range

of proportions from zero to 100% of kaolin clay content. The results are presented quantitatively and graphically in Table 5.3 and Figure 5.3.

Table 5.3 The compaction characteristics of sand-kaolin clay mixtures

Mixture	MDD (kN/m^3)	OWC (%)	Void ratio
100:0	17.0	13	0.50
95:5	18.3	11	0.41
90:10	19.7	9.8	0.31
80:20	20.3	9.1	0.27
60:40	19.4	12.8	0.33
0:100	15.2	20.1	0.70

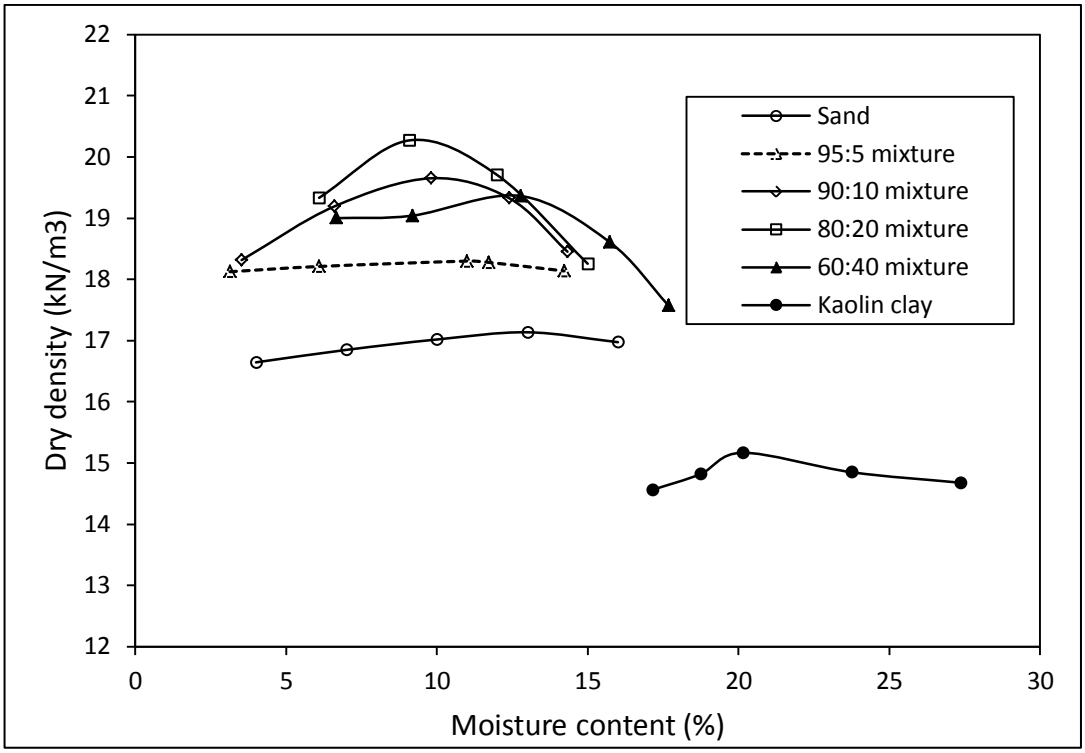

Figure 5.2 Compaction curves of specimens

For the poorly graded sand, the density due to compaction was mainly caused by rearrangement of the particles. During compaction, the particles of sand move to find the best position. The voids become narrower and the specimen becomes denser and more compact. However, due to the lack of smaller particles, the pore spaces in poorly graded sand remain relatively unfilled. Assuming that the particles of poorly graded sand are uniform and round, the packing arrangement of the specimens may be close to one of packing arrangements proposed by Mitchell and Soga (2005) as described in Chapter 3. According to their findings, simple cubic and tetrahedral

packing have the highest and lowest void ratios respectively. The increase in water content of the specimen to some extent allows the particles to move more easily, causing an increase in dry density. However, excessive compaction water content may cause sand particles to float in the water, causing the dry density to decrease.

The change of mixture proportions from sand to 95:5 caused the composition of the specimen to change. During compaction, the smaller particles of the clay filled some pores of sand causing a decrease in void ratio (from 0.50 to 0.41), and as a consequence causing the dry density to increase (from 1.7 to 1.83 t/m^3). The change in composition was also associated with the change of optimum water content (from 13 % to 11 %). A similar situation occurred in the 90:10 mixture, when the remaining pores amongst sand particles of 95:5 mixture were occupied by adding more kaolin clay particles. Due to the compaction, the void ratio decreased from 0.41 in the 95:5 mixture to 0.31 in the 90:10 mixture. The dry density increased from 1.83 t/m3 in the 95:5 mixture to 1.93 t/m3 in the 90:10 mixture. The addition of 10 % of kaolin clay to the sand contributed to an increase of 15% in the maximum dry density (from 1.7 of sand to 1.97 t/m^3).

It can be assumed from Figure 5.3 that to some extent (up to 20%), the increase in kaolin clay content would cause the increase in dry density and the decrease in void ratio. However, the void ratio starts to increase when the kaolin clay content of the mixture was > 20 %. This result is in accordance with the results of Mullin and Panayiotopoulos (1984a). It can be concluded that the addition of kaolin clay to sand to some extent could produce a new material with beter properties.

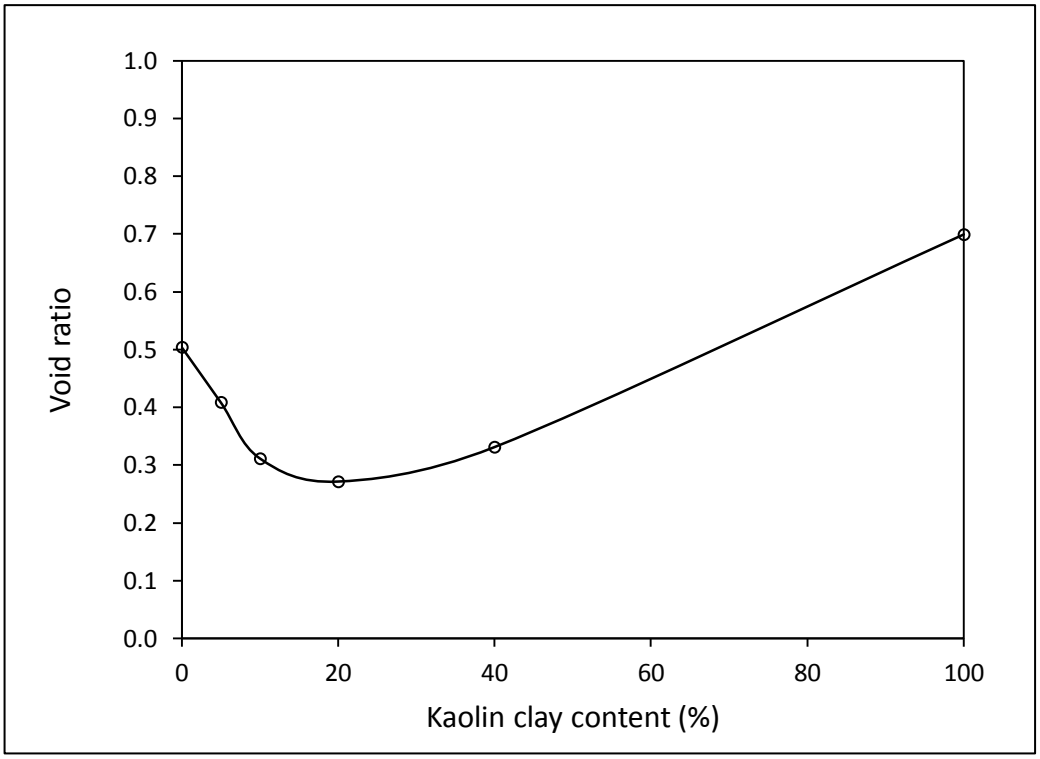

Figure 5.3 Kaolin clay content versus void ratio of sand-kaolin clay mixture from compaction test

5.4 Soil water characteristic curve (SWCC)

Coarse-grained material such as sand usually has a very low air entry value, low residual suction and low volume change. Conversely, fine-grained material such as clay would have a high air entry value, high residual suction, and high volume change. Two methods were used for the SWCC test; tensiometers and filter paper as previously described in Chapter 4. For the specimens without kaolin clay or very low kaolin clay content such as 100:0 and 95:5 mixtures, tensiometers were utilised, whereas for the higher kaolin clay content such as the 90:10 mixture, the combination of tensiometer and filter paper method was employed. The reason for employing such methods is as follows. The tensiometer method was suitable for measuring low suction (< 80 kPa), but it was unable to be used for suction higher than 80 – 90 kPa. The filter paper method exhibited effective performance in high and very high suction conditions, but it was not suitable for very low suction. The results of the SWCC test on those specimens are shown in Figures 5.4, 5.5, and 5.6.

In this study, the mathematical model proposed by Fredlund and Xing (1994) was employed to obtain the best-fit curve of SWCC data, using equation (2.33). The equation was solved using a least squares method by minimising the sum of squared deviation of the measured data from the calculation with respect to parameters a, m, and n as follows:

$$f(a,m,n) = \sum_{i=1}^{M}\left[\theta_i - \theta(\psi_i, a, m, n)\right]^2 \qquad (5.1)$$

where $f(a,m,n)$ is the objective function, M is the total number of measurements, and θ_i and ψ_i are the measured data. The Solver program of Excel was utilised to obtain the solution. The best-fit curves and the parameters are presented in each figure, and the best-fit curves of SWCCs for all mixtures are shown in Figure 5.7. It can be observed from this figure that the sand has the highest storage capacity, followed by the 95:5 mixture, and finally the 90:10 mixture with the lowest storage capacity. This order also occurred in the compaction characteristics of the specimen, where the 100:0 mixture exhibited the highest OWC, followed by the 95:5 and 90:10 mixture respectively.

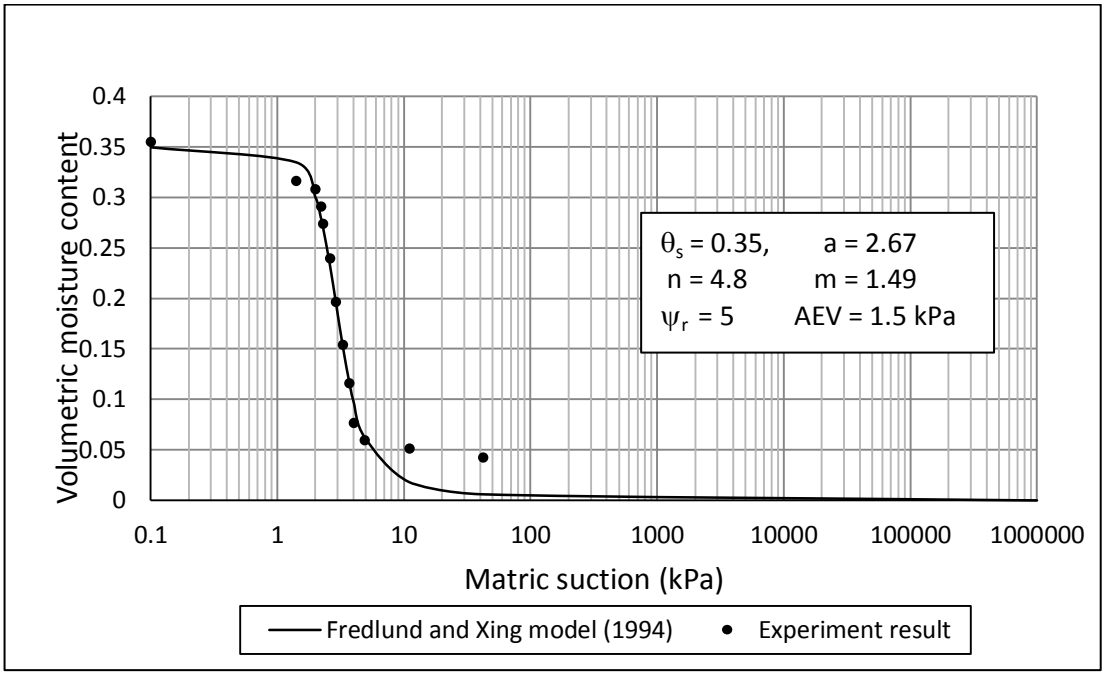

Figure 5.4 SWCC of sand

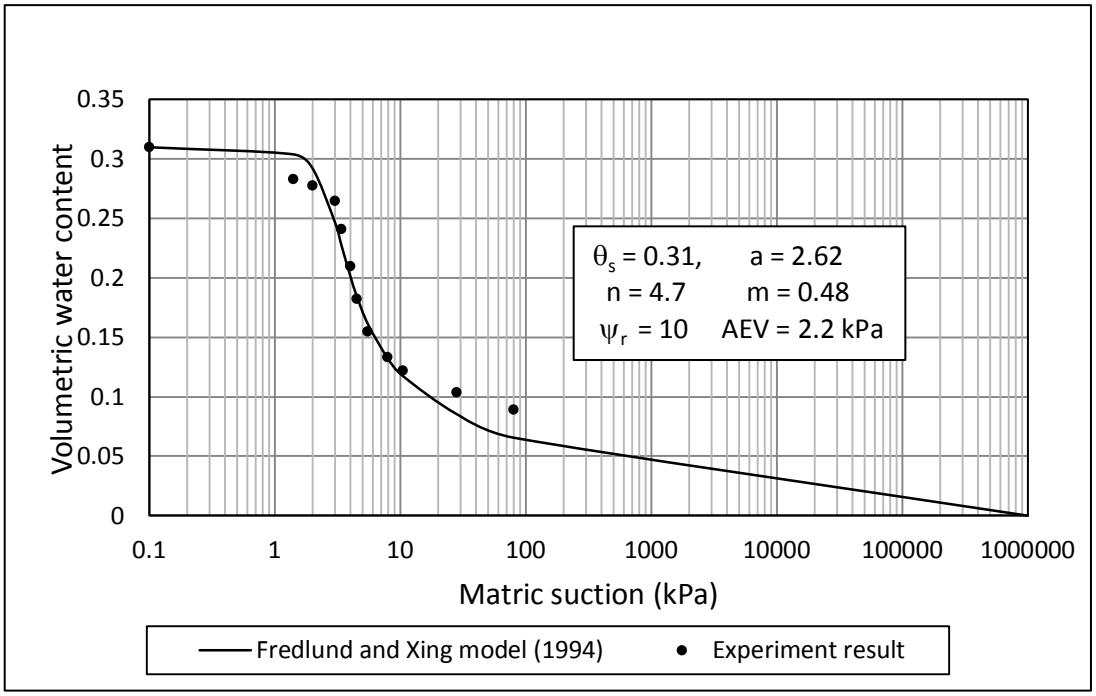

Figure 5.5 SWCC of 95:5 mixture

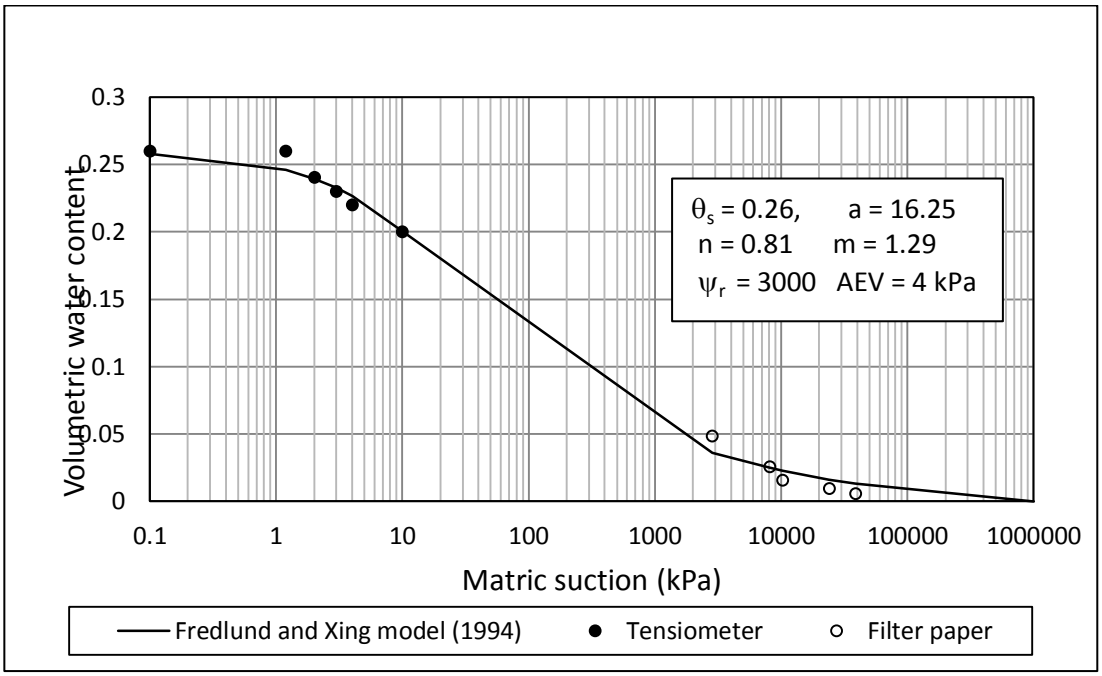

Figure 5.6 SWCC of 90:10 mixture

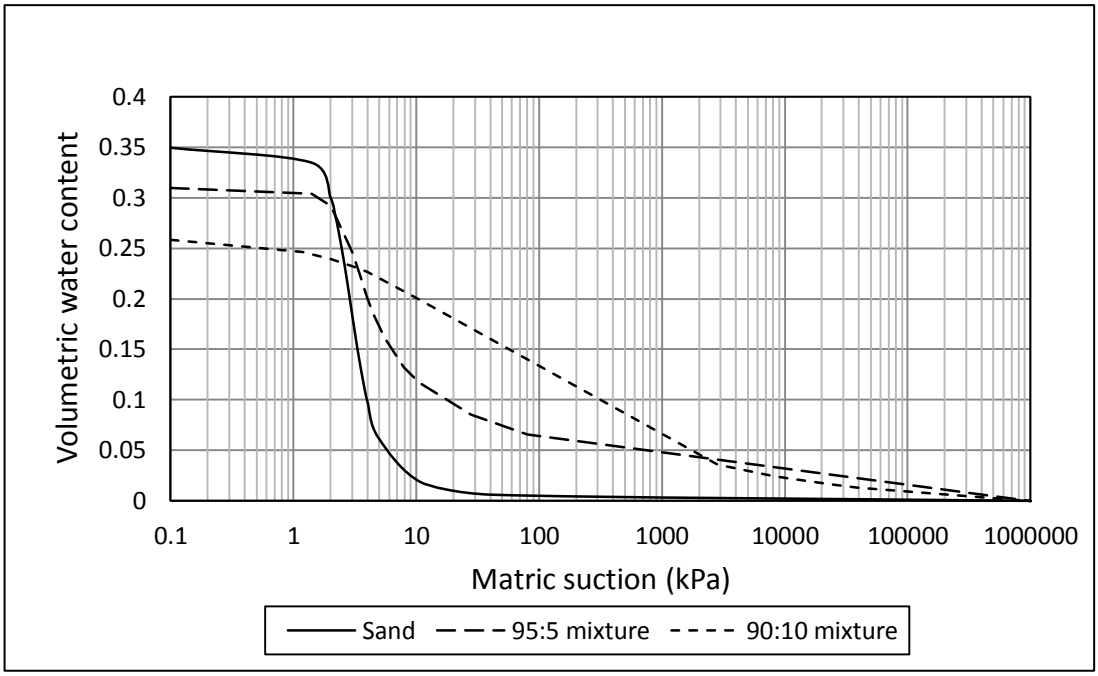

Figure 5.7 Best-fit curves of SWCC for all mixtures

In some cases, it is more effective to present the SWCC in matric suction versus gravimetric water content diagram as shown in Figure 5.8.

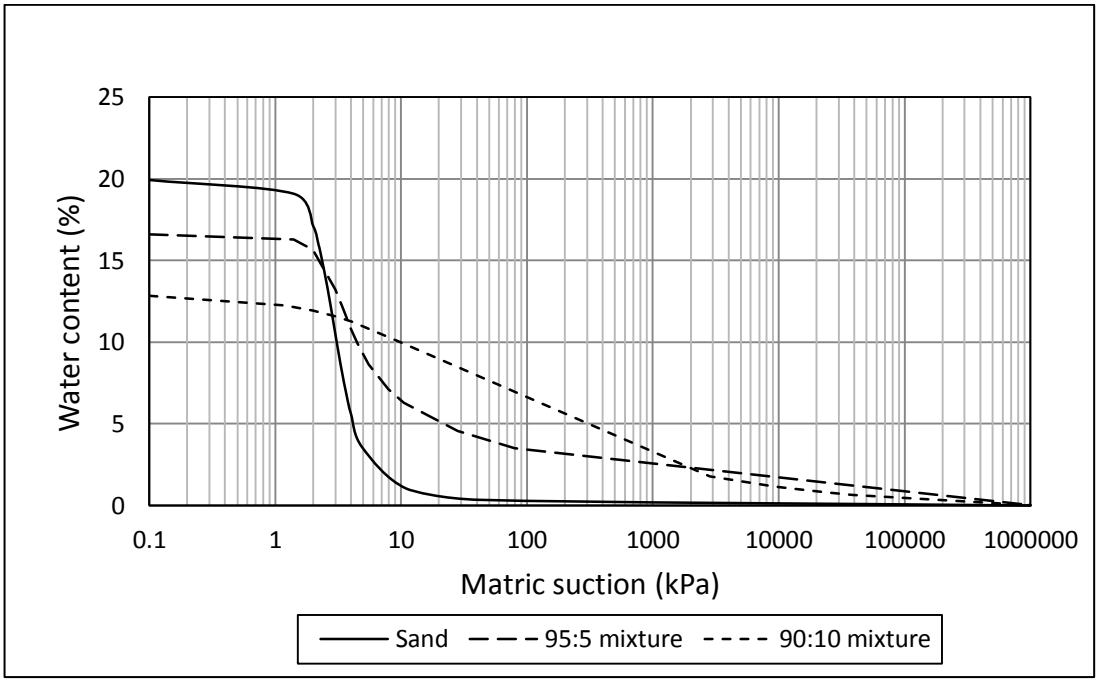

Figure 5.8 Best-fit curves of SWCC for all mixtures in matric suction versus water content

5.5 Direct shear test

5.5.1 Determination of shearing rate

In the consolidated-drained direct shear test, the maximum shearing rate has to be determined to have drained conditions in which there is no excess pore pressure at failure. According to ASTM D 3080, the maximum shearing rate can be calculated using equation (4.2) as described in Chapter 4. The displacement at failure d_f = 12 mm can be chosen for normally consolidated/lightly fine grained soil and 5 mm for other soil. The minimum time required from start to failure can be estimated using equation (4.3) and the settlement-square root of the time curve.

Figure 5.9 shows the curves of the settlement-square root of the time curve of all mixtures from a normal load of 14 kg (initial normal stress of 39.2 kPa). It can be observed from that figure that the time-settlement curves exhibited quick drainage and were not well defined for estimating the displacement rate. ASTM D 3080 recommends using t_f = 10 min (0.5 mm/min) for clean dense sand and t_f = 60 min (0.08 mm/min) for sand with more than 5 % fines. In this study, the moderate value of t_f = 40 min was used, resulting in the maximum displacement rate of d_r = 0.125 mm/min. This value was set for all direct shear tests in both saturated and unsaturated conditions.

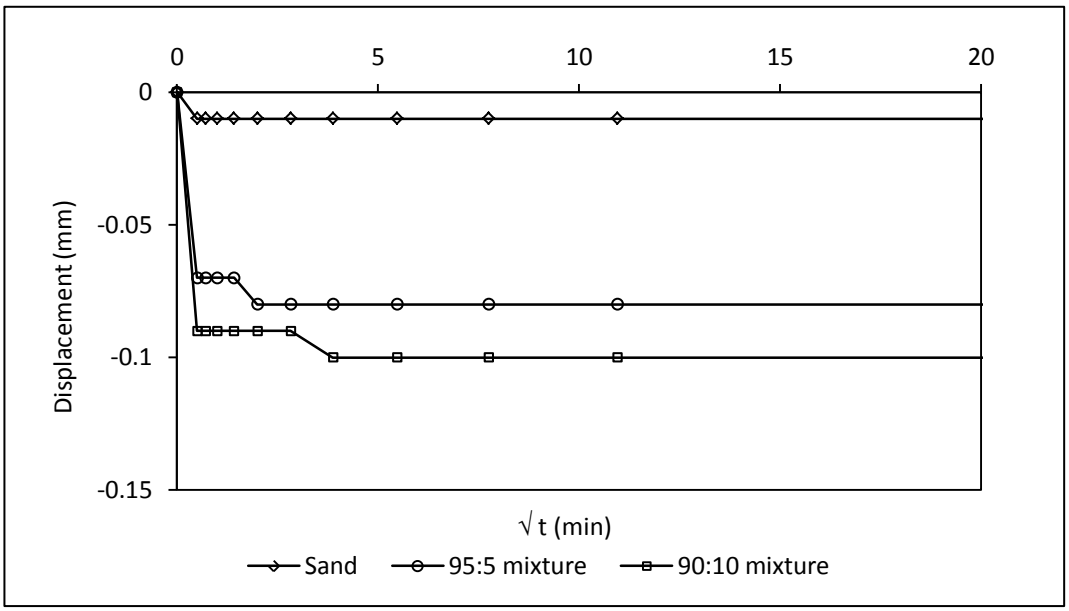

Figure 5.9 The curves of settlement-square root of time at initial normal stress of 39.2 kPa

5.5.2 Direct shear test on saturated specimens

A series of direct shear test on saturated specimens was performed to obtain the effective shear strength parameters (c' and ϕ') for all mixtures. Three different normal forces of 4 kg, 14 kg, and 24 kg were given to each mixture to impose an initial normal stress of 11.2 kPa, 39.2 kPa, and 67.1 kPa. During shear, this normal stress changes due to the change in the shearing area of the sample. The results and analysis of each mixture are presented in tabulation and graphic.

5.5.2.1 Saturated direct shear on sand

Figure 5.10 shows the shear stress-displacement curves of the saturated direct shear test on sand specimens, indicating that all curves exhibit hardening behaviour until peak value, followed by softening. According to shear strength theory, the behaviour of cohesionless soil under direct shear testing is dependent on the compactness of the soil (Das, 2008). For dense and medium sand, the shear stress increases with shear displacement to a peak value, and then decreases to an approximate constant value. For loose sand, shear stress increases with shear displacement and then remains relatively constant up until ultimate value is reached.

Figure 5.10 (b) shows the plot of the vertical and horizontal displacement of sand during the direct shear test. It can be observed from the figure that all curves exhibit the expansion phenomenon (dilation). During the test, the applied normal and shearing stresses cause the movement of specimen particles. In dense sand, the particles tend to move over the neighbouring particles in the shearing direction, causing an increase in volume (dilation). In loose sand, the particle movement does not travel in the direction of the shearing, rather the particles tend to fill the gaps among the particles. In this situation, the volume of the specimen tends to decrease. According to Wu and Sun (2008), volume change is due to the slipping and rotating of particles. After expansion (or compaction) the interlocking state will change toward a more stable state. The strength characteristics shown in Figure 5.10 (b) indicate that the specimens were in a dense/medium state.

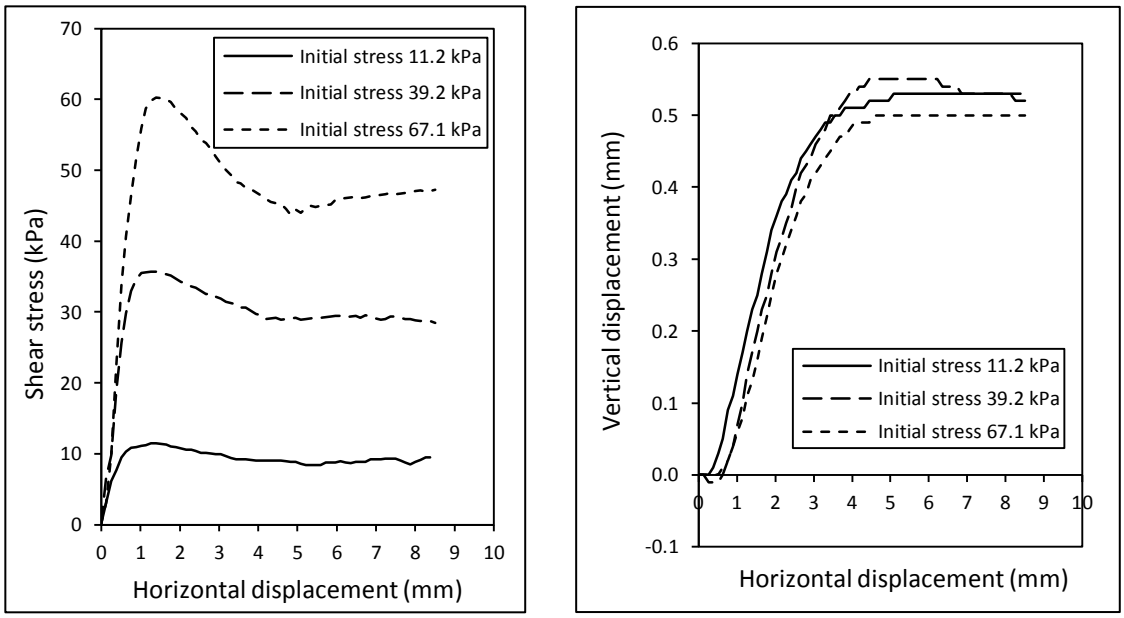

(a) (b)

Figure 5.10 Shear strength behaviour of saturated direct shear test on sand. (a) Shear stress versus displacement curves, and (b) Vertical versus horizontal curve

Table 5.4 shows the summary of the saturated direct shear test on sand. The effective shear strength parameters were obtained by plotting these values on normal versus shear stresses as shown in Figure 5.11. The curve was forced to intercept at (0 ; 0) to comply with the property of cohesionless soil (c' = 0), resulting in the effective internal shear angle of $\phi' = 41.4^{o}$.

Table 5.4 Stresses at failure of sand in saturated direct shear test.

Normal force (kg)	Peak stress (kPa)	
	Normal	Shear
4	11.45	11.48
14	40.09	39.57
24	68.72	68.87

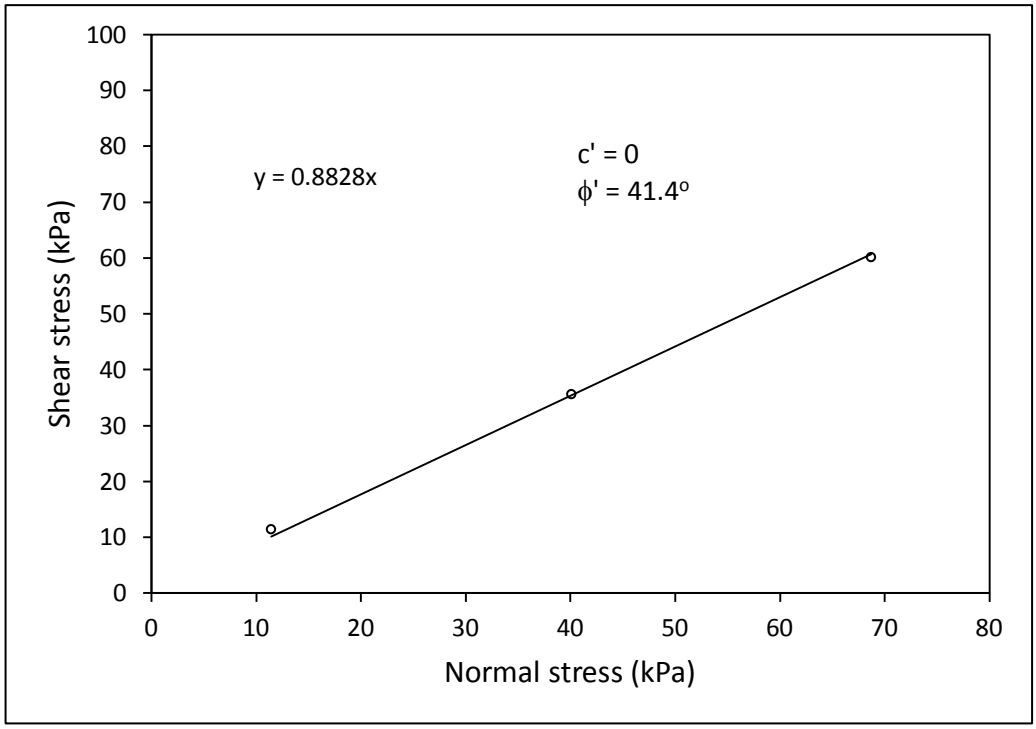

Figure 5.11 Failure envelope of sand from saturated direct shear test.

5.5.2.2 Saturated direct shear on sand-kaolin clay mixtures

Figure 5.12 (a) shows the horizontal displacement versus shear stress curves of the saturated direct shear test on the 95:5 mixture. It can be observed from the figure that the strain hardening behaviour was clearly taking place, starting from zero displacement to displacement at peak stress, followed by strain softening behaviour until a residual value was reached. The lowest dilation was experienced by the specimen when the normal stress of 67.1 kPa was applied, whereas the highest was when the normal stress of 11.2 was imposed (Figure 5.12 (b)). In general, the higher the normal stress, the lower the dilation.

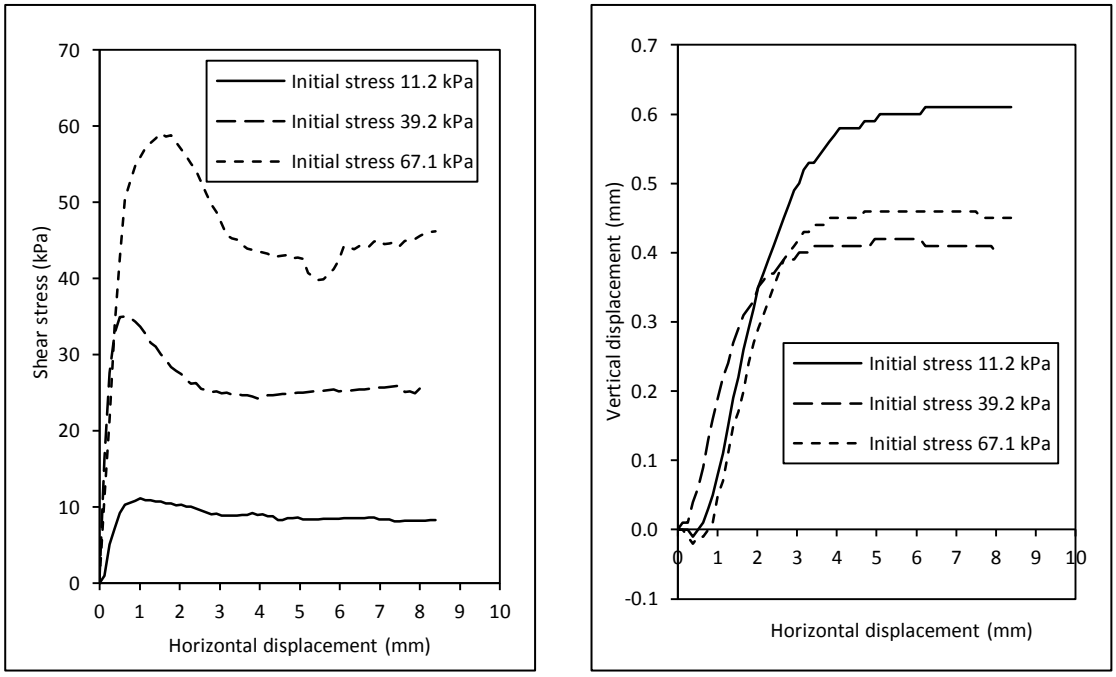

(a) (b)

Figure 5.12 Saturated direct shear result of 95:5 mixture of (a) Shear stress-displacement, and (b) Horizontal versus vertical displacement

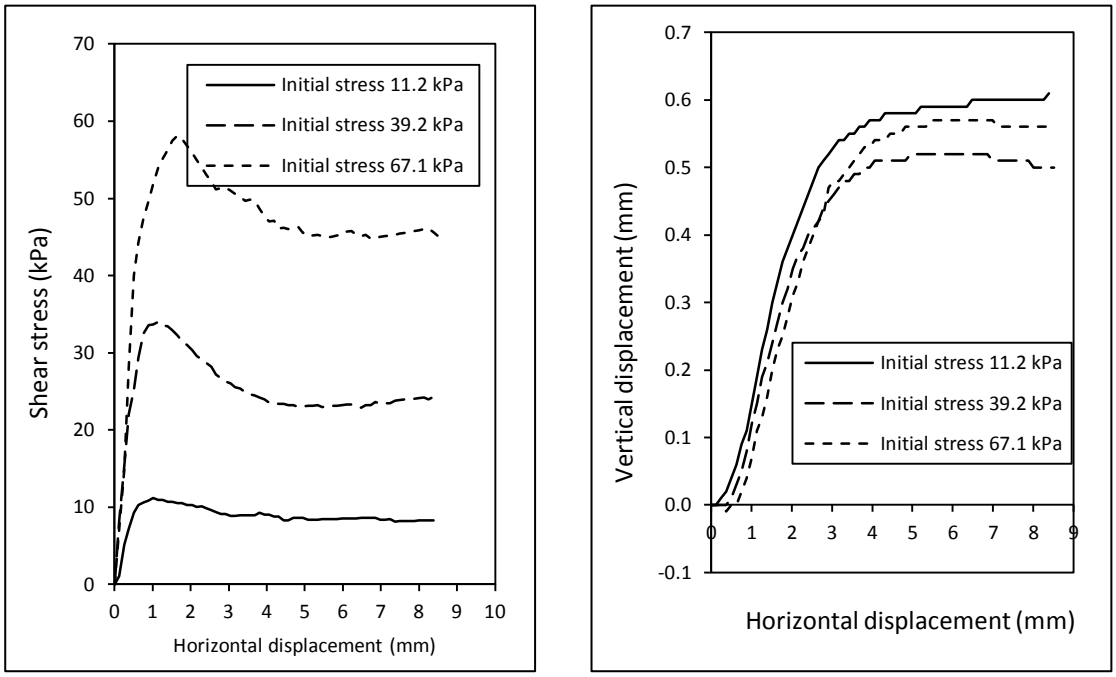

(a) (b)

Figure 5.13 Saturated direct shear result of 90:10 mixture of (a) Shear stress-displacement, and (b) Horizontal versus vertical displacement

Figure 5.13 (a) and (b) shows the shear strength behaviour of 90:10 mixture from the saturated direct shear test. The specimen also exhibited relatively similar (strain hardening and dilation) behaviour to the 95:5 mixture. Table 5.5 shows the summary of the saturated direct shear test on sand and sand-kaolin clay mixtures.

Table 5.5 The summary of saturated direct shear test on sand and sand-kaolin clay mixtures

Normal Load	Sand		95:5 mixture		90:10 mixture	
	Normal stress (kPa)	Peak stress (kPa)	Normal stress (kPa)	Peak s tress (kPa)	Normal stress (kPa)	Peak Stress (kPa)
4 kg	11.45	11.47	11.48	10.71	11.38	11.14
14 kg	40.09	35.73	39.57	35.01	39.91	33.96
24 kg	68.72	60.24	68.87	59.06	69.02	58.14

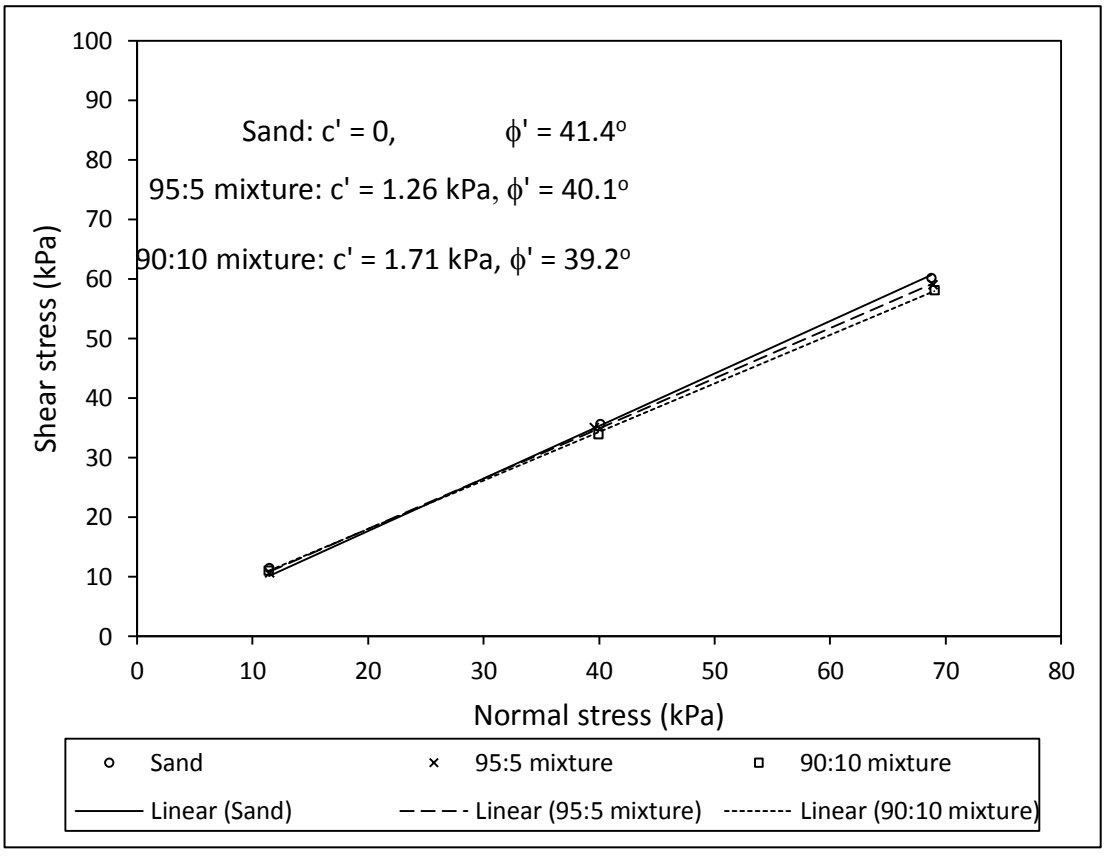

Figure 5.14 Failure envelopes of sand and sand-kaolin clay mixtures resulting from saturated direct shear test

The failure envelopes of sand-kaolin clay mixtures are presented in Figure 5.14. As a comparison, the failure envelope of sand is also presented. It can be observed that the

behaviour of the sand and sand-kaolin clay mixture in saturated conditions was slightly affected by the amount of kaolin (kaolin clay content). The increase in kaolin clay content led to an increase in effective cohesion c' and a decrease in the effective internal friction angle ϕ'.

5.5.3 Direct shear test on unsaturated specimens

Unlike the test for saturated conditions, the unsaturated direct shear test was more complex. Before and during the test, care was taken with the specimen, devices and suction apparatus as described in Chapter 4. In this study, the tensiometer was only used for suction measurement during the unsaturated direct shear test. The result, analysis and discussion are presented in the following section.

5.5.3.1 Equilibration before shearing

Immediately after compaction, the specimen may not be in a homogenous state. Some parts of the specimen may have a higher water content than others. Re-equilibration was then required to achieve homogeneity of the specimen. For this purpose, a preliminary test was carried out to find out the minimum time for equilibration of the specimen before shearing. Three samples were prepared; sand, and mixtures of 95:5 and 90:10. The tensiometer HAED was placed on the surface of the specimens, and suction measurement was performed. Figure 5.15 shows the result of matric suction monitoring, commencing immediately after compaction and continuing for 12 hours. It can be observed that at least 7 hours were required for the specimen to achieve a matric suction equilibrium state. The same test was performed for the specimen when it was air dried. Figure 5.16 shows the matric suction-time curves during the equilibration of the specimen after one day of air-drying. It also indicates that the time period of 12 hours is sufficient for equilibration before shearing.

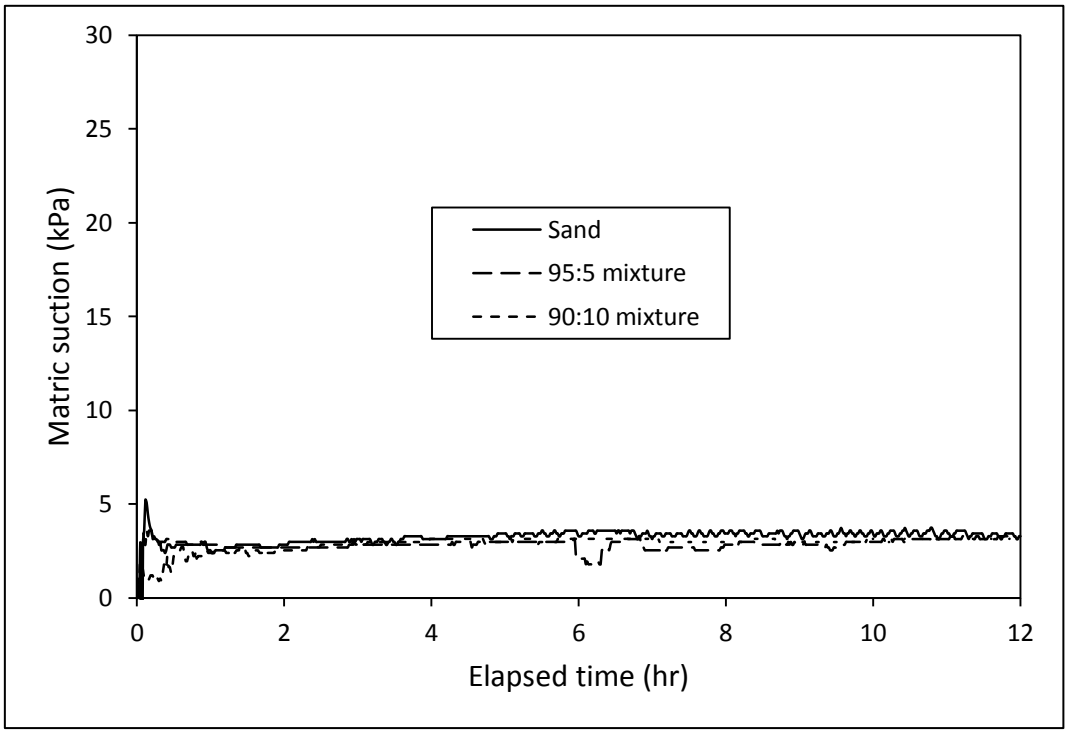

Figure 5.15 Matric suction monitoring for determination of equilibration period before shearing on samples immediately after compaction

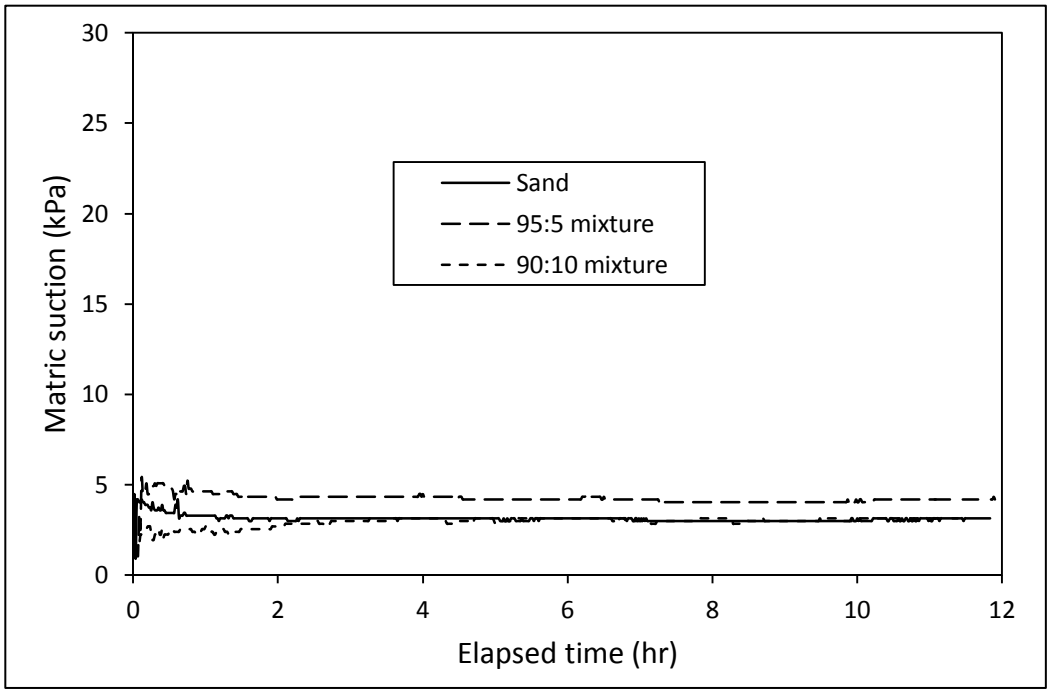

Figure 5.16 Test result of required equilibration period before shearing on samples after one day air drying

5.5.3.2 Unsaturated direct shear test on sand

Figure 5.17 shows the shear stress-displacement curves resulting from the unsaturated direct shear test on sand specimens. There were at least 12 combinations of sand specimens that underwent different treatments. Each specimen/treatment was named as follows: SC denoted sand specimens immediately after compaction, SD1, SD2, SD3 and SD4 denoted sand specimens after drying treatment for the different time periods being: T1, T2, T3, and T4, at which T1 < T2 < T3 < T4. Due to drying after compaction, the water content of SD1 was higher than SD2, and SD3 > SD4 > SD4.

During shear, the matric suction for each test was recorded. Figure 5.18 shows the typical result of the matric suction measurement on sand specimens during shear at an initial normal stress of 11.2 kPa. It can be seen from the figure that the longer the drying period, the higher the negative pore water pressure (matric suction).

The peak stress and the corresponding matric suction of each test and each normal load including the peak stresses from the saturated direct shear tests were plotted to construct the unsaturated failure envelopes. The average normal stresses were calculated from the normal stress at failure from the saturated and unsaturated data as summarised in Table 5.6. Figure 5.19 shows the failure envelopes of sand resulting from unsaturated direct shear tests. Note that the shear strengths with zero matric suction were obtained from previous saturated direct shear tests. It can be seen from Figure 5.19 that the variation of shear strength with respect to matric suction is non-linear. The slope of the curve, denoted by ϕ^b, indicated the rate of shear strength increase due to the increase in matric suction. According to Fredlund and Rahardjo (1993), the magnitude of ϕ^b was normally equal to or smaller than the effective friction angle ϕ'. However, there were many cases in which $\phi^b > \phi$' (e.g. Donald (1957), Likos, et al., (2010), Nam et al., (2011)). According to Likos, et al., (2010), this phenomenon occurred due to the effect of dilation as a result of the complex response of unsaturated sand.

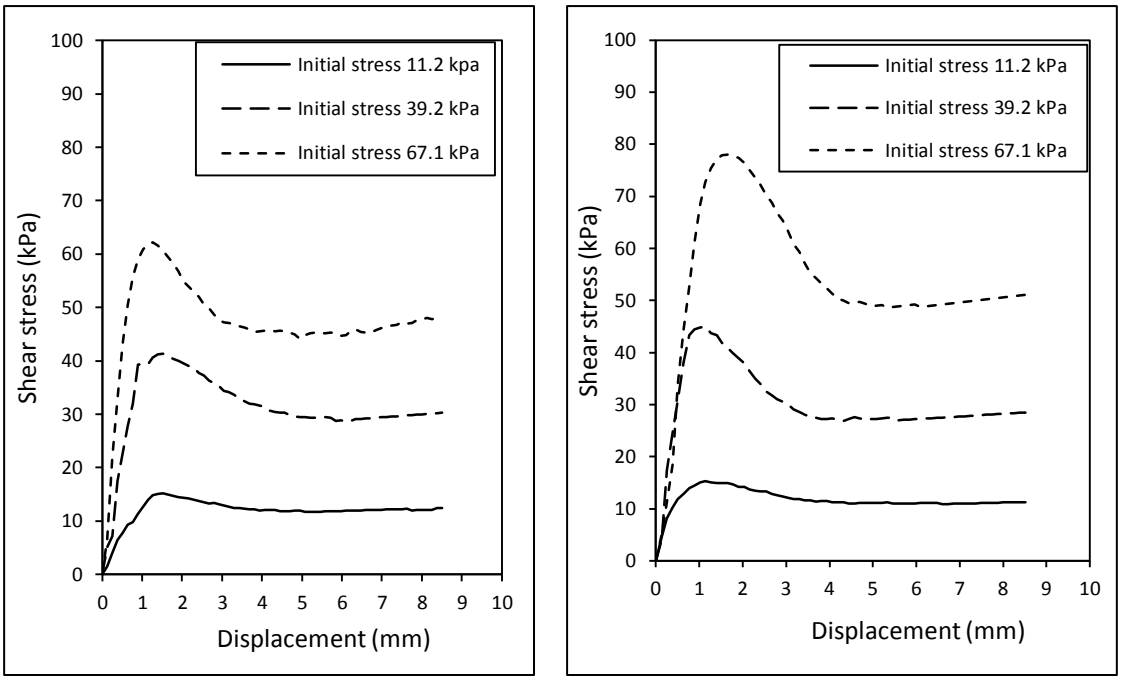

(a) (b)

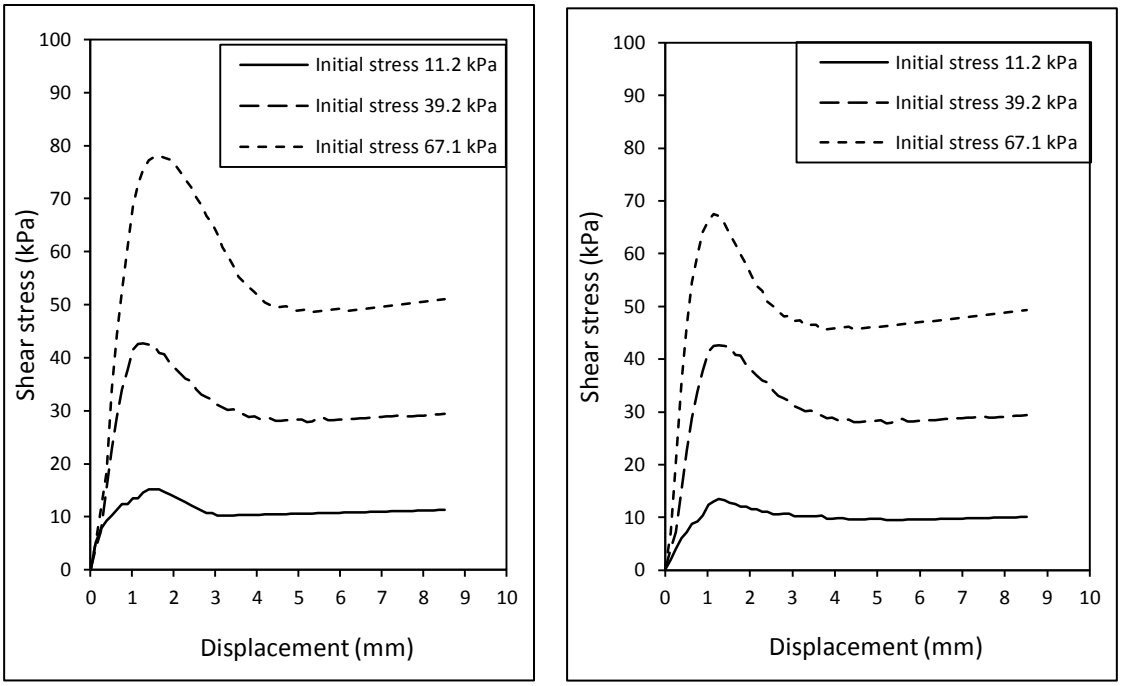

(c) (d)

Figure 5.17 Shear-displacement curves of unsaturated direct shear test on sand at different drying periods, (a) specimen SC, (b) Specimen SD1, (c) specimen SD2, and (d) specimen SD3

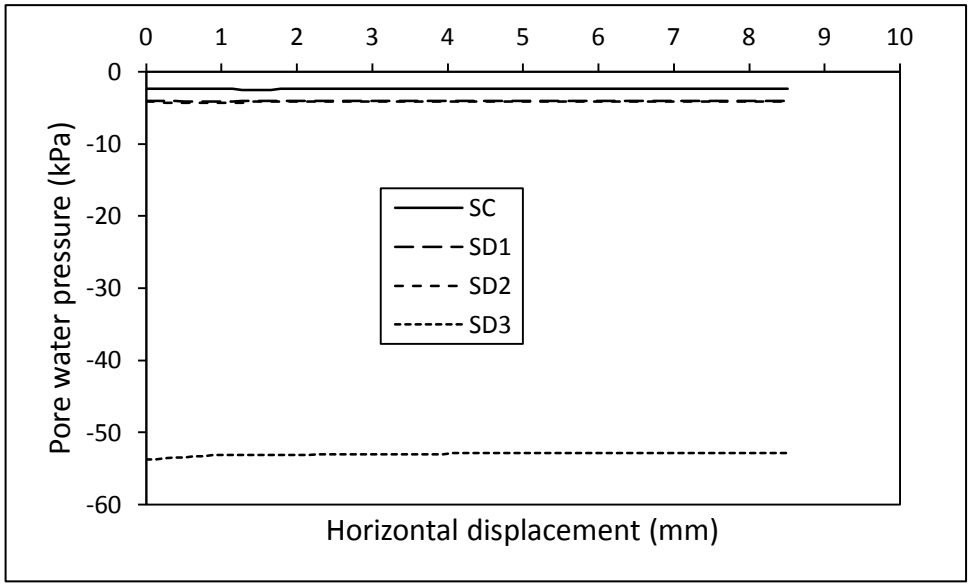

Figure 5.18 Typical plot of horizontal displacement versus pore water pressure (matric suction) on sand at initial normal stress of 11.2 kPa

Table 5.6 Average normal stresses at failure of sand (in kPa)

Specimen	Initial normal stress 11.2 kPa			Initial normal stress 39.2 kPa			Initial normal stress 67.1 kPa		
	Suction	Shear	Normal	Suction	Shear	Normal	Suction	Shear	Normal
Sat	0	11.47	11.45	0	35.72	40.09	0	60.23	68.72
SC	2.54	15.16	11.48	2.69	41.29	40.17	2.24	60.63	68.87
SD1	4.18	15.32	11.40	4.48	44.92	39.91	4.18	78.05	69.02
SD2	4.18	15.19	11.50	4.63	46.32	40.00	5.52	77.71	68.72
SD3	53.13	13.53	11.43	65.82	42.67	40.00	56.87	67.51	68.42
		Ave	11.5		Ave	40.2		Ave	68.7

The curve formed two lines with two different slopes. Starting from zero suction until residual suction (ψ_r = 5 kPa), the slope ϕ^b was steep, with $\phi^b > \phi$'. Beyond the residual suction, the increase in matric suction caused a decrease in shear strength (the magnitude ϕ^b was negative). This result agreed with the common behaviour of unsaturated sand as stated by Vanapalli and Lacasse (2010).

It can be observed from Figure 5.19 that the change of ϕ^b clearly started and took place in the suction range between the air entry value (AEV) and residual suction ψ_r. Vanapalli (1999) named this range of suction as the transition zone. The magnitude of ϕ^b was also affected by the magnitude of applied normal stress. The higher the

normal stress applied, the higher the angle ϕ^b. The difference value of ϕ^b was presumably caused by different mechanisms of particle interaction due to different initial void ratios. From the studied literature it has been found that this phenomenon occurred in most cases.

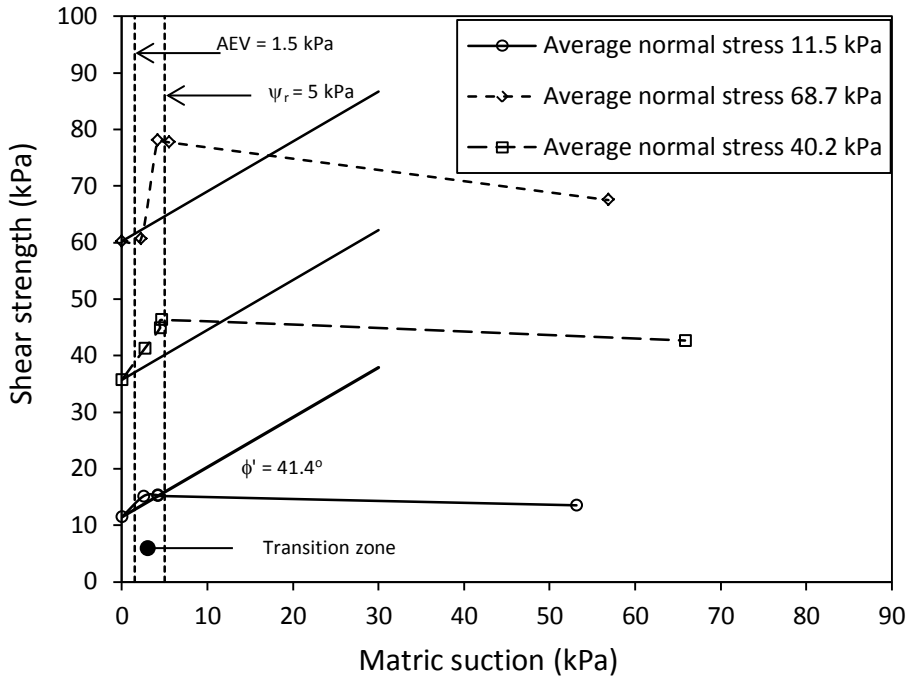

Figure 5.19 Plot of variation of shear strength with respect to matric suction of sand.

5.5.3.3 Unsaturated direct shear test on 95:5 mixture

Similar to the the test on sand, a number of specimens of 95:5 mixtures were also prepared. For simplification purposes, each specimen was named according to its treatment. M95C denoted the 95:5 mixture immediately after compaction, whereas M95D1, M95D2, M95D3, and M95D4 denoted the 95:5 mixture after drying for the periods of time T1, T2, T3, and T4 respectively at which T1 < T2 < T3<T4.

Figure 5.20 shows the shear stress-displacement curves resulting from the unsaturated direct shear test on the 95:5 mixture. The average normal stresses were calculated from the saturated and unsaturated data, as summarised in Table 5.7.

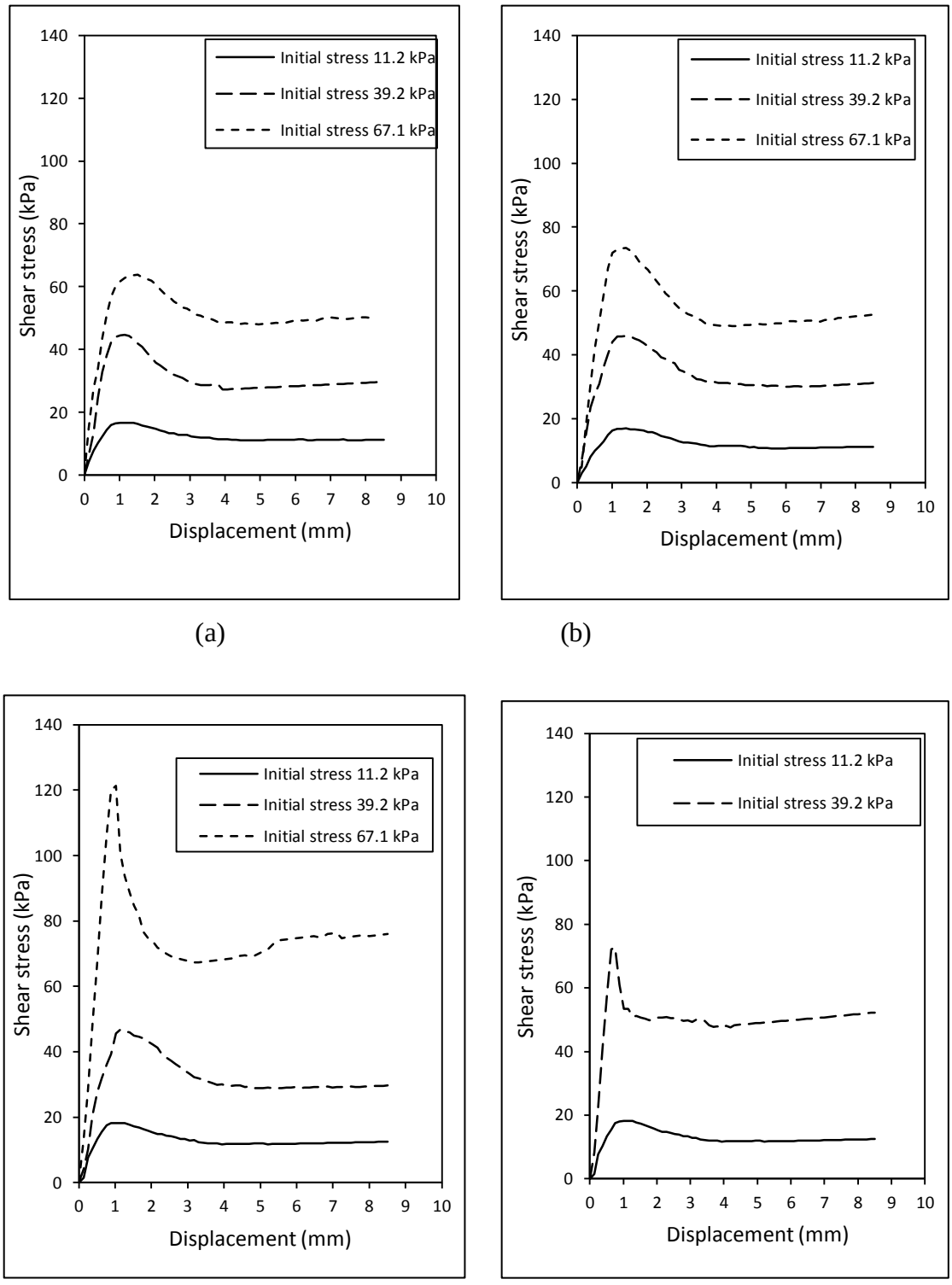

Figure 5.20 Shear stress-displacement curves of unsaturated direct shear test of 95:5 mixture at different drying periods, (a) specimen M95C, (b) specimen M95D1, (c) specimen M95D2, and (d) specimen M95D3

Table 5.7 Average normal stresses at failure of 95:5 mixture (in kPa)

Specimen	Initial normal stress 11.2 kPa			Initial normal stress 39.2 kPa			Initial normal stress 67.1 kPa		
	Suction	Shear	Normal	Suction	Shear	Normal	Suction	Shear	Normal
Sat	0	10.71	11.48	0	30.05	39.57	0	59.06	68.87
M95C	2.69	16.69	11.45	3.13	44.66	39.91	2.99	63.77	68.87
M95D1	5.22	16.95	11.45	7.31	46.74	39.91	4.93	73.54	68.72
M95D2	11.49	18.21	11.43	15.67	50.48	40.00	68.66	121.25	68.27
M95D3	29.10	20.47	11.38	65.67	72.75	39.65			
		Ave	11.4		Ave	39.9		Ave	68.7

Figure 5.21 shows the failure envelopes of the 95:5 mixture resulting from unsaturated direct shear tests. The curves also formed a bi-linear pattern as exhibited by the sand specimens in Figure 5.19. From zero suction until air entry value (AEV), the slope of shear strength with respect to matric suction was linear with $\phi^b > \phi'$. After AEV, the rate of shear strength increase with respect to matric suction was smaller than the previous one, with the result that the magnitude of ϕ^b was smaller than the effective shear angle ($\phi^b < \phi'$). In other words, the magnitude of ϕ^b was always lower than that the magnitude of ϕ', except for where matric suction was less than the AEV. As previously discussed, the high ϕ^b was presumably caused by the effect of dilation.

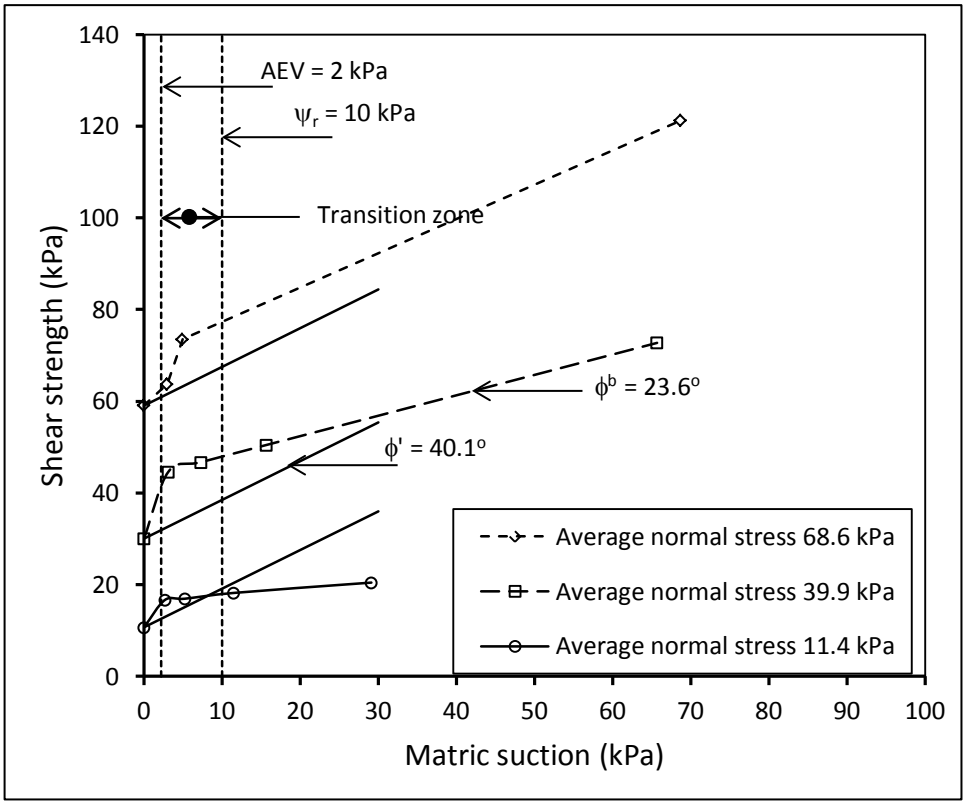

Figure 5.21 Plot of variation of shear strength with respect to matric suction of 95:5 mixture

5.5.3.4 Unsaturated direct shear test on 90:10 mixture

Figure 5.22 shows the shear stress-displacement curves resulting from the unsaturated direct shear test of 90:10 mixture. The average normal stresses are summarised in Table 5.8. Each specimen was named according to its treatment; M90C denoted the 90:10 mixture immediately after compaction, M90D1 denoted the specimen after the drying period T1, and M90D2 was the specimen after drying period T2.

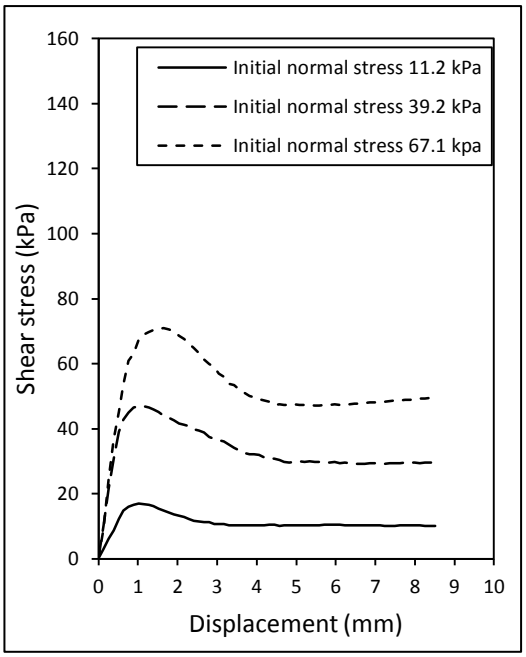

(a)

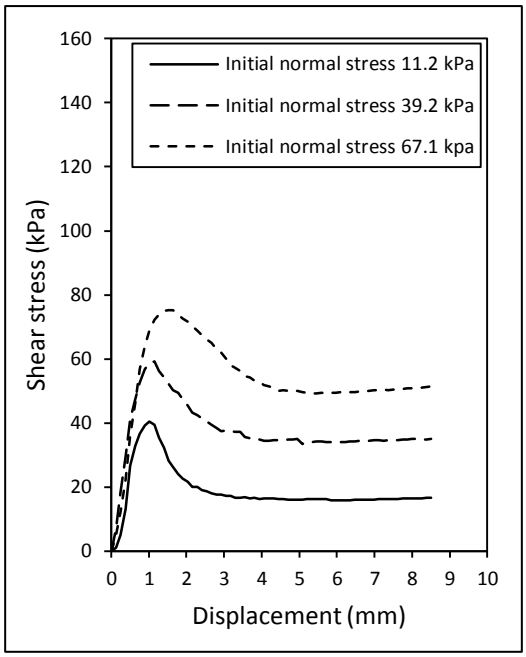

(b)

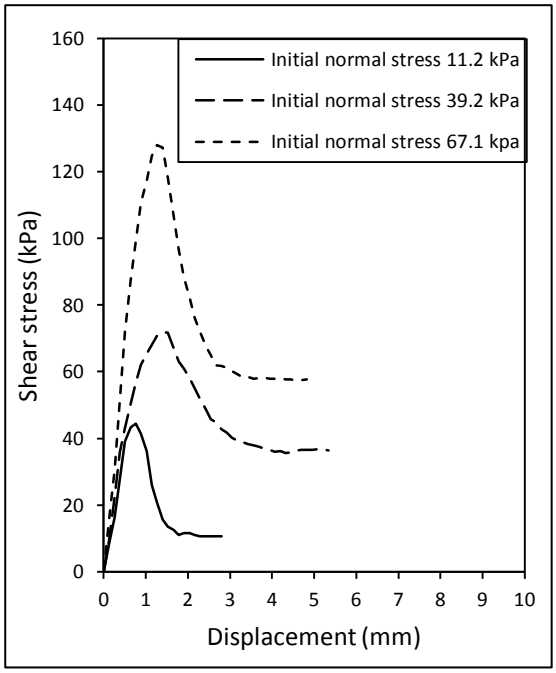

(c)

Figure 5.22 Shear stress-displacement curves of unsaturated direct shear test of 90:10 mixture at different drying periods, (a) specimen M90C, (b) specimen M90D1, (c) specimen M90D2

Table 5.8 Average normal stresses at failure of 90:10 mixture (in kPa)

Specimen	Initial normal stress 11.2 kPa			Initial normal stress 39.2 kPa			Initial normal stress 67.1 kPa		
	Suction	Shear	Normal	Suction	Shear	Normal	Suction	Shear	Normal
Sat	0	11.14	11.38	0	33.68	39.91	0	61.42	68.72
M90C	3.73	17.10	11.38	4.63	47.00	39.91	4.33	70.98	69.02
M90D1	55.07	40.42	11.38	22.99	59.20	39.91	12.99	96.59	68.42
M90D2	64.18	44.37	11.38	48.51	71.97	40.09	55.82	128.02	68.57
		Ave	11.4		Ave	39.9		Ave	68.7

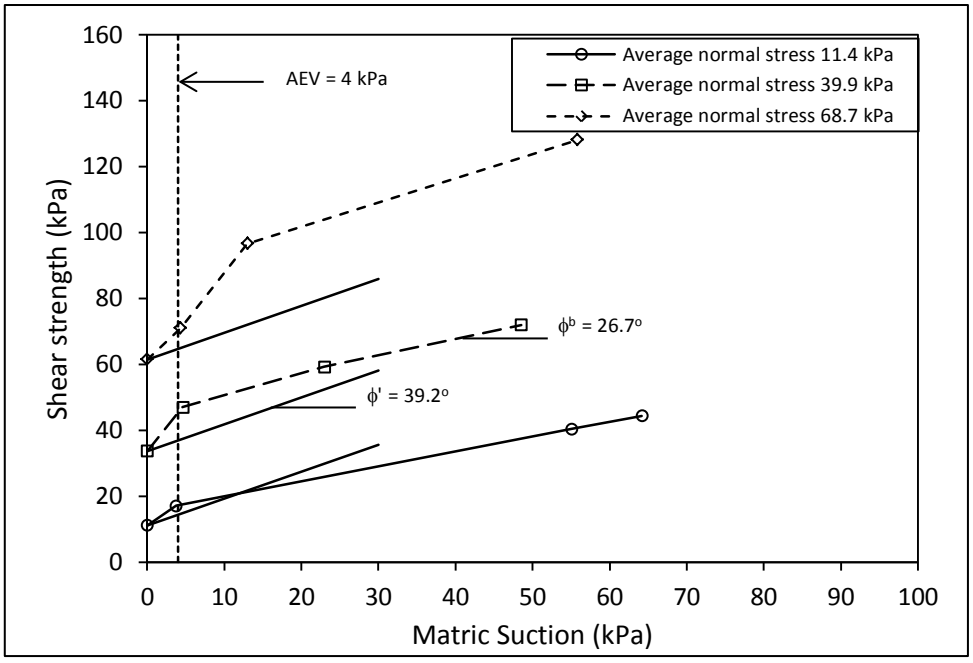

Figure 5.23 Plot of variation of shear strength with respect to matric suction of 90:10 mixture.

Figure 5.23 shows failure envelopes of 90:10 mixture. The results indicate that the failure envelopes formed a bi-linear pattern as exhibited by sand specimens and the 95:5 mixture in the previous tests. From zero suction up to the AEV, point, the slope ϕ^b was higher than the effective friction angle ϕ'. Beyond the AEV, the slope ϕ^b was lower than the effective friction angle ϕ'.

5.6 CBR test

The CBR with suction measurement was performed following the procedure described in section 4. The set-up of the CBR test was made in such a way that the tensiometers were able to monitor the suction during the test. For simplification, the specimen was assumed to have two layers or upper and bottom halves. The matric suction of the upper layer was obtained from the average values obtained from tensiometer T1 (top) and tensiometer T2 (middle). Tensiometer T3 (bottom) was placed to record the matric suction in the bottom half of the specimen. Figure 5.24 shows the illustration of the tensiometer placement during the test.

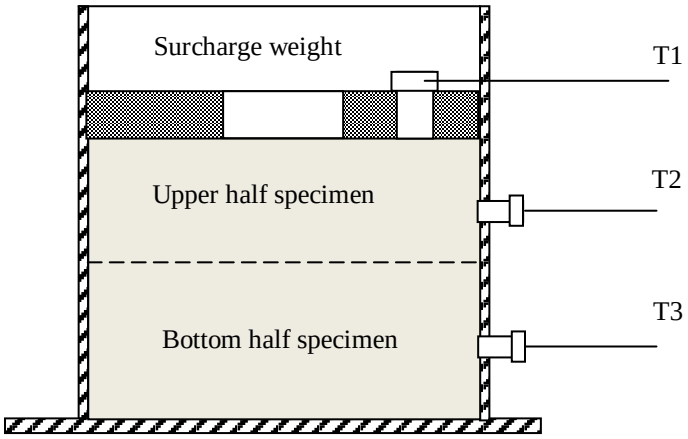

Figure 5.24 Tensiometer placement of CBR test

Due to the penetration of the CBR piston, the upper half of the specimen deformed in a vertical direction. The relation between the CBR value and the matric suction of the upper half of specimen was investigated in this study. The result, analysis and discussion are presented as follows.

5.6.1 CBR test on sand

Figure 5.25 shows the typical plot of the CBR test of sand from the soaked specimen (soaked CBR). The displacement versus force during penetration is presented in Figure 5.25 (a). The CBR was defined as the magnitude of force resulting from 0.1 in. (2.5 mm) of penetration after correction. The CBR was calculated as:

$$CBR = \frac{2}{13.2} \times 100\ \% = 15.2\ \%$$

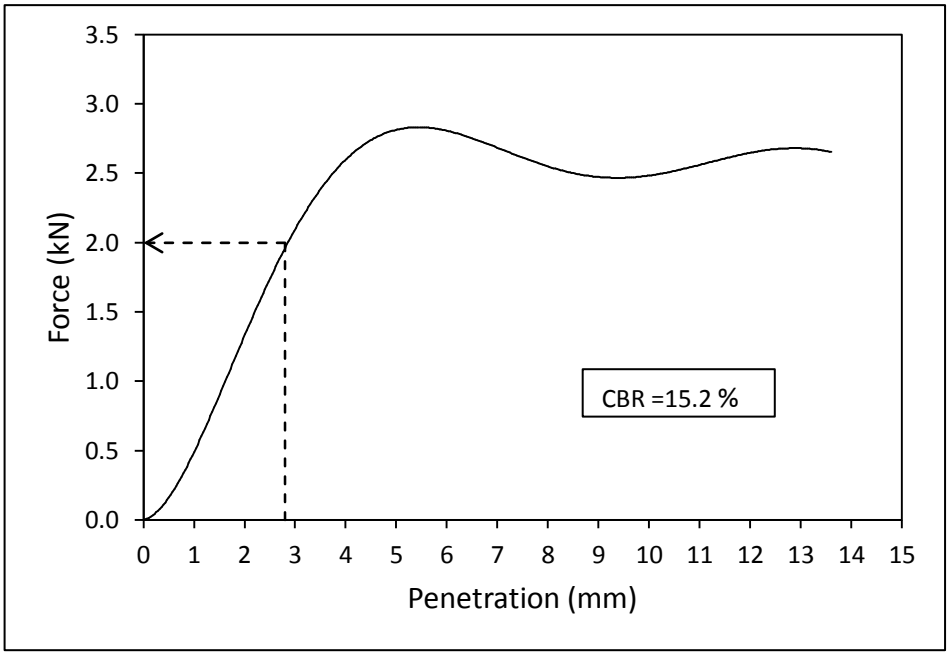

(a)

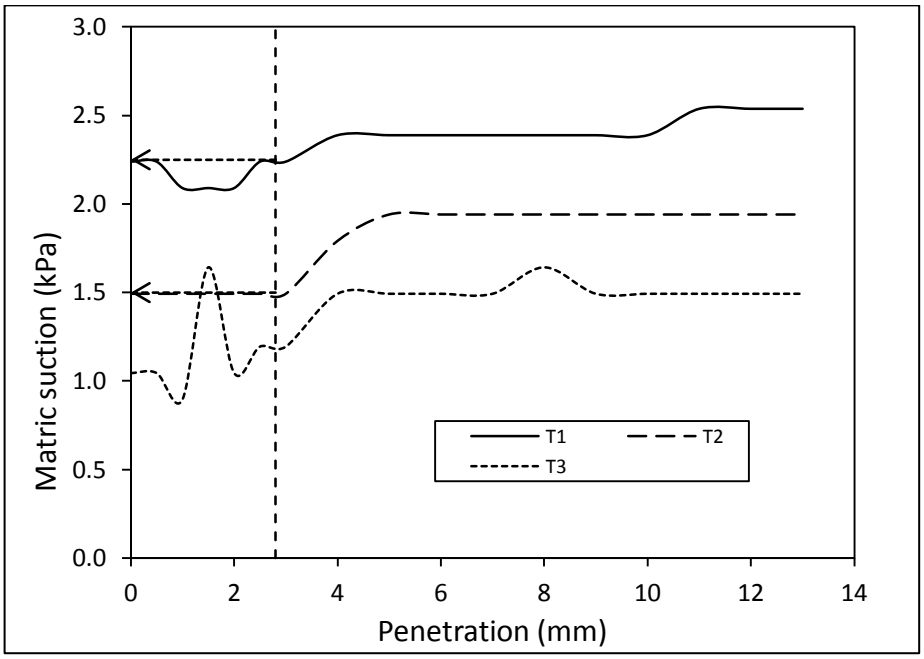

(b)

Figure 5.25 Typical result of soaked CBR test with suction measurement of sand. (a) Force versus penetration. (b) Matric suction versus penetration during test

Figure 5.25 (b) shows the corresponding matric suction during the test. T1, T2, and T3 denote the matric suction recorded from the top, middle and bottom tensiometers respectively. It can be observed from this figure that different parts of the specimen

caused different matric suction readings. Seemingly this was due to the different water content in different parts of the specimen; the lower the water content, the higher the matric suction. The movement of pore water during the penetration may have caused the change in matric suction. For the sand specimen, the matric suction of the upper half was 1.9 kPa, obtained from the average matric suction of T1 and T2. After completing the CBR test, the specimen given a water content test of the upper and bottom layers.

Figure 5.26 (a) and (b) show the plot of penetration versus force and the corresponding matric suction during the test on unsoaked specimens. The result indicated that both CBR and matric suction were slightly higher compared to the soaked CBR. The matric suction of T1, T2 and T3 were slightly different due to lack of homogeneity of the water content in the specimen. Immediately after compaction, the water content in the bottom half of the specimen was lower than the water content in the upper half, and as a consequence, matric suction in the bottom half was higher than matric suction in the upper half.

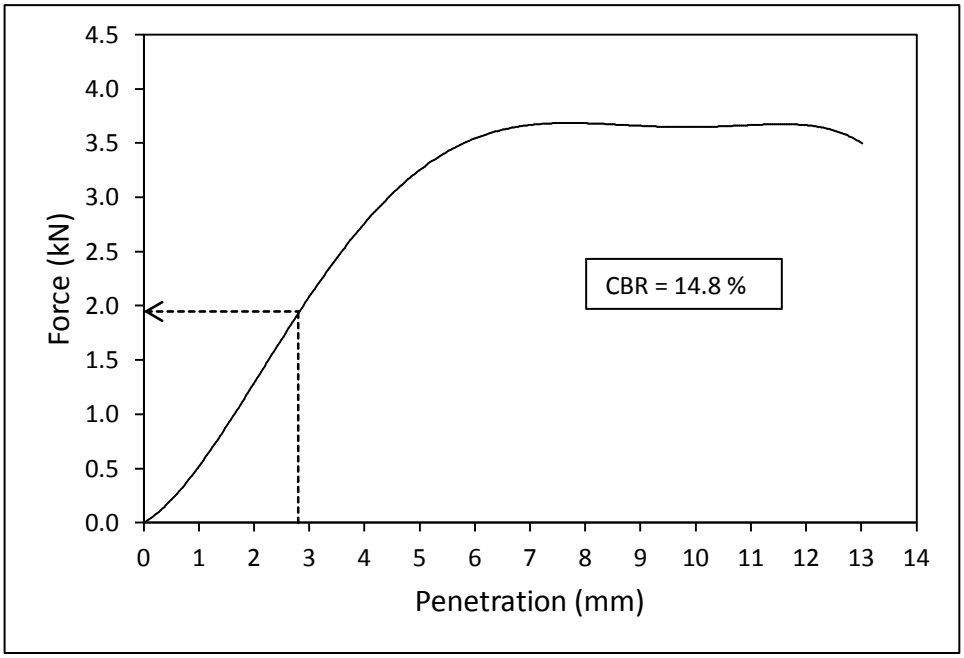

(a)

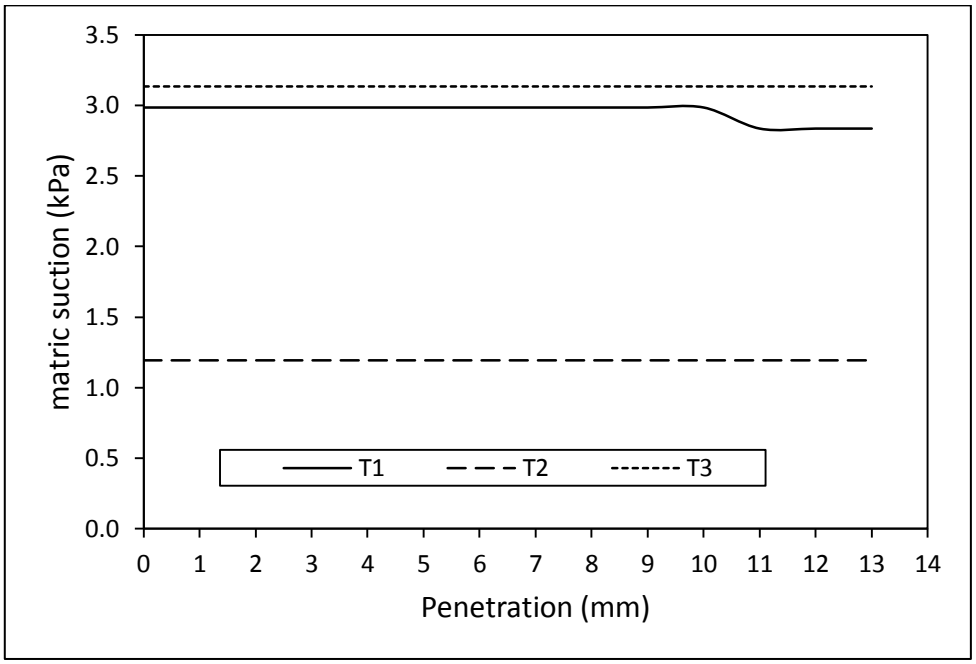

(b)

Figure 5.26 Plot of CBR test of sand from unsoaked CBR. (a) Force versus penetration and (b) Matric suction versus penetration during test

A similar test was also performed on other sand specimens with different water content. The purpose of the differing water contents was to generate different matric

suction by the air drying method, as previously described in the Chapter 4. The plots of all sand specimens are presented in the Appendices. The CBR versus matric suction and water content from all tests on sand specimen were summarised in Table 5.9, and presented graphically as shown in Figure 5.27. Starting from the air entry value suction (AEV) until near residual suction, the increase in matric suction caused an increase in CBR. After residual suction, the increase in matric suction caused a decrease in CBR. It can be observed that an approximate bi-linear curve was formed from this plot. As a comparison, the plot of CBR versus water content is also presented here, as shown in Figure 5.28.

Table 5.9 The summary of CBR and corresponding matric suction and water content of sand

CBR (%)	15.15	14.77	20.08	22.73	20.83	19.32
Matric suction (kPa)	1.9	2.1	6.1	6.7	27.0	42.5
Water content (%)	16.9	11.6	4.0	3.3	4.2	3.2

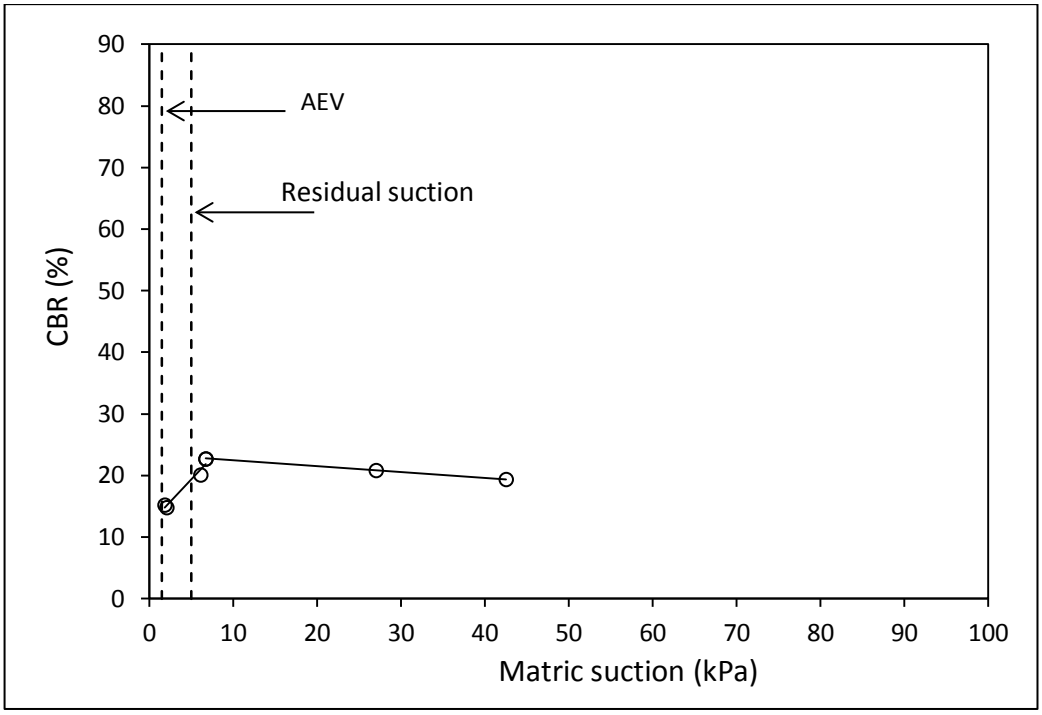

Figure 5.27 Plot of matric suction versus CBR of sand specimen

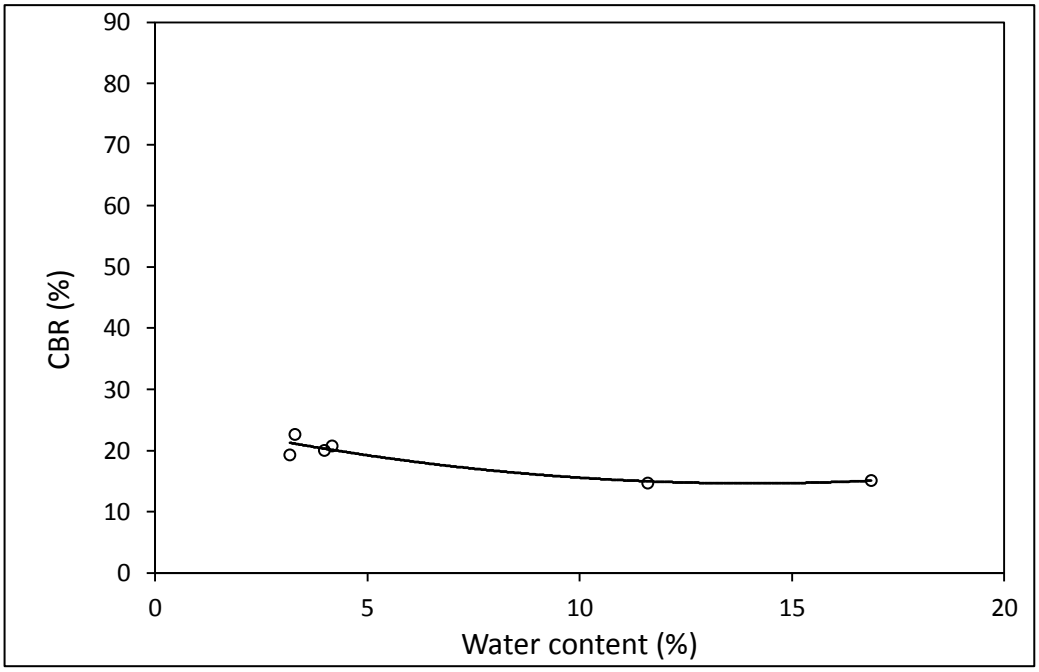

Figure 5.28 Plot of water content versus CBR of sand specimen

5.6.2 CBR test on sand-kaolin mixtures

Figure 5.29 shows the plot of water content versus CBR of all specimens (sand, 95:5 mixture, and 90:10 mixture). The curves of the 95:5 and 90:10 mixtures illustrate the non-linear relation of CBR-water content due to the decrease in water content from air-drying. Until its water content reached the optimum (OWC), the CBR increased slightly as the water content decreased. The significant increase rate in the CBR occurred when the water content of the specimen was less than that of the OWC. Similar behaviour was reported by Ampadu (2007) for the CBR test on lateritic soil.

Figure 5.30 shows the plot of matric suction versus the CBR. It can be observed from the figure that the relation between the CBR and matric suction forms a bi-linear curve. The first part of the curve starts from near zero matric suction (soaked sample) to near air entry value (AEV) with a significant increase in CBR. The second part starts from near AEV with a relatively slower increase in CBR. Matric suction never attained a zero value even though the sample was soaked for four days. The reason for this is that the test was performed 15 minutes after removing the mould from the bath. Some of the water in the specimen may infiltrate through the base, and some may evaporate. In general, the matric suction versus the CBR of these particular

specimens exhibited a bi-linear curve with the inflection points occurring after passing the AEV point.

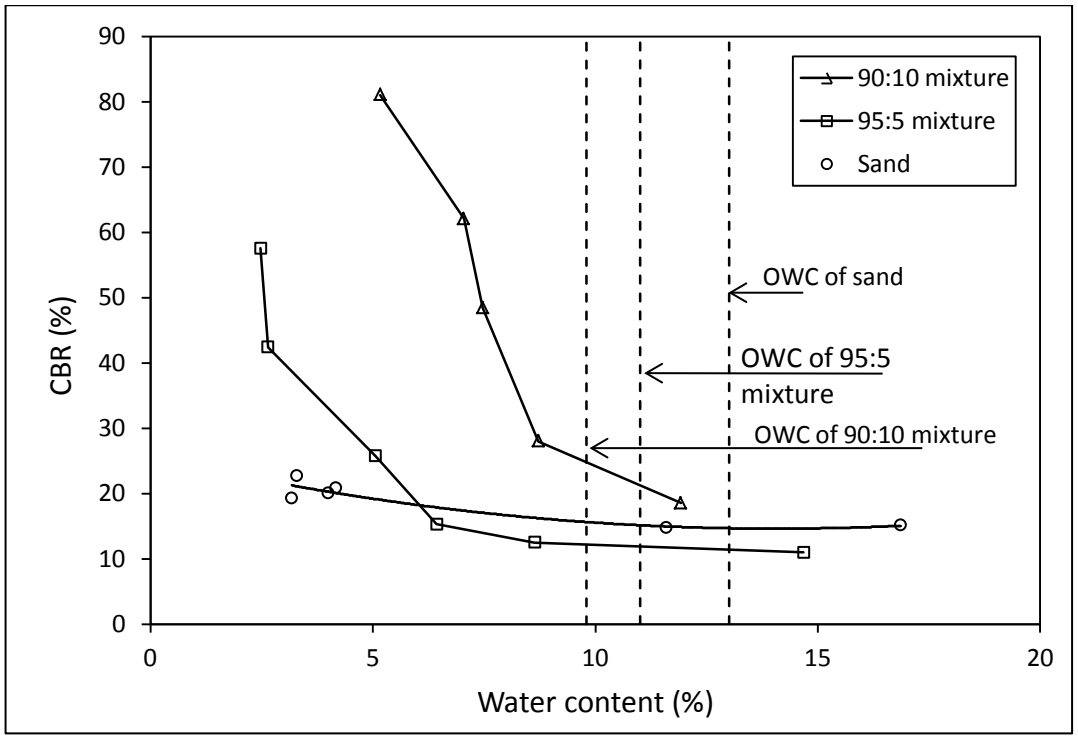

Figure 5.29 Plot of water content versus CBR of sand and sand-kaolin clay mixtures

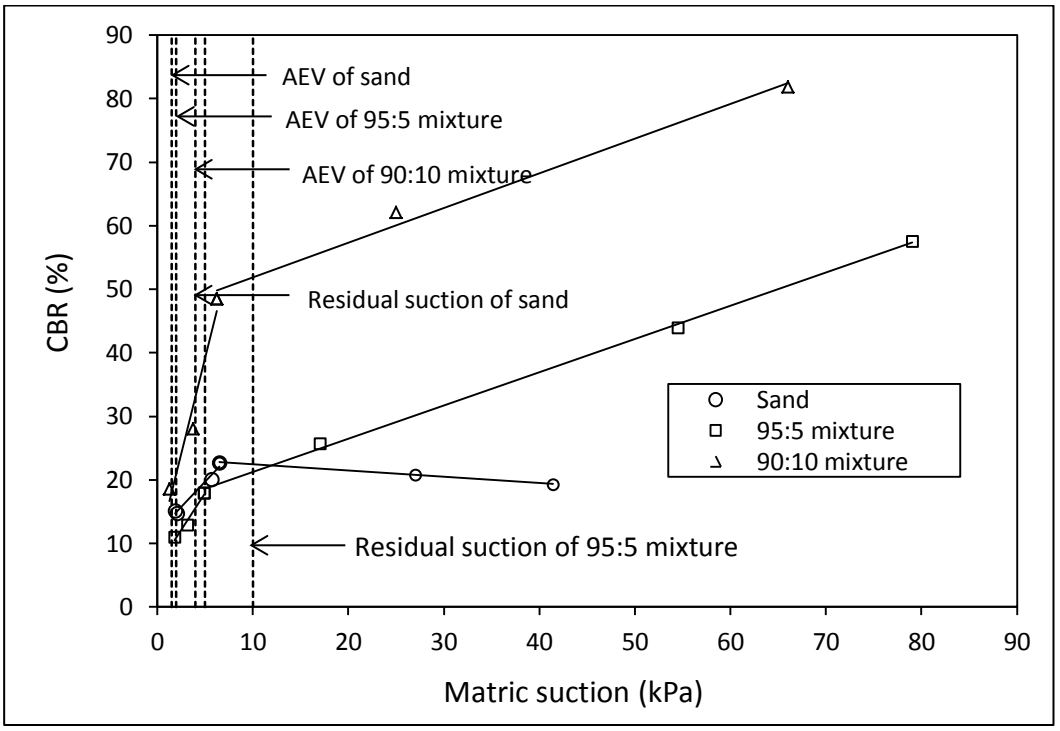

Figure 5.30 Plot of matric suction versus CBR of sand and sand-kaolin clay mixtures

5.7 Correlation between CBR and unsaturated shear strength

The CBR and shear strength tests in which suction was taken into consideration can be time consuming and costly. The laboratory procedure associated with the devices and specimen preparation of both tests is complex. The correlation was based on the data from both suction-monitored-CBR and suction-monitored direct shear tests on sand, 95:5, and 90:10 sand-kaolin clay mixtures. Due to the limited range of suction measurements, this correlation may only be valid for the particular range of suction from zero to 80 kPa.

The correlation was developed by plotting 5 kPa interval of suction of the failure envelopes of sand from Figure 5.19 in Section 5.5.3.2 and the suction-CBR curve for sand from Figure 5.30. The results are presented in Figure 5.31 below. It can be seen that the single value of the CBR can be obtained from the failure envelopes of unsaturated sand, from initial normal stresses of 11.2 kPa, 39. 2 kPa, or 67.1 kPa. The range of R-square values between 0.87 and 0.92 indicated that these correlations were reasonable.

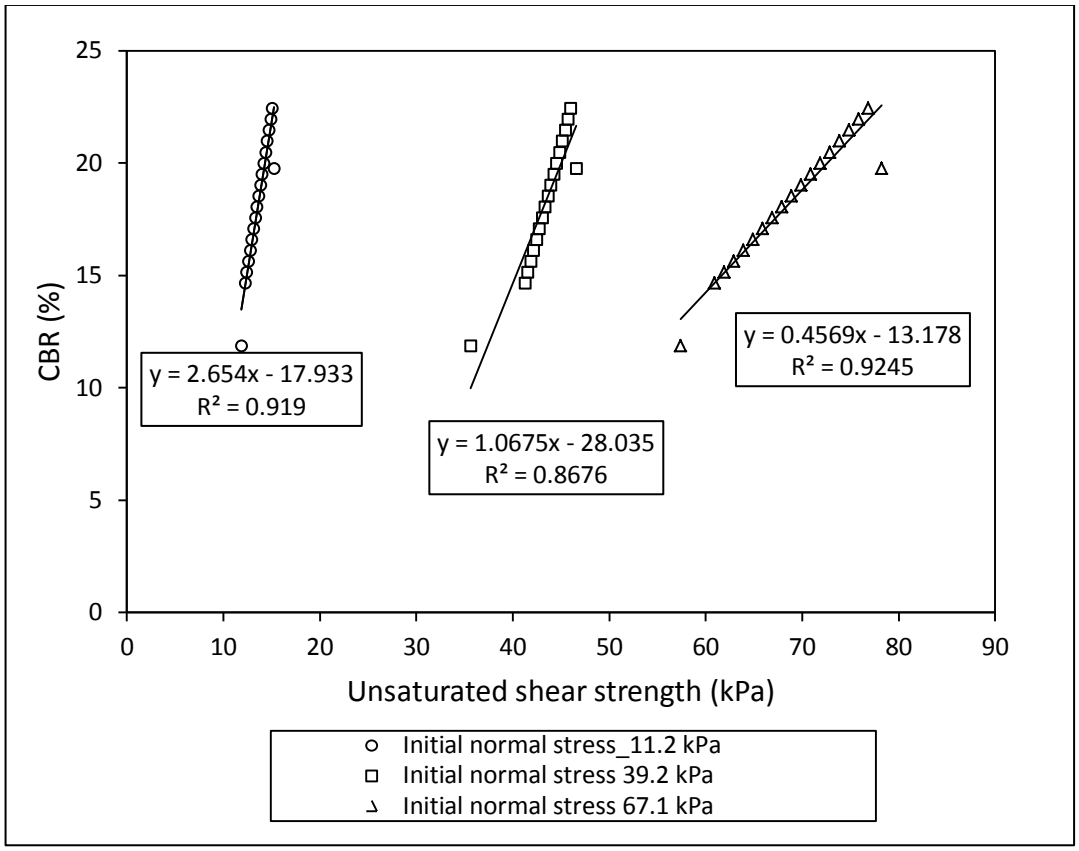

Figure 5.31 The correlation between unsaturated shear strength and CBR for sand

A similar method was adopted to correlate the CBR and unsaturated shear strength for the 95:5 and 90:10 mixtures. The equations and R-square values are presented in Figure 5.32 and Figure 5.33 respectively. The high R-square values of these equations indicated a positive correlation between the CBR and unsaturated shear strength. Table 9.10 summarises the correlations for all specimens.

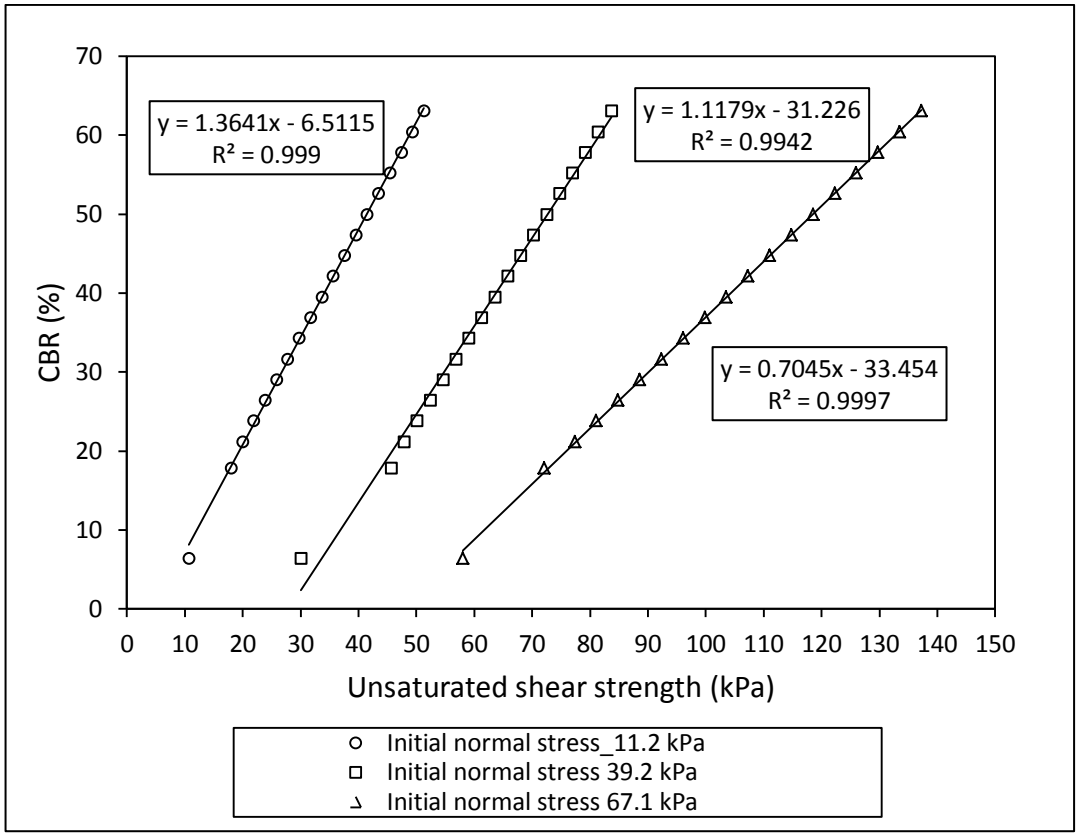

Figure 5.32 The correlation between unsaturated shear strength and CBR for 95:5 mixture

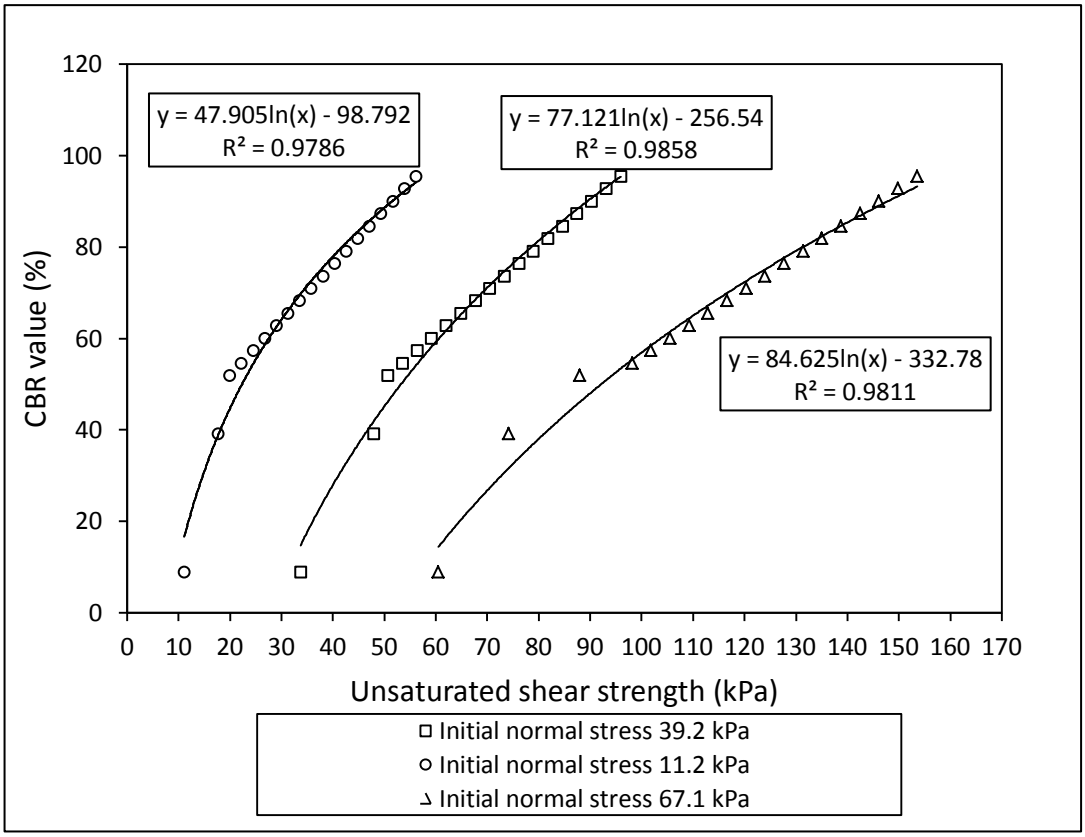

Figure 5.33 The correlation between unsaturated shear strength and CBR for 90:10 mixture

Table 5.10 The summary of correlations for all specimens

Specimen	σ_n (kPa)	Correlation	Equation
Sand	11.2	$CBR_u = 2.7\tau_u - 17.9$	(5.2)
	39.2	$CBR_u = 1.07\tau_u - 28$	(5.3)
	67.1	$CBR_u = 0.46\tau_u - 13.2$	(5.4)
95:5 mixture	11.2	$CBR_u = 1.36\tau_u - 6.5$	(5.5)
	39.2	$CBR_u = 1.12\tau_u - 31.2$	(5.6)
	67.1	$CBR_u = 0.7\tau_u - 33.45$	(5.7)
90:10 mixture	11.2	$CBR_u = 47.9\ln(\tau_u) - 98.8$	(5.8)
	39.2	$CBR_u = 77.1\ln(\tau_u) - 256.54$	(5.9)
	67.1	$CBR_u = 84.63\ln(\tau_u) - 332.78$	(5.10)

Note: CBRu is unsaturated CBR, σ_n is initial net normal stress of direct shear

As examples, Figure 5.34, 5.35, and 5.36 demonstrates the comparison resulting from experimental and correlations of sand, 95:5, and 90:10 mixtures using the equations (5.3), (5.6) and (5.9) respectively. It can be seen that the plot of unsaturated shear strength-CBR resulting from the experiment is very similar to the plot resulting from correlation. It has been observed that a slight difference between the experiment and correlation was taken place near the air entry value (AEV) of the

specimen, at which the inflection point between the first line and the second line of the bi-linear curve took place.

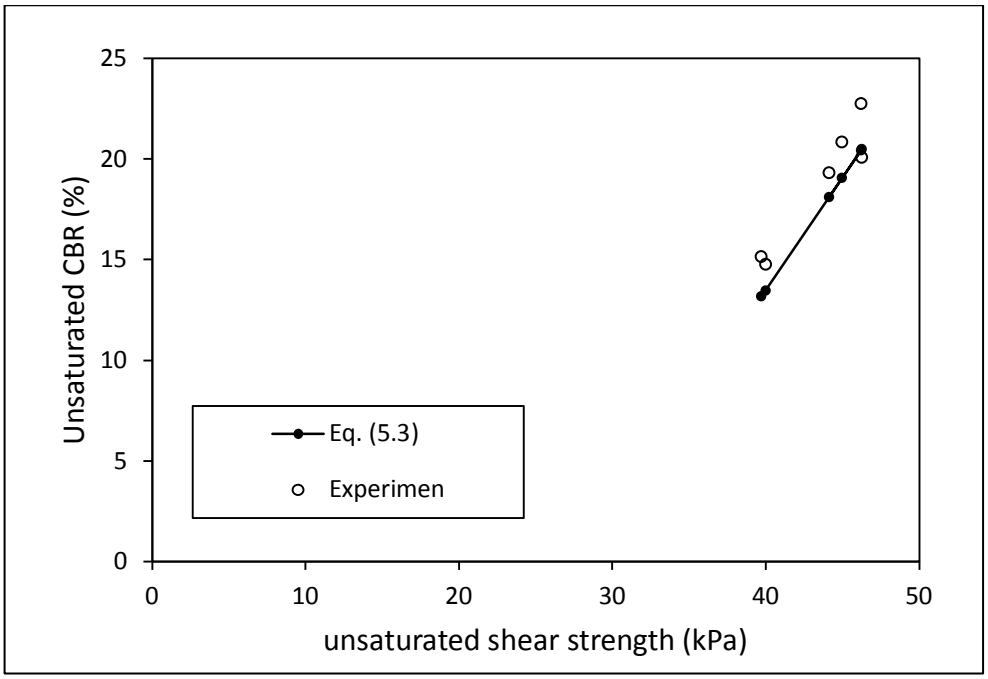

Figure 5.34 The comparison of experimental and correlation results of sand

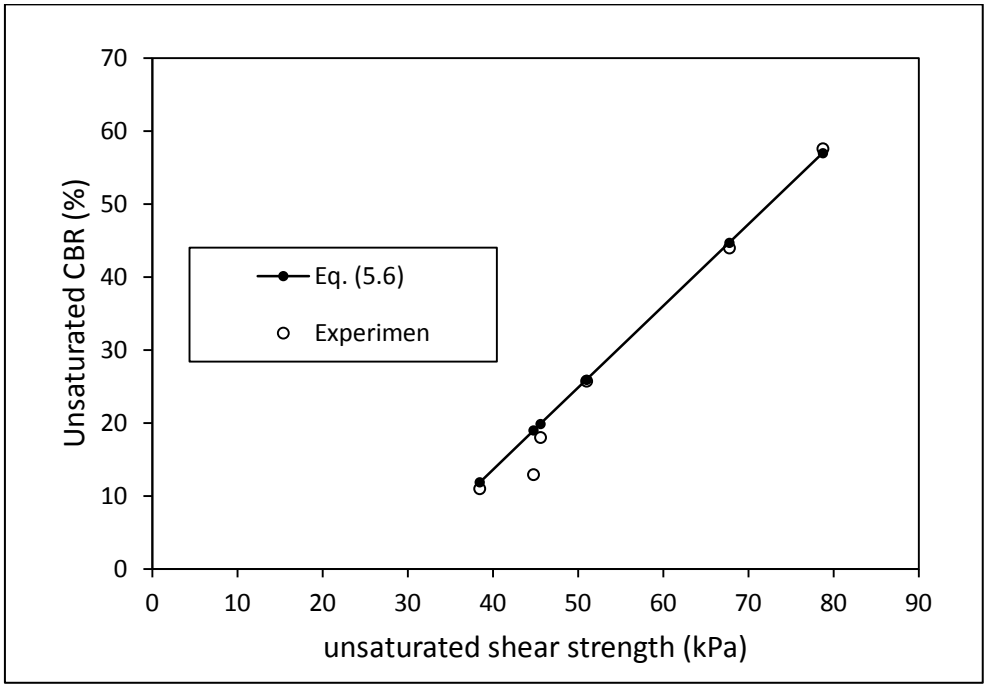

Figure 5.35 The comparison of experimental and correlation results of 95:5 mixture

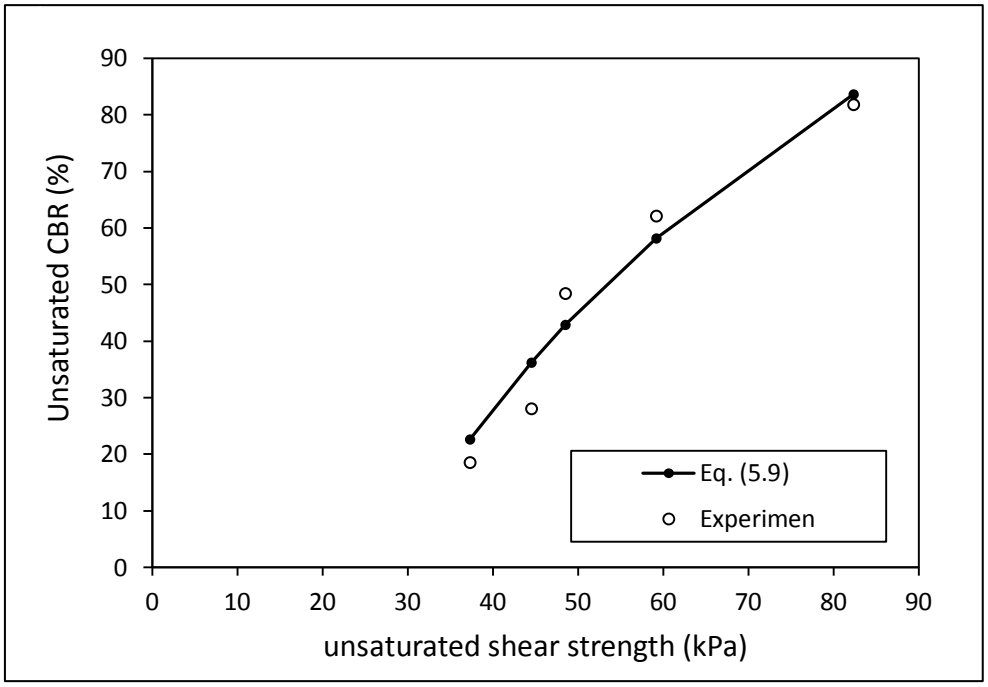

Figure 5.36 The comparison of experimental and correlation results of 90:10 mixture

5.8 Summary

1. A preliminary test was performed on sand and a sand-kaolin clay mixture of 95:5 and 90:10 proportions to obtain their index properties. The results indicated that the specimens could be classified as SP, SP, and SC-SM according to ASTM standards.
2. The standard compaction test indicated that the specimens had a maximum dry density of 17, 18.3, and 19.7 kN/m^3 respectively, with their optimum water content being 13, 11, and 9.8%. The presence of 5% and 10% of kaolin clay contributes 7.6% and 15% respectively to the increase in maximum dry density.
3. A tensiometer was used for obtaining the soil water characteristic curve (SWCC) of material with a low air entry value (AEV) and low residual suction such as sand and a 95:5 kaolin clay mixture. However, for the specimens with a relatively high AEV or high residual suction such as the 90:10 mixture, the tensiometer alone was not enough. The combination of the tensiometer for low suction and the filter paper for high suction was employed in this study.

4. The suction-monitored direct shear device has been successfully used for the specimens where matric suction was less than 80 kPa. The tensiometer was fully effective during the test. Care has been taken to ensure that matric suction of the specimen was always under 80 kPa. The SWCC was a very useful tool for predicting the desired specimen water content.
5. The result of the saturated direct shear test indicated that the increase in kaolin clay content caused an increase in effective cohesion and a decrease in the effective internal friction angle.
6. The result of saturated and unsaturated direct shear indicated that the failure envelopes formed a bi-linear pattern. From zero suction until AEV, the increase in shear strength due to suction (denoted as ϕ^b) was higher than the effective friction angle ϕ'. Beyond the AEV, the slope ϕ^b was lower than the effective friction angle ϕ'.
7. The results also indicated that in unsaturated conditions, the presence of kaolin clay in the mixture contributes to the increase in shear strength.
8. The CBR test with direct suction measurement using tensiometers was successfully performed. The results indicated that in general, the matric suction versus the CBR of these particular specimens exhibited a bi-linear curve with the inflection points take place after passing the AEV point.
9. In general, to some extent, the presence of kaolin clay in the mixture led to an increase in maximum dry density, unsaturated shear strength and CBR.
10. The correlation between the CBR and unsaturated shear strength was created by plotting the failure envelopes resulting from unsaturated direct shear and unsaturated CBR tests. The range of the R-square was between 0.87 and 0.99. The high R-square value of the equations indicated that the correlations were reasonable. These correlations may be applicable only for these particular specimens in the range of suction between 0 and 80 kPa.

CHAPTER 6
CONCLUSIONS AND RECOMMENDATIONS

6.1 Conclusions

An experimental study using suction-monitored direct shear and suction monitored CBR was conducted effectively. The overall objectives of this study on the behaviour of the devices and the behaviour of the soil in unsaturated conditions has been achieved. Based on the results and analyses, it can be concluded that:

1. The preliminary study on natural sub-grade samples from different locations in Perth deemed three samples classifiable as poorly graded sand (SP), and another as poorly graded sand with clay (SP-SC). For the purposes of this study and to ensure the repeatability of the test, an artificial soil composed of sand and differing proportions of sand-kaolin clay mixture of 95:5 and 90:10 were used to resemble natural soil.
2. A standard compaction test was performed on the artificial specimens. The results indicated that the presence of 5% and 10% kaolin clay contributes 7.6% and 15% to the increase in maximum dry density respectively.
3. In this study, two suction measurement methods of tensiometer and filter paper method were used in the soil water characteristic curve (SWCC) test. The SWCC test using tensiometer on the sand and 95:5 mixture was successfully performed. The air entry value (AEV) and residual suction of these specimens was lower than the maximum reading capacity of the tensiometer. However, for the specimens with relatively high AEV or high residual suction, such as the 90:10 mixture, the tensiometer alone was not enough. For this reason, the combination of tensiometer for low suction and filter paper for high suction was employed.
4. Suction-monitored direct shear devices were successfully used for the specimens where matric suction was less than 80 kPa. The tensiometer performed effectively during the test. Care was taken to ensure that the matric suction of the specimen was always under 80 kPa. For this the SWCC was highly useful for predicting the desired specimen water content.
5. The result of the direct shear test in saturated and unsaturated conditions on sand and sand-kaolin clay mixtures indicated that the failure envelopes

formed a bi-linear pattern. From zero suction until AEV, the increase in shear strength due to suction (denoted as ϕ^b) was higher than the effective friction angle ϕ'. Beyond the AEV point, the slope ϕ^b was lower than the effective friction angle ϕ'. The results also indicated that in unsaturated conditions, the presence of kaolin clay in the mixture contributes to the increase in shear strength.

6. The CBR test with direct suction measurement using tensiometers was introduced as a new method for conducting the unsaturated CBR test. Direct suction measurement using tensiometers was successfully performed. The results indicated that the present of kaolin clay in the mixture, to some extent, led to the increase in CBR. In general, matric suction versus the CBR curve exhibits a bi-linear curve with the inflection points taking place near AEV. Until AEV, the increase of the CBR due to suction was high. Beyond the AEV, the increase in the CBR due to suction was lower.
7. It can be observed from the unsaturated CBR and direct shear tests results that both suction-CBR and suction-shear strength curves of these particular specimens formed a similar pattern, i.e., bi-linear. Based on this, the correlation between them was developed.
8. The correlation between CBR and unsaturated shear strength was created by plotting the failure envelopes resulting from unsaturated direct shear and unsaturated CBR tests. The range of the R-square was between 0.87 and 0.99. The high R-square value of the equations indicated that the correlations were reasonable. These correlations may be applicable only for these particular specimens in a range of suction between 0 and 80 kPa.

6.2 Recommendations

Based on the literature review, experimental work, analysis and discussion, some further work and study is recommended for the future:

1. Most of the unsaturated direct shear devices use suction-controlled methods. These methods are relatively complex and require continuous control to maintain constant suction. Suction-monitored direct shear tests are much simpler in practice and laboratory test costs are relatively low. Therefore

these can be deemed as one of the alternatives for a low-cost unsaturated shear strength test.

2. One unit of a direct shear machine usually has only one unit of shear box. For a suction-monitored direct shear test, it is recommended that more than one unit of shear box for one unit of direct shear machine be used. From this, one shear box can be used for shearing, whilst others may be used for specimen preparation.
3. In this study, artificial soil composed of sand and sand-kaolin clay mixtures with small proportions of kaolin clay were used to ensure low suction (due to the low capacity of the tensiometer). In future, studies could be conducted using high proportions of kaolin clay/fine grained material and studies could be conducted on natural soil using a high capacity tensiometer (suction probe).
4. Due to the limited time of this study, the compacted specimens in the unsaturated CBR test were not in suction equilibrium. Suction equilibration can be created by leaving the specimen for several days in a closed-air tight CBR mould after air drying. In suction equilibrium, the number of tensiometers can be reduced to two or even one for one CBR mould.

REFERENCES

Agus, S.S., Leong, E.C. and Rahardjo, H., 2001. Soil-water characteristic curves of Singapore residual soils. Geotechnical and Geological Engineering, 19: 285-309.

Al-Khafaf S. and Hanks, R.J., 1974. Evaluation of filter paper method for estimating soil water potential. Soil Science, 117(4): 194-199.

Ampadu, S., 2007. A laboratory investigation into the effect of water content on the CBR of a subgrade soil. In: T. Schanz (Editor), Experimental Unsaturated Soil Mechanics. Springer Berlin Heidelberg, pp. 137-144.

Anand J. Puppala, P.E., Punthutaecha, K. and Sai K. Vanapalli, P.E., 2006. Soil-water characteristic curves of stabilized expansive soils. Journal of Geotechnical and Geoenvironmental, 132(6): 736-751.

AS-1726, 1993. Geotechnical site investigation. Australian Standard.

ASTM-D422-63, 2007. Standard test method for particle-size analysis of soils. ASTM International, West Conshohocken, PA.

ASTM-D5298-10, 2010. Standard test method for measurement of soil potential (suction) using filter paper. ASTM International, West Conshohochen, PA, pp. 1-6.

ASTM-D-698-07, 2007. Standard test method for laboratory compaction characteristic of soil using standard effort (12,400 fr-lbf/ft3 (600 kN-m/m3)). ASTM International, Pennsylvania.

ASTM-D-854-06, 2006. Standard test method for specific gravity of soil solid by water pycnometer. ASTM International, Pennsylvania, pp. 1-7.

ASTM-D-1883-07, 2007. Standard test method for CBR (California Bearing Ratio) of laboratory-compacted soils. ASTM International, Pennsylvania.

ASTM-D-2487-06, 2006. Standard practice for classification of soils for engineering purposes (Unified Soil Classification System). ASTM International, Pennsylvania, pp. 1-11.

ASTM-D-3080-04, 2004. Standard test method for direct shear test of soils under consolidated drained conditions. ASTM International, Pennsylvania.

ASTM-D-4318-05, 2005. Standard test method for liquid limit, plastic limit, and plasticity index of soils. ASTM International, Pennsylvania.

Bishop, A.W., 1959. The principle of effective stress. Lecture delivered in Oslo, Norway, 1955. Technisk Ukeblad, Oslo.

Black, W.P.M., 1962. A method of estimating the California bearing ratio of cohesive soils from plasticity data. Geotechnique, 12(4): 271-282.

Boutin, C., Kacprzak, G. and Thiep, D., 2011. Compressibility and permeability of sand-kaolin mixtures. Experiments versus non-linear homogenization schemes. International Journal for Numeric and Analytical Methods in Geomechanics, 35: 21-52.

Bulut, R. and Wray, W.K., 2005. Free energy of water-suction-in filter paper. Geotechnical Testing Journal, 28(4): 1-10.

Chahal, R.S., 1965. Effect of temperature and trapped air on matric suction. Soil Science, 100(4): 262-266.

Chandler, R.J. and Gutierrez, C.I., 1986. The filter-paper method of suction measurement. Geotechnique, 36(2): 265.

Chiu, T.F. and Shackelford, C.D., 1998. Unsaturated hydraulic conductivity of compacted sand-kaolin mixtures. Journal of Geotechnical and Geoenvironmental Engineering, 124(2): 160-170.

Corey, A.T., Slayter, R.O. and Kemper, W.D., 1967. Comparative terminologies for water in the soil-plant-atmosphere system in irrigation in agricultural soils, R.M. Hagan et.al. American Society of Agronomy, 11.

Das, B.M., 2008. Advanced Soil Mechanics. Taylor & Francis, New York.

Davis, E.H., 1946. The California bearing ratio method for the design of flexible roads and runway. Geotechnique, 1(4): 249-263.

Donald, I.B., 1956. Shear strength measurements in unsaturated, non-cohesive soils with negative pore pressure., 2nd Australia and New Zealand Conference on Soil Mechanics and Foundation Engineering. University, Christchurch, New Zealand, pp. 200-205.

Donald, I.B., 1957. Effective Stresses in Unsaturated Non cohesive Soils with Controlled Negative Pore Pressure, University of Melbourne, Australia, Melbourne.

Fawcett, R.G. and Collis-George, N., 1967. A filter paper method for determining the moisture characteristics of soil. Australian Journal of Experimental Agriculture and Animal Husbandary, 7: 162-167.

Fredlund, 1996. The Emerge of Unsaturated Soil Mechanics, The fourth spencer J. Buchanan Lecture, Texas.

Fredlund, D.G., 1979. Second Canadian Geotechnical Colloquium: Appropriate concepts and technology for unsaturated soils. Canadian Geotechnical Journal, 16(1): 121-139.

Fredlund, D.G., 2000. The 1999 R.M. Hardy Lecture: The implementation of unsaturated soil mechanics into geotechnical engineering. Canadian Geotechnical Journal, 37: 963-986.

Fredlund, D.G. and Houston, S.L., 2009. Protocol for the assessment of unsaturated soil properties in geotechnical engineering practice. Canadian Geotechnical Journal, 46(6): 694-707.

Fredlund, D.G. and Morgenstern, N.R., 1977. Stress state variables for unsaturated soils. Journal of Geotechnical Engineering Division, 103: 447–466.

Fredlund, D.G., Morgenstern, N.R. and Widger, R.A., 1978. The shear strength of unsaturated soil. Canadian Geotechnical Journal, 15(3): 313-321.

Fredlund, D.G. and Rahardjo, H., 1993. Soil Mechanics for Unsaturated Soil. A Wiley-Interscience Publication, Canada.

Fredlund, D.G. and Xing, A., 1994. Equations for the Soil-water Chracteristic curve. Canadian Geotechnical Journal, 31: 521-532.

Fredlund, M.D., Fredlund, D.G. and Wilson, G.W., 1997. Prediction of the soil water characteristic curve from Grain Size Distribution and Volume-Mass Propreties, 3rd Symposium on Unsaturated Soil, Rio de Janeiro, Brazil, pp. 1-11.

Fredlund, M.D., Wilson, G.W. and Fredlund, D.G., 2002. Use of the grain-size distribution for estimation of the soil-water characteristic curve. Canadian Geotechnical Journal, 39: 1103-1117.

Frenkel, H. and Levy, G.J., 1992. Clay dispersion on hydraulic conductivity of clay-sand mixtures as affected by addition of various anions. . Clay and Clay Minerals, 40(5): 515-521.

Gan J.K.M., Fredlund D.G. and Rahardjo H., 1988. Determination of the shear strength parameters of an unsaturated soil using the direct shear test. Canadian Geotechnical Journal, 25: 500_510.

Gardner, R., 1937. A method of measuring capillary tension of soil moisture over a wide moisture range. Soil Science, 43(5): 277-283.

Grim, R.E., 1962 a. Clay Mineralogy. Science, 135(3507): 890-898.

Grim, R.E., 1962 b. Applied Clay Mineralogy. Mc Graw-Hill Company Inc., New York.

Hamblin, A.P., 1981. Filter paper method for routin measurement of field water potential. Journal of Hydrology, 53: 355-360.

Hilf, J.W., 1956. An Investigation of Pore-Water Pressure in Compacted Cohesive Soils, PhD dissertation, Tech. Memo. No. 654. U.S. Dept. of the Interior, Bureau of Reclamation, Design and Construction Div., , Denver.

Holtz, R.D. and Kovacs, W.D., 1981. An Introduction to Geotechnical Engineering. Prantice-Hall Inc., New Jersey.

Houston, S.L., Houston, W.N. and Wagner, A.-m., 1994a. Laboratory filter paper suction measurements. Geotechnical Testing Journal, 17(2): 185-194.

Houston, S.L., Houston, W.N. and Wagner, A.M., 1994b. Laboratory Filter Paper Suction Measurement. Geotechnical Testing Journal, 7(2): 185-194.

Jigheh, H.S. and Zare, C., 2012. Mechanical behaviour of over consolidated clay-sand mixtures. Journal of Civil Engineering and Urbanism, 2(1): 40-44.

Jotisankasa, A., 2010. KU-Tensiometers/Piezometers, Geotechnical Innovation Laboratory, GERD Centre, Dept. of Civil Engineering, Kasetsart University, Bangkok.

Jotisankasa, A. and Mairaing, W., 2010. Suction-monitored direct shear testing of residual soils from landslide-prone areas. Journal of Geotechnical and Geoenvironmental Engineering, 136(3): 533-537.

Jotisankasa, A., Sawangsurriya, A., Booncharoenpanich, P. and Soralump, S., 2012. Influence of kaolin mixture on unsaturated shear strength of decomposed granitic silty sand, Unsaturated Soils: research and applications. Springer, pp. 385-390.

Jotisankasa, A., Tapparnich, J., Booncharoenpanich, P., Hunsachainan, N. and Soralump, S., 2010. Unsaturated soil testing for slope studies, International Conference on Slope 2010: Geotechnique and Geosynthetic for Slope. Department of Highway, Thailand, Chiangmai, Thailand.

Khanzode, R.M., Vanapalli, S.K. and Fredlund, D.G., 2002. Measurement of soil-water characteristic curves for fine-grained soils using a small-scale centrifuge. Canadian Geotechnical Journal, 39(5): 1209-1217.

Leong, E.C., He, L. and Rahardjo, H., 2002. Factors affecting the filter paper method for total and matric suction measurements Geotechnical Testing Journal, 25(3): 1-12.

Leong, E.C. and Rahardjo, H., 1996. Soil-water characteristic curves from drying and wetting of a residual soil, 7th Australia New Zealand Conference on Geomechanics: Geomechanics in Chaning World, Barton, pp. 418-423.

Likos, W.J., Wayllace, A., Godt, J. and Lu, N., 2010. Modified Direct Shear Apparatus for Unsaturated Sands at Low Suction and Stress. Geotechnical Testing Journal, 33(4): 1-12.

Lourenço, S.D.N., Gallipoli, D., Toll, D.G., Augarde, C.E. and Evans, F.D., 2011. A new procedure for the determination of soil-water retention curves by continuous drying using high-suction tensiometers. Canadian Geotechnical Journal, 48(2): 327-335.

Lu, N. and Likos, W.J., 2004. Unsaturated Soil Mechanics. John Wiley and Sons Inc., New York.

Mackenzie, R.C. and Mitchell, B.D., 1966. Clay mineralogy. earth Science Reviews, 2: 47-91.

Marinho, F.A.M., 2005. Nature of soil–water characteristic curve for plastic soils. Journal of Geotechnical and Geoenvironmental Engineering, 131(5): 654-661.

McQueen, I.S. and Miller, R.F., 1968. calibration and evaluation of wide-range gravimatric method for measuring moisture stress. Soil Science, 106(3): 225-231.

Miller, C.J., A.M., Y., Yaldo, K. and Merayyan, S., 2002. Impact of soil type and compaction conditions on soil water characteristic. Journal of Geotechnical and Geoenvironmental, 128(9): 733-742.

Mitchell, J.K. and Soga, K., 2005. Fundamentals of Soil Behavior. John Wiley and Sons, New Jersey.

Mullins, C.E. and Panayiotopoulos, K.P., 1984a. Compaction and shrinkage of sands and sand-kaolin mixtures. Soil & Tillage Research, 4: 191-198.

Mullins, C.E. and Panayiotopoulos, K.P., 1984b. The strength of unsaturated mixtures of sand and kaolin and concept of effective stress. Journal of Soil Science, 35: 459-468.

Murray, E.J. and Sivakumar, V., 2010. Unsaturated soils a fundamental interpretation of soil behaviour Wiley-Blackwell Iowa.

Murray, H.H., 1991. Overview-clay mineral application. Applied Clay Science, 5: 379-395.

Nam, S., Gutierrez, M., Diplas, P. and Petrie, J., 2011. Determination of the shear strength of unsaturated soils using the multistage direct shear test. Engineering Geology, 122(3-4): 272-280.

Ng, C.W.W. and Menzies, B., 2007. Advanced Unsaturated Soil Mechanics Engineering. Taylor and Francis e-Library.

Ng, C.W.W. and Pang, Y.W., 2000. Experimental investigations of the soil-water characteristics of a volcanic soil. Canadian Geotechnical Journal, 37: 1252-1264.

Paraire, J., 1987. Suction tests on CBR-diameter specimens. The bearing capacity-suction relation, Transport and Road Research Lab. (TRRL).

Poulovassilis A., 1962. Hysterisis of pore water, an application of the concept of independent domain. J. Soil Science, 93: 405-412.

Purwana, Y.M., Jitsangiam, P., Nikraz, H. and Josinakasa, A., 2011. Experimental studies on suction-monitored direct shear apparatus on Perth poorly graded sand, International Conference on Advances in Geotechnical Engineering, Perth, Western Australia, pp. 273-278.

Rahardjo H and Leong, E.C., 2006. Suction Measurement. In: G.A. Miller, C.E. Zapata, S.L. Houston and D.G. Fredlund (Editors), Unsaturated Soil. ASCE, Carefree, Arizona, pp. 81-104.

Ridley, A.M. and Burland, J.B., 1999. Use of the tensile strength of water for the direct measurement of high suction: Discussion. Canadian Geotechnical Journal, 36: 178-180.

Ridley, A.M. and Wray, W.K., 1995. Suction measurement: A review of current theory and practices. In: E.E. Alonso and P. Delage (Editors), Unsaturated Soils: Proc. 1st Int. Conf. on Unsat. Soils, Paris, pp. 1293-1322.

Shankar, P., Teo, J., Leong, Y.-K., Fourie, A. and Fahey, M., 2010. Adsorbed phosphate additives for interrogating the nature of interparticles forces in kaolin clay slurries via rheological yield stress. Advanced Powder Technology, 21(4): 380-385.

Sillers, W.S., Fredlund, D.G. and Zakerzaheh, N., 2001. Mathematical attributes of some soil–water characteristic curve models. Geotechnical and Geological Engineering, 19(3): 243-283.

Sivakumar, V. and Tan, W.C., 2002. CBR, undrained strength and yielding characteristics of compacted tills. In: d.C. Juca, Marinho (Editor), Unsaturated Soils: proceedings of the Third International Conference on Unsaturated Soils, UNSAT 2002, Recife, Brazil, pp. 657-661.

Skempton, A.W., 1953. The colloidal activity of clay, 3rd Int. Conf. soil mech. Found. Eng, pp. 57-61.

Slavéková, J., 1967. Dependence of the root suction force on the soil water content. Biologia Plantarum, 9(2): 149-156.

Soos, P. and Bohac, J., 2002. Properties of soils and rocks and their laboratory determination. In: U. Smoltczyk (Editor), Geotechnical Engineering Handbook. Ernst and Sohn, Berlin, pp. 119-206.

Swarbrick, G.E., 1995. Measurement of soil suction using the filter paper method, 1st International Conference on Unsaturated Soils. A. A. Balkema, Rotterdam, pp. 653-658.

Tarantino, A. and Tombolato, S., 2005. Coupling of hydraulic and mechanical behaviour in unsaturated compacted clay. Geotechnique, 55(4): 307-317.

Terzaghi, K., 1943. Theoretical Soil Mechanics. John Wiley and Sons, New York.

Tinjum, J.M., Benson, C.H. and Blotz, L.R., 1997. Soil-water characteristic curve for compacted clays. Journal of Geotechnical and Geoenvironmental, 123(11): 1060-1069.

Vanapalli, S.K., Fredlund, D.G. and Pufahl, D.E., 1999. The influence of soil structure and stress history on the soil-water characteristics of a compacted till. Geotechnique, 49(2), 143-159. Geotechnique, 49(2): 143-159.

Vanapalli, S.K. and Lacasse, F., 2010. Comparison between the measured and predicted shear strength behaviour of four unsaturated sands. In: F.S. Buzzi (Editor), Unsaturated Soils. Taylor & Francis Group, London, pp. 121-127.

Wilkinson, G.E. and Klute, A., 1962. The temperature effect on the equilibrium energy status of water held by porous media. Soil Sci. Soc. Am. J., 26(4): 326-329.

Wu, A. and Sun, Y., 2008. Granular Dynamic Theory and Its Applications. Metallurgycal Industry Press, Beijing.

Yang, H., Rahardjo, H., Leong, E.C. and Fredlund, D.G., 2004. Factors affecting drying and wetting soil-water characteristic curves of sandy soils. Canadian Geotechnical Journal, 41: 908-920.

APPENDIX

CBR TEST

AND

CORRESPONDING MONITORED SUCTION

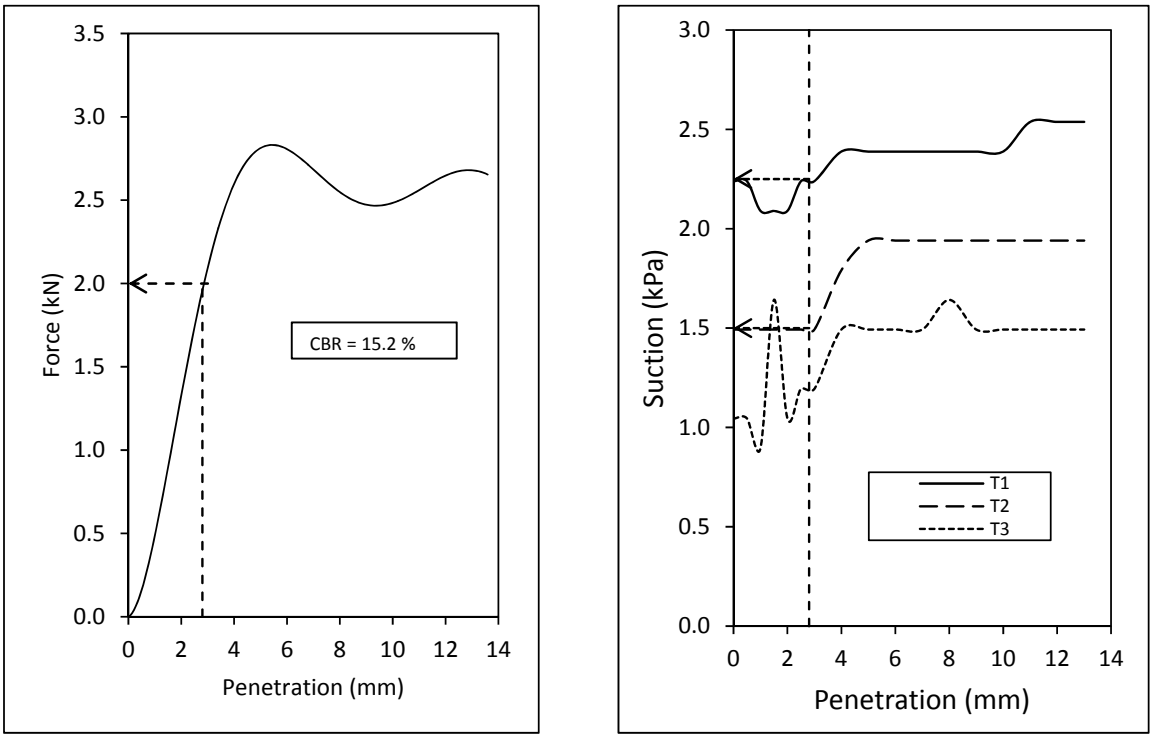

Figure A1: CBR test on SS specimen

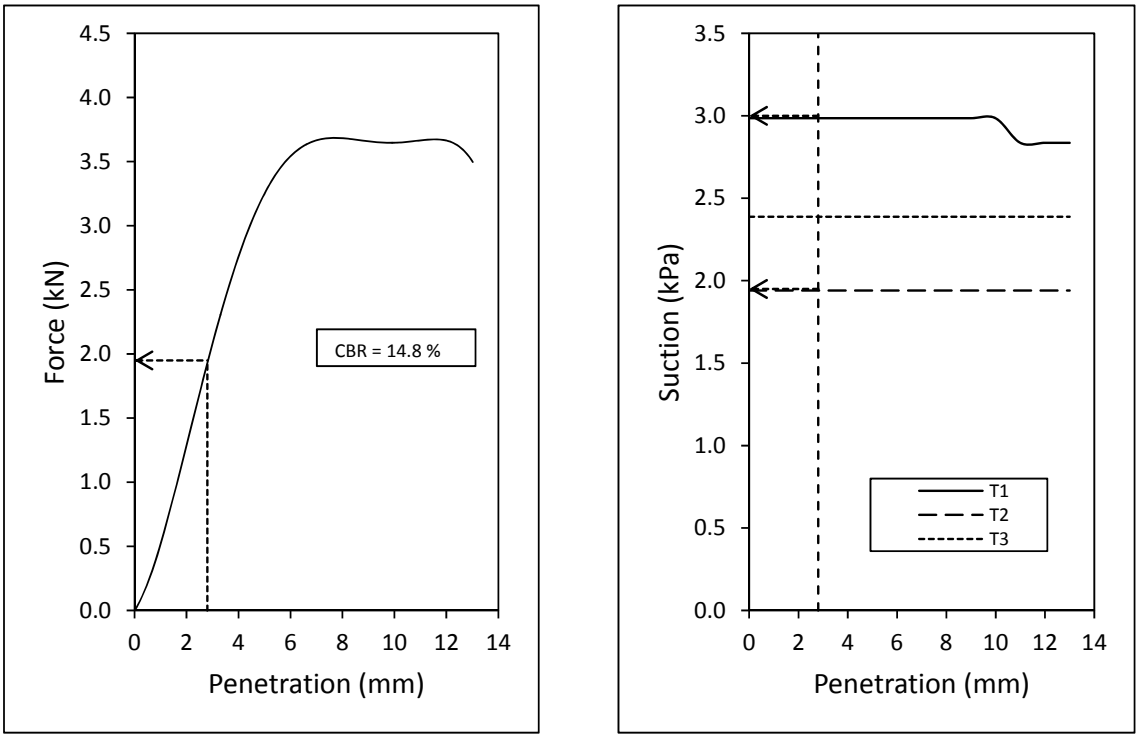

Figure A2: CBR test on SU1 specimen

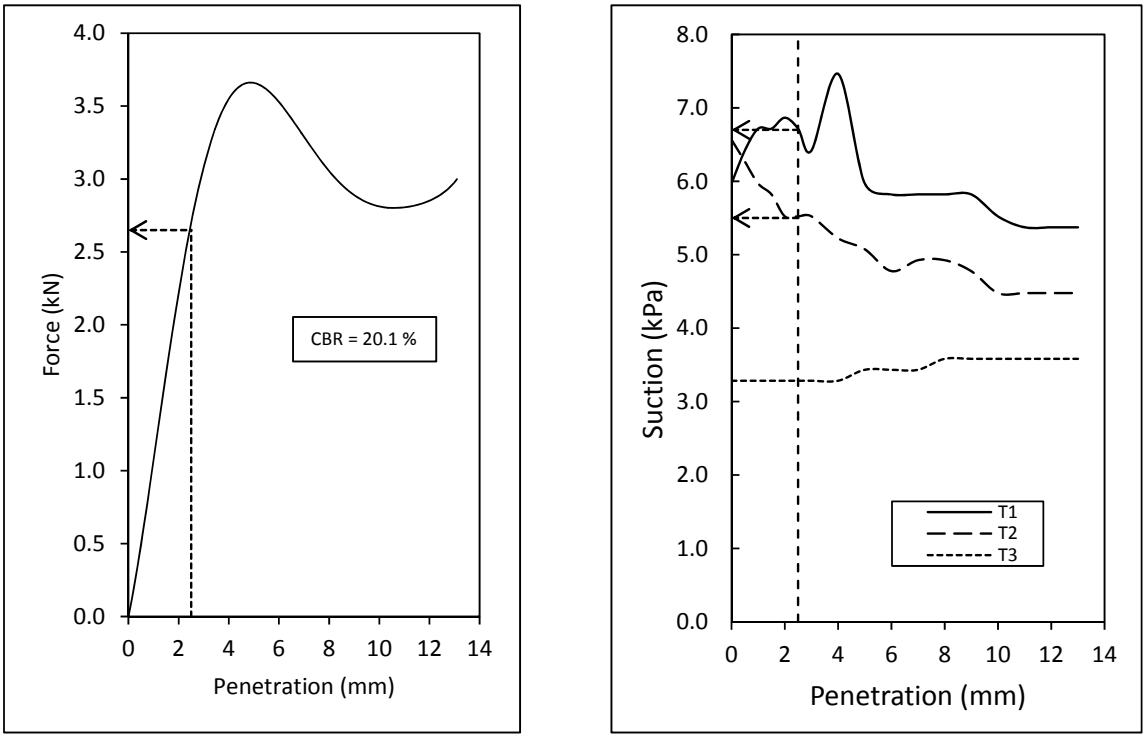

Figure A3: CBR test on SU2

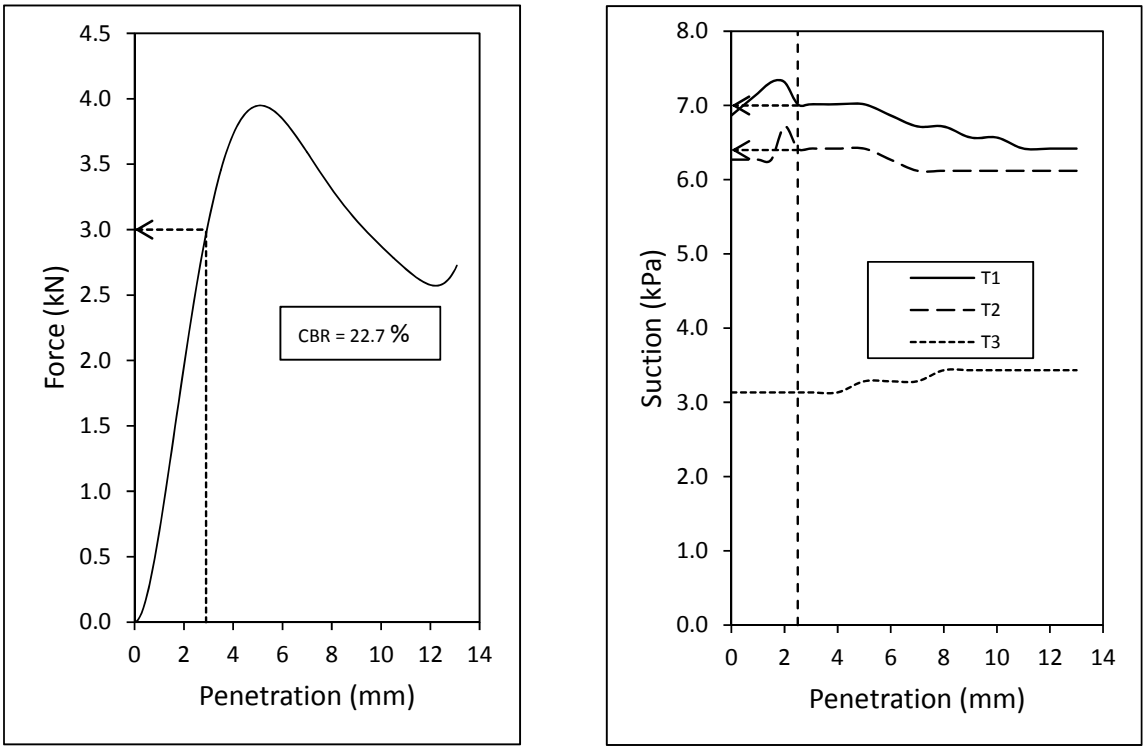

Figure A4: CBR test on SU3

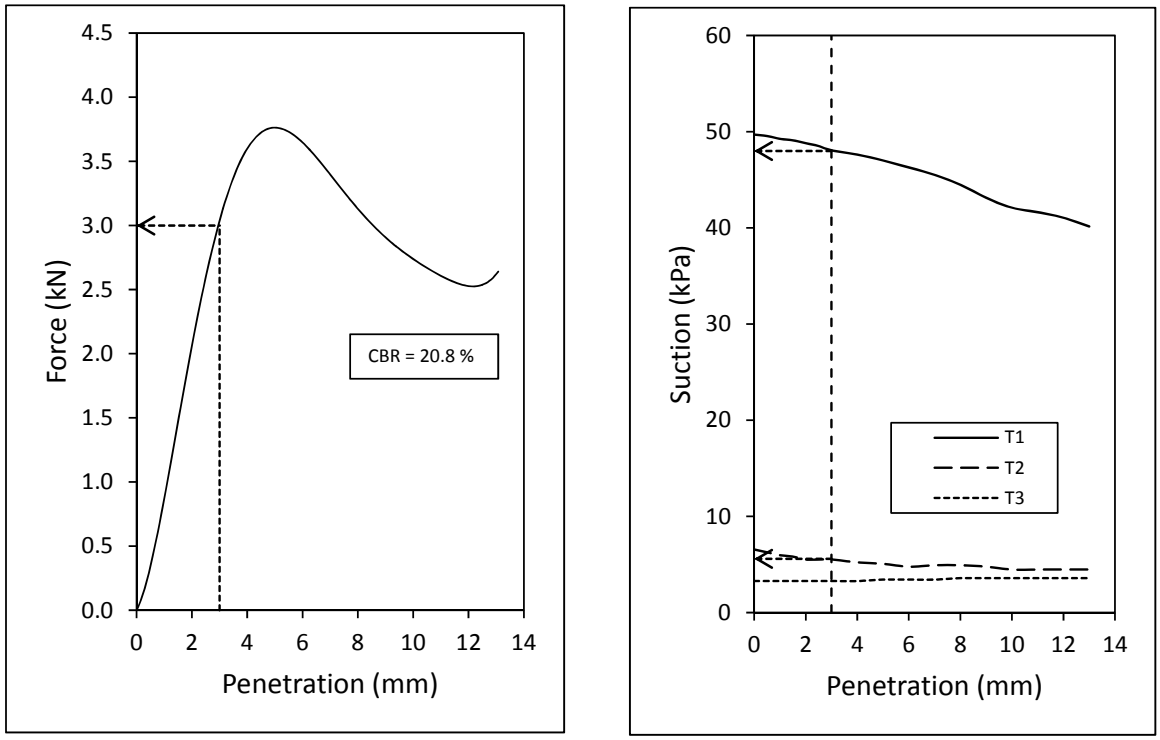

Figure A5: CBR test on SU4

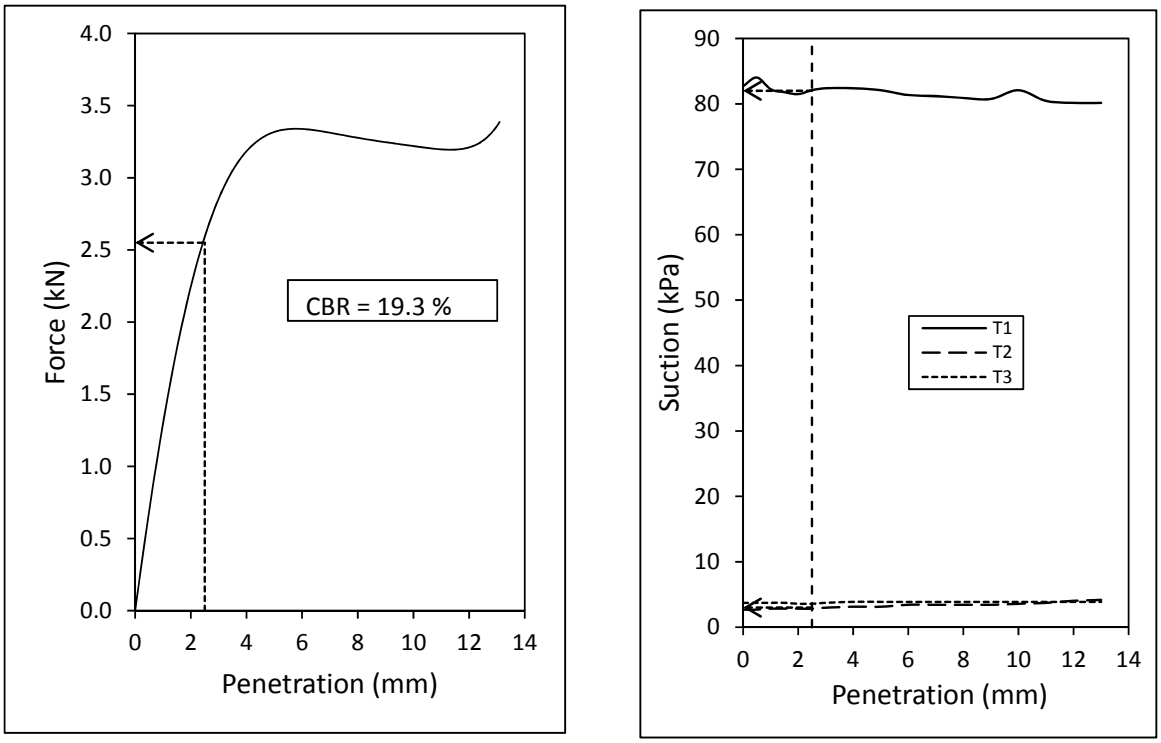

FigureA6: CBR test on SU5

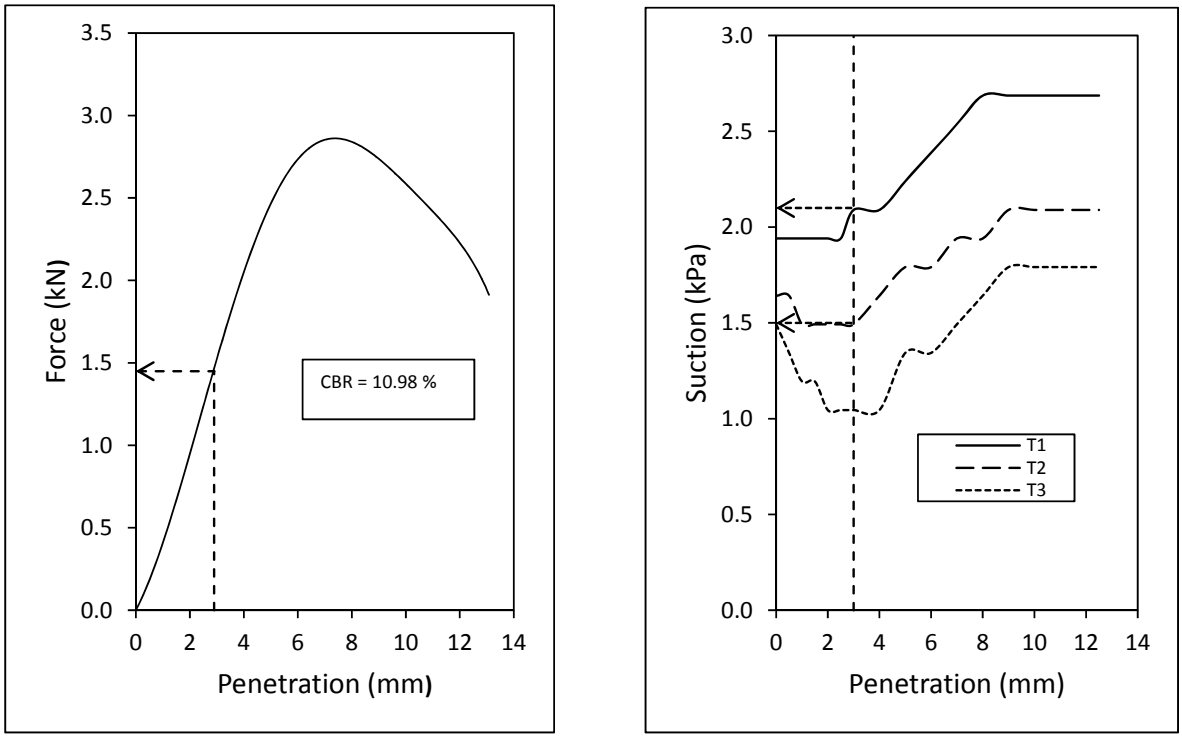

Figure A7: CBR test on M95S

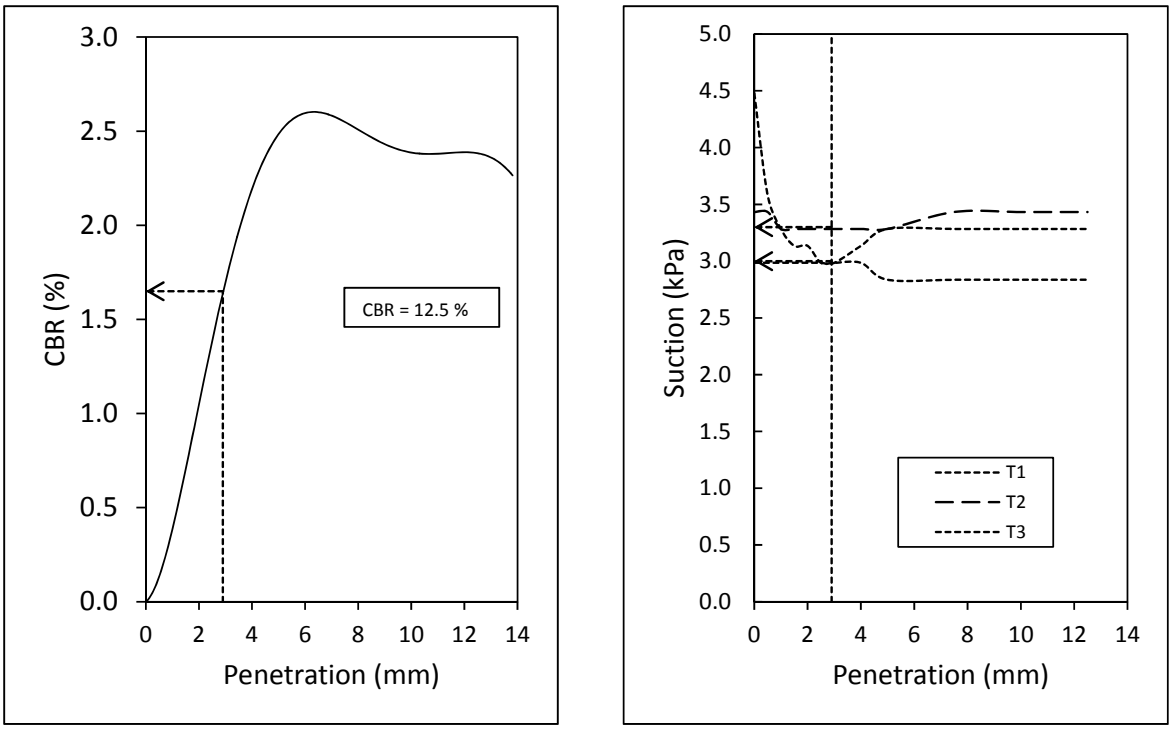

Figure A8: CBR test on M95U1

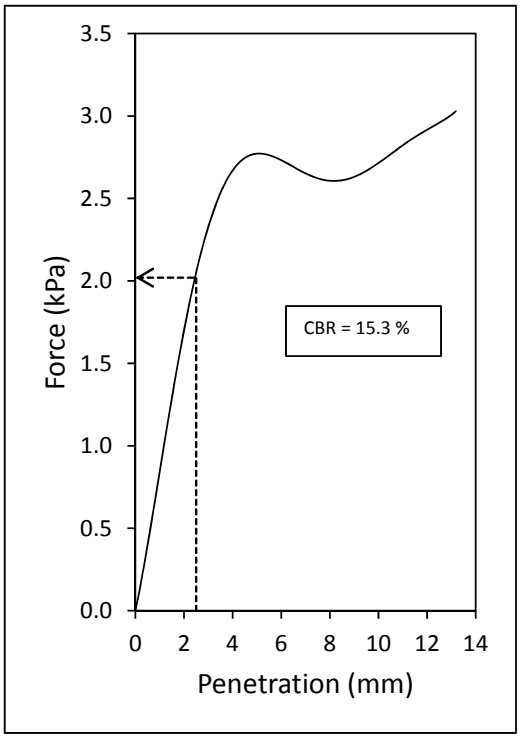

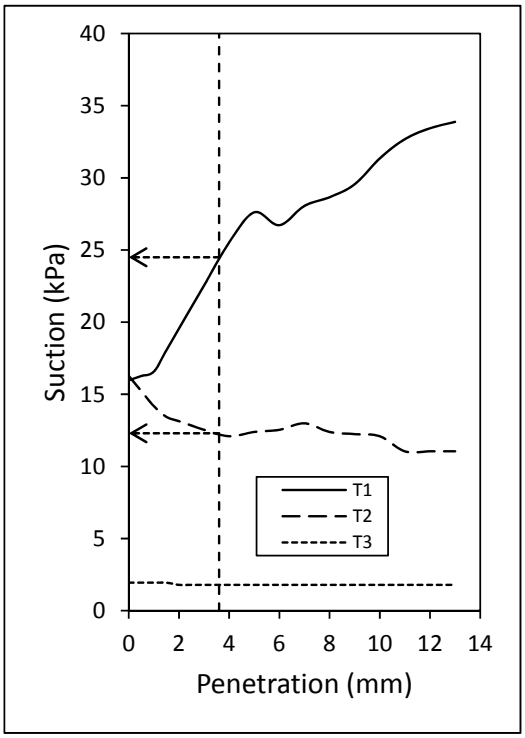

Figure A9: CBR test on M95U2

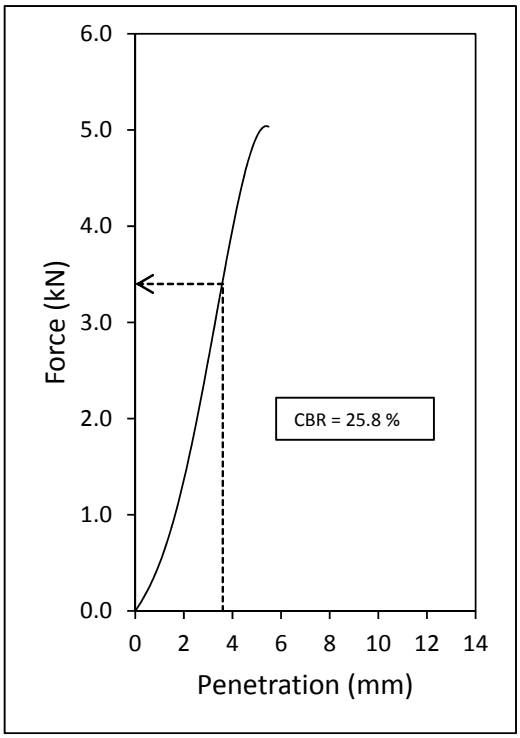

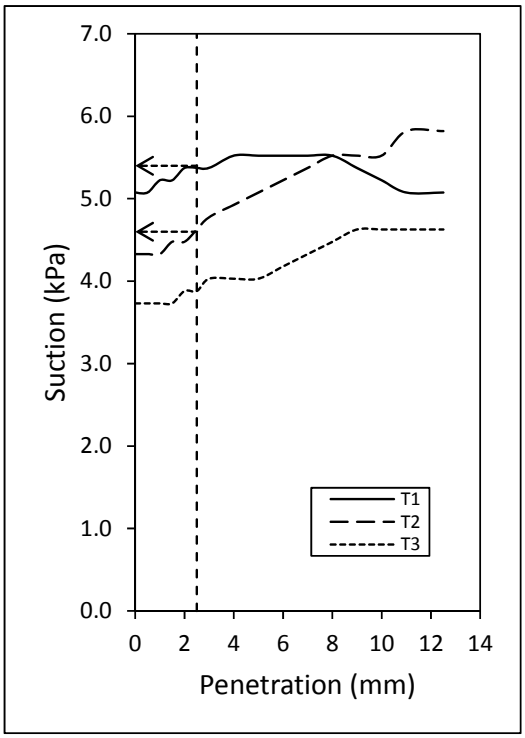

FigureA10: CBR test on M95U3

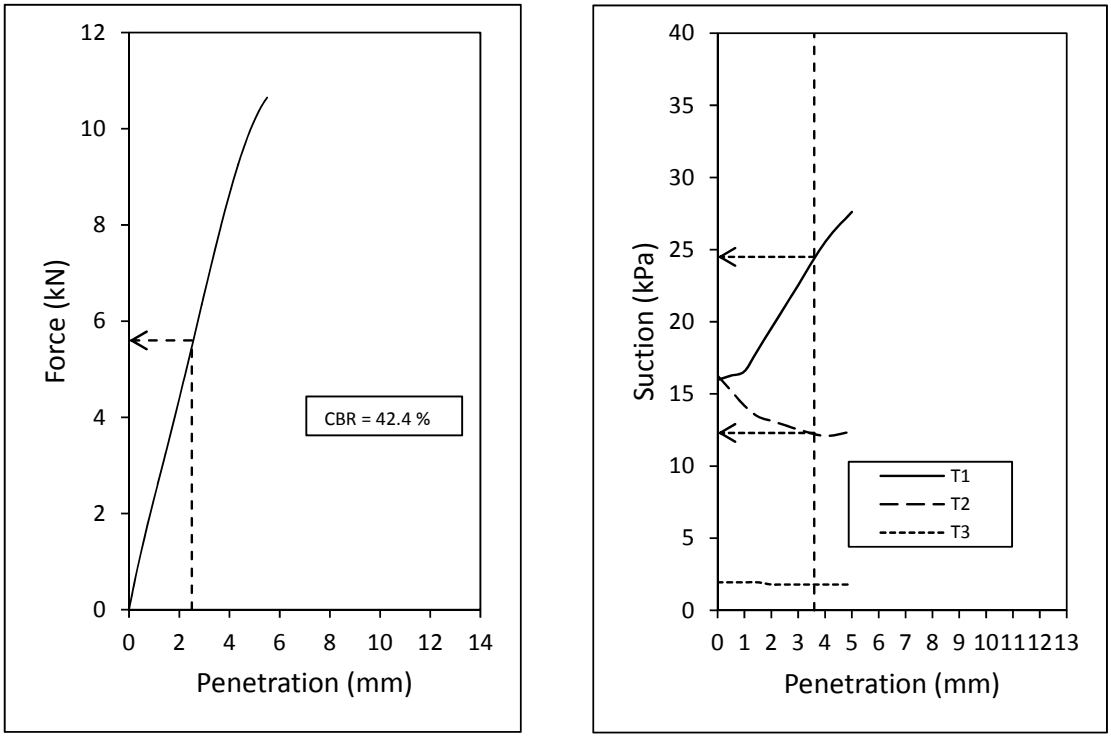

Figure AB11: CBR test on M95U4

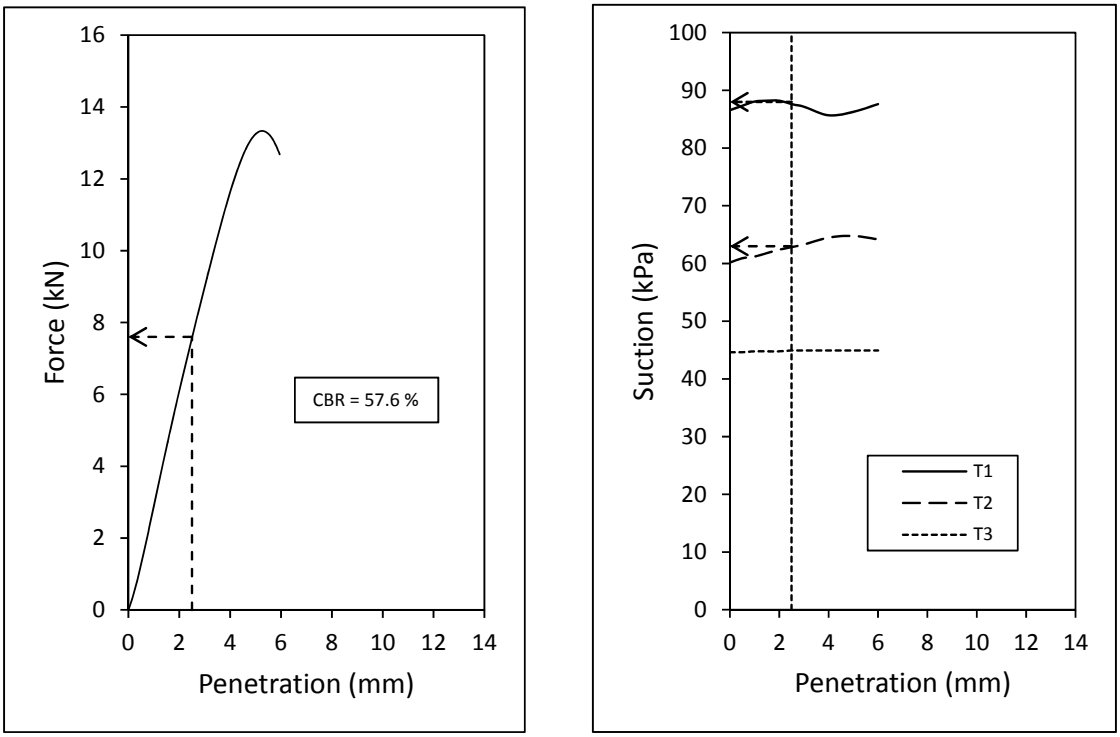

Figure A12: CBR test on M95U5

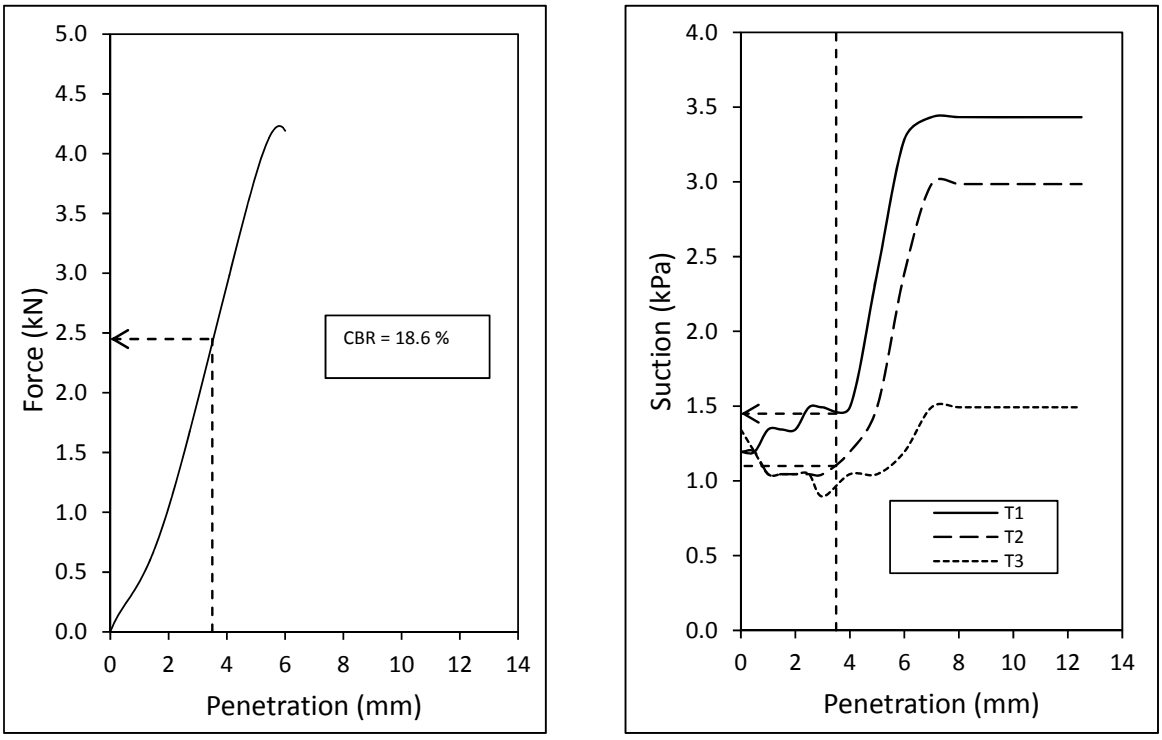

Figure A13: CBR test on M90S

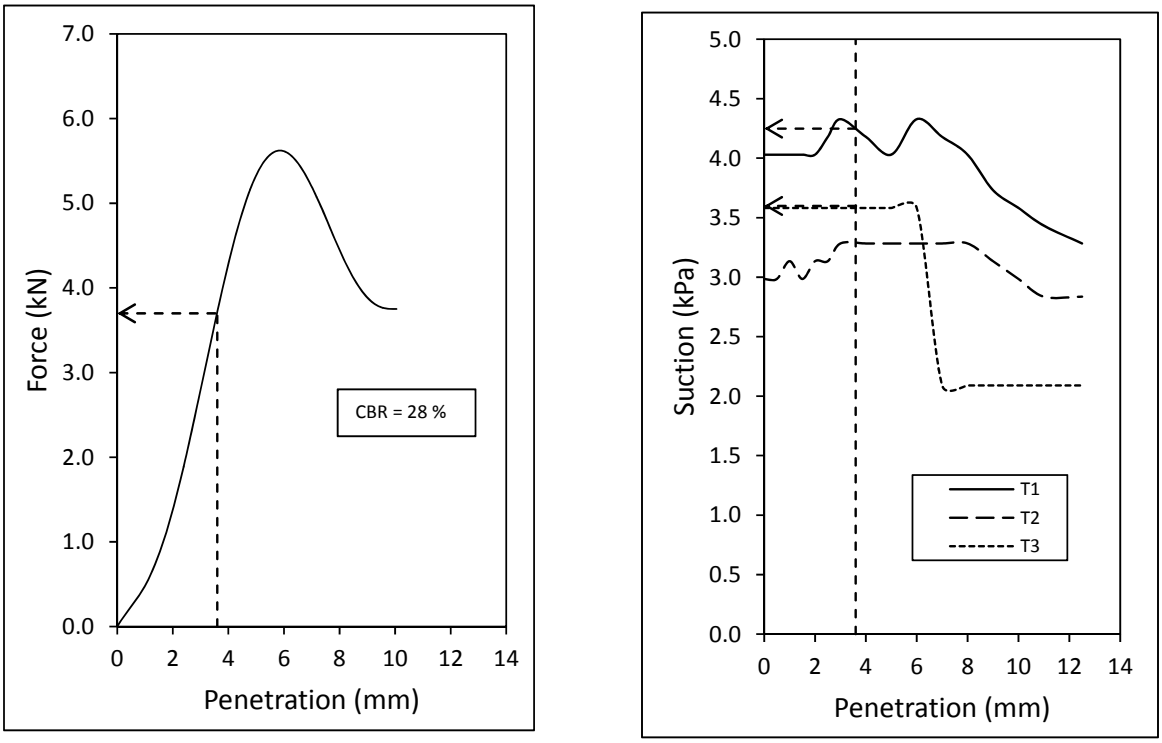

Figure A14: CBR test on M90U1

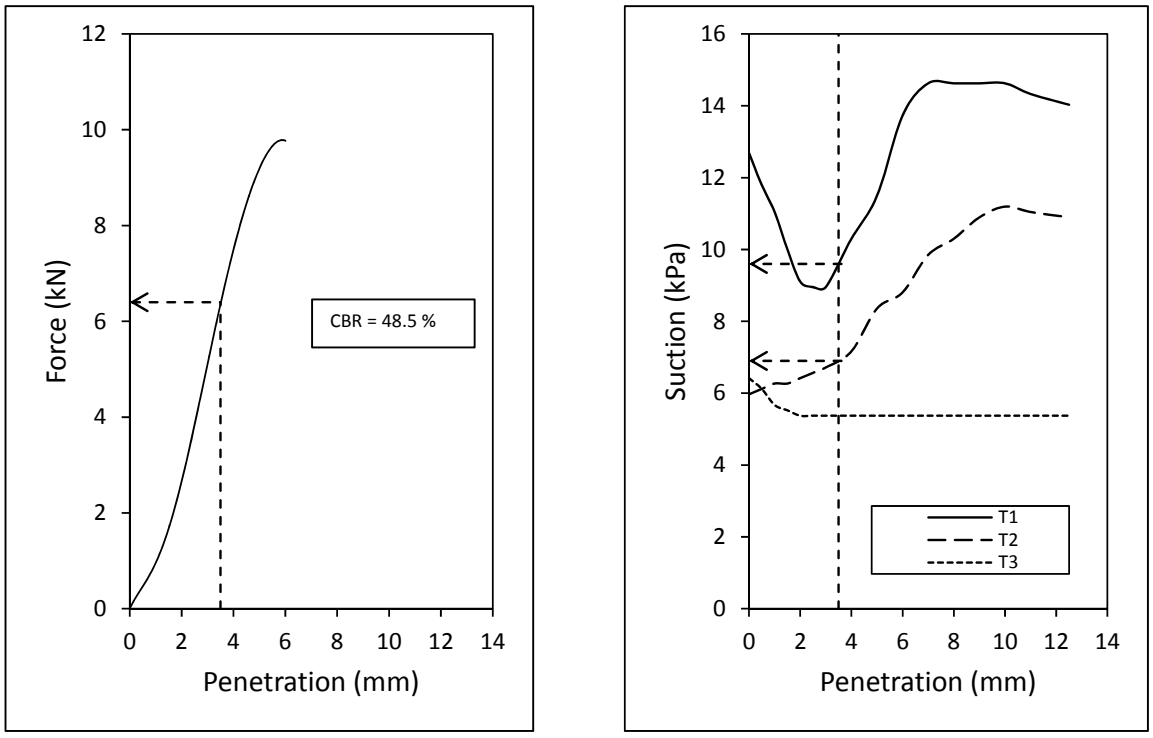

Figure A15: CBR test on M90U2

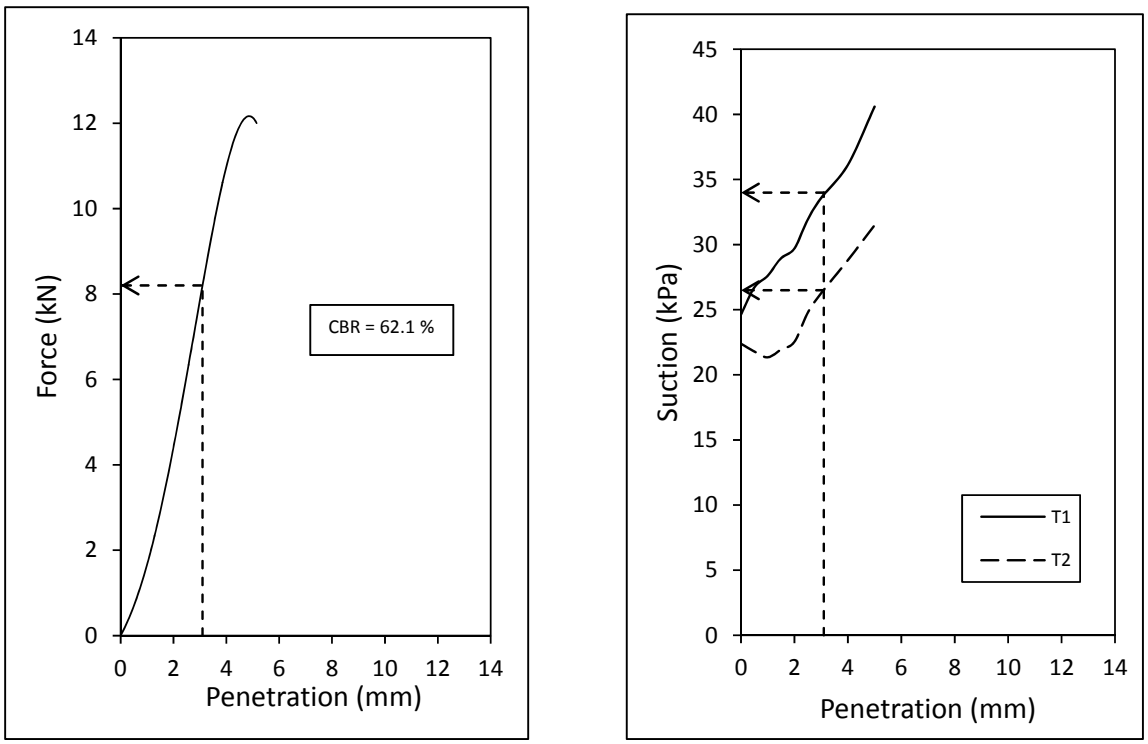

Figure A16: CBR test on M90U3

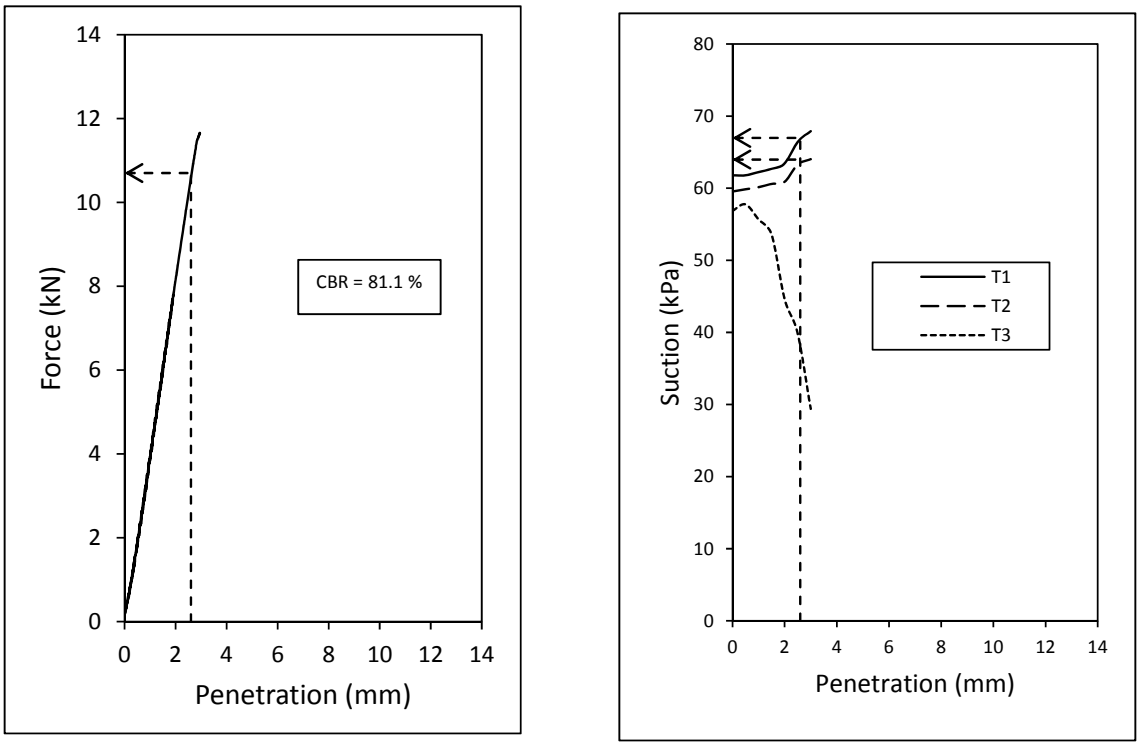

Figure A17: CBR test on M90U4